Improvement of Pedestrian Safety: Response of detection systems to real accident scenarios

Hedi Hamdane

▶ **To cite this version:**

Hedi Hamdane. Improvement of Pedestrian Safety: Response of detection systems to real accident scenarios. Modeling and Simulation. Aix Marseille Université ; University of Adelaide, 2016. English. NNT : . tel-01450696v2

HAL Id: tel-01450696
https://hal.science/tel-01450696v2

Submitted on 9 Feb 2017

HAL is a multi-disciplinary open access archive for the deposit and dissemination of scientific research documents, whether they are published or not. The documents may come from teaching and research institutions in France or abroad, or from public or private research centers.

L'archive ouverte pluridisciplinaire **HAL**, est destinée au dépôt et à la diffusion de documents scientifiques de niveau recherche, publiés ou non, émanant des établissements d'enseignement et de recherche français ou étrangers, des laboratoires publics ou privés.

Aix-Marseille University
Faculté des Sciences du Sport de Luminy

The University of Adelaide

The French institute of science and technology
for transport, development and networks

PhD THESIS

In: Human Movement Science

Presented by

Hédi HAMDANE

For the qualification for the award of the degree of Doctor of Philosophy
under a Cotutelle Agreement between Aix-Marseille University and The University of Adelaide

Improvement of Pedestrian Safety: Response of detection systems to real accident scenarios

Defended on December 5th 2016 in front of the committee:

Mr. Robert ANDERSON	University of Adelaide	Co-supervisor
Mr. Matthew BALDOCK	University of Adelaide	Examiner
Mr. Reinoud BOOTSMA	Aix-Marseille University	President
Mr. Johan DAVIDSON	Chalmers University of Technology	Reviewer
Ms. Catherine MASSON	IFSTTAR/Aix-Marseille University	Invited
Mr. Thierry SERRE	IFSTTAR	Co-supervisor
Mr. Remy WILLINGER	University of Strasbourg	Reviewer

École Doctorale Sciences du Mouvement Humain – ED 463

Contents

Figures

Tables

Preface

Through common activities shared in the field of pedestrian safety, collaboration has been materialised between two institutes, the French institute of science and technology for transport, development and networks (IFSTTAR) in France, and the University of Adelaide (through its research centre, the Centre for Automotive Safety Research – CASR) in Australia. This collaboration started in 2007 through the framework of the IHRA (International Harmonization Research Activities) that aims to develop standard safety evaluation procedures in vehicle technologies. Based on these events, a Memorandum of Understanding has been signed by both institutes in 2009[1].

Over the years, IFSTTAR and CASR have been performing common research activities such as comparison of accident investigation methods, accident reconstruction modelling and numerical simulation of pedestrian accidents. Exchange of researchers and students have been realized resulting in effective work and several articles published in common.

This PhD project is a continuation of this collaboration between the two institutes IFSTTAR and CASR. It is enrolled within a "cotutelle agreement" signed between the University of Aix-Marseille and the University of Adelaide. It is performed in cooperation with CASR and two research laboratories of IFSTTAR (the LMA –Accident mechanism laboratory– and the LBA –Applied biomechanics laboratory–).

[1] At that time, IFSTTAR was named INRETS. A renewal of the Memorandum of Understanding has been signed in 2013 to extend the duration to 4 years.

Abstract

The scope of this research concerns pedestrian active safety. Several primary safety systems have been developed for vehicles in order to detect a pedestrian and to avoid an impact. These systems analyse the forward path of the vehicle through the processing of images from sensors. If a pedestrian is identified on the vehicle trajectory, these systems employ emergency braking and some systems may potentially employ emergency steering. Methods for assessing the effectiveness of these systems have been developed. But, it appears difficult to determine the relevance of these systems in terms of pedestrian protection. The general objective of this research was to test the response of these systems in many accident configurations.

The first step consisted of gathering a sample of a hundred of accidents involving vehicles with pedestrians. These accidents were provided from accident databases of two laboratories LMA and CASR. Data of these accidents were recorded in sufficient detail from in-depth investigation which enables reconstructing the trajectory of the vehicle and pedestrian prior to the collision.

The second step was to analyse qualitatively and quantitatively the data of the selected accidents. These accidents were reconstructed to simulate the pre-crash conditions. From this accident reconstruction, factors relevant to the primary safety of pedestrians were deduced.

The next step consisted of coupling the vehicle dynamic behaviour with a primary safety system in order to confront these systems to real accident configurations. The potential of these systems is studied by verifying the feasibility of deploying an autonomous emergency manoeuvre during the timeline of the accident and according to the vehicle dynamic capabilities: i.e. verifying the possibilities in terms of crash avoidance. Based on this procedure, three modelling methods were developed: a first method testing a system to each accident configuration and two others using graphs of evaluation from a parametric study realised on a generic system. The results of the three methods were then discussed.

Finally, as a perspective, the last study will approach crash mitigation. As a consequence of an active safety system response, the vehicle impact speed is reduced. The effect of speed reduction on variations in impact conditions will be then addressed to measure the potential safety impact of these systems on pedestrian protection.

Abstract in French

Le contexte général de cette recherche concerne la sécurité active des piétons. De nombreux systèmes embarqués dans les véhicules sont actuellement développés afin de détecter un piéton sur la chaussée et d'éviter une collision soit par une manœuvre de freinage d'urgence soit par une manœuvre de déport. La plupart de ces systèmes d'aide à la conduite sont basés sur des systèmes de détection (caméras, radars, etc). Ils analysent la scène en temps réel, puis effectuent un traitement d'images dans le but d'identifier un potentiel danger. Or il apparaît difficile de déterminer la pertinence de ces systèmes en termes de sécurité routière. L'objectif général de ce travail est ainsi d'estimer cette pertinence en confrontant les systèmes à de multiples configurations d'accidents réels.

Une première étape a consisté à sélectionner une centaine de cas d'accidents réels impliquant des piétons percutés par des véhicules motorisés. Ce recueil s'est effectué à la fois dans les laboratoires LMA et CASR. Ces deux laboratoires ont des méthodes similaires d'investigation des accidents de la route. La qualité et la quantité d'information sur chaque accident recueilli permet de récupérer les données nécessaires pour la reconstruction cinématique d'un accident.

Dans une seconde étape, une analyse qualitative et quantitative est réalisée sur l'échantillon d'accidents sélectionnés. Ces accidents ont été par la suite reconstruits cinématiquement modélisant avant impact les trajectoires des véhicules et piétons impliqués. Une analyse de ces reconstructions a permis de dégager les enjeux dans l'espace et dans le temps qui influencent la sécurité primaire du piéton.

L'étape suivante a pour but de tester les systèmes de détection des piétons dans les configurations d'accidents reconstruits en les associant à la cinématique des véhicules. Le test de performance de ces systèmes a été alors réalisé en vérifiant leurs compatibilités au regard de la chronologie des accidents; i.e. vérifier la possibilité d'évitement des accidents. À partir de cette procédure, trois différentes méthodes de modélisation ont été développées : une première méthode évaluant un système pour chaque configuration d'accidents et deux autres méthodes utilisant des graphes tracés à partir d'une étude paramétrique d'un système générique. Ces méthodes ont été par la suite évaluées.

Enfin, une extension de la méthodologie précédemment décrite est proposée comme perspective pour aborder la phase d'impact du piéton contre le véhicule. En conséquence d'un déclenchement d'un système actif, la vitesse d'impact est réduite et donc les conditions du choc sont modifiées. Une méthode a été développée pour étudier les effets de cette réduction de vitesse en analysant les conséquences sur les risques lésionnels du piéton.

Statement of originality

To the best of my knowledge and belief, this work contains no material which has been accepted for the award of any other degree or diploma in any university or other tertiary institution that was not mentioned in the agreement signed between the University of Adelaide and the Aix-Marseille Université. It contains no material previously published or written by another person, except where due reference has been made in the text.

I give consent to this copy of my thesis when deposited in the University Library, being made available for loan and photocopying, subject to the provisions of the Copyright Act 1968.

The author acknowledges that copyright of published works contained within this thesis (as listed in the following page) resides with the copyright holder(s) of those works.

I also give permission for the digital version of my thesis to be made available on the web, via the University's digital research repository, the Library catalogue, the Australasian Digital Theses Program (ADTP) and also through web search engines, unless permission has been granted by the University to restrict access for a period of time.

Hédi HAMDANE

List of publications

- H. Hamdane, T. Serre, C. Masson and R. Anderson (2016). Relevant factors for active pedestrian safety based on 100 real accident reconstructions. International Journal of Crashworthiness, Volume 21 (1), p. 51-62.

- H. Hamdane, T. Serre, C. Masson, R. Anderson (2015). Issues and challenges for pedestrian active safety systems based on real world accidents. Accident Analysis & Prevention, Volume 82, September 2015, p. 53–60.

- H. Hamdane, T. Serre, R. Anderson, C. Masson and J. Yerpez (2014). Description of pedestrian crashes in accordance with characteristics of Active Safety Systems, Proceedings of the 2014 IRCOBI conference, Berlin, Germany, 10-12 September 2014.

- H. Hamdane, T. Serre, R. Anderson and J. Yerpez (2014). Accident simulation and reconstruction for enhancing pedestrian safety: issues and challenges, Proceedings of the 6th ESAR conference, Hannover, Germany, 20-21 June 2014.

- H. Hamdane, R. Anderson, C. Masson, M. Llari and T. Serre (2014). Assessment methodology of Active Pedestrian Safety Systems: an estimation of safety impact, Proceedings of the 3rd SIMBIO-M conference, Marseille, France, 19-20 June 2014.

Acknowledgement

I would like to thank everyone who has contributed and helped me in achieving this research work:

Thierry Serre, my principal co-supervisor at IFSTTAR-LMA, for giving me the opportunity to carry out this work, for tutoring me and sharing knowledge and expertise in the field of traffic safety.

Robert Anderson, my principal co-supervisor at CASR, at the University of Adelaide, for guidance throughout my research work and for the valuable feedback provided during the writing process of the thesis.

Catherine Masson, my co-supervisor at IFSTTAR-LBA, at the University of Aix-Marseille, for the helpful assistance and support with the writing of my thesis and my papers.

Christophe Perrin, head of the in-depth crash investigation team at IFSTTAR-LMA, and Joël Magnin and Bastien Canu, two other members of this team, for sharing their expertise in the field of crash investigation.

Craig Kloeden, Tori Lindsay, Giulio Ponte and Sam Doecke, Research Fellows at CASR in charge of conducting in-depth crash investigation, for their valuable assistance with the use of data from the CASR crash database.

Andrew van den Berg, Impact Lab Manager at CASR, for his priceless insights about active safety systems.

Paul Hutchinson, Senior Research Fellow at CASR, for the valuable discussions we had about modelling active safety systems.

Thierry Brenac, Research Fellow at IFSTTAR-LMA, for sharing his expertise in the field of traffic safety.

Maxime Llari, Engineer at IFSTTAR-LBA, for always being available to assist me with the Madymo simulations.

Michèle Bidal, Library Assistant at IFSTTAR-LMA, and Jaime Royals, Information Manager at CASR, for their assistance with providing materials for my research.

All the colleagues of CASR for making me feel like home.

The colleagues of IFSTTAR-LMA/LBA for their support.

The PhD students encountered in the three research centres for making the work place more pleasant.

Special thanks to two colleagues/friends for their invaluable support pushing me forward to finish writing the thesis.

Last but not least, my family and my friends for their support.

List of abbreviations

- ADAS: Advanced Driver Assistance System
- AEB: Autonomous Emergency Braking
- AES: Autonomous Emergency Steering
- AIS: Abbreviated Injury Scale
- CASR: Centre for Automotive Safety Research
- Euro NCAP: European New Car Assessment Program
- FoV: Field of View
- GIDAS: German In-Depth Accident Study
- IFSTTAR-LMA: French institute of science and technology for transport, development and network, Laboratory of accident mechanisms analysis
- LTTB: Last Time To Brake
- TTB: Time-To-Brake
- TTC: Time-To-Collision
- Ped-AEBS: Pedestrian Autonomous Braking System
- Ped-CAMS: Pedestrian Collision Avoidance and Mitigation System
- WAD: Wrap Around Distance

Chapter 1

Introduction

Each year, more than 1.2 million people are killed in road traffic accidents and, according to WHO's 2004 study Global Burden of Disease, traffic accidents are the 10th leading cause of death worldwide (WHO, 2009). Such figures make road injuries a major global public health concern and have lead the UN to declare 2011-2020 the "Decade of Action for Road Safety".

Half of world traffic deaths occur amongst vulnerable road users, including motorcyclists (23%), pedestrians (22%) and cyclists (5%) while car occupants comprise 31% of mortalities. A further 19% of fatalities are unspecified types of road users. On a yearly basis, more than 270,000 pedestrians are killed on the road while millions more suffer injuries (WHO, 2013). These numbers are likely to rise in the coming years given the global trends toward development and urbanization.

The European Union has undertaken a Framework Programme for Research and Innovation outlining a set of objectives and actions in order to reduce the number of traffic deaths (European program horizon2020[1]). Among these objectives and actions is the promotion of new technologies in the vehicle market specifically to enhance pedestrian protection.

1.1. State of art of pedestrian safety systems

As with all vehicle safety technology, pedestrian safety technology may be classified as either passive or active, depending on the phase of a crash during which they operate (Figure 1.1).

[1] http:ec.europa.eu/programmes/horizon2020

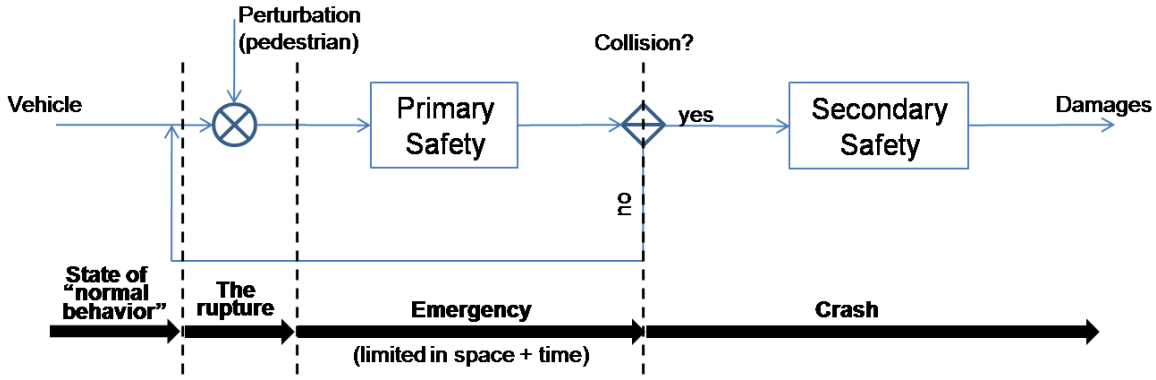

Figure 1.1. Illustration of event sequences of a crash

The transition from a Normal Driving condition to an Imminent Crash is caused by a Critical Event; i.e. the advent of a pedestrian on the path of the vehicle. After this, the driver has to take appropriate countermeasures, which are limited in time and space, to avoid the crash. This phase is called Primary or Active Safety Phase. During this phase, Advanced Driver Assistance Systems (ADAS) can operate to assist the driver to avoid the collision. ADAS may include, braking assistance or autonomous braking or steering (Broggi et al., 2009; Hayashi et al., 2012; Keller et al., 2011a). They are called Pedestrian Collision Avoidance and Mitigation systems (Ped-CAMS).

If the crash is unavoidable, the entire system formed by the pedestrian, the driver, the vehicle and the driving environment move to a collision phase called Secondary or Passive Safety Phase. The Pedestrian Safety Systems involved in this phase are activated in response to a first impact detected with the bumper and exceeding a certain threshold. Car manufacturers have designed vehicles with pop-up bonnets that provide additional clearance from the rigid components underneath before the head impact occurs. Also, a manufacturer has recently developed a pedestrian airbag that is deploying in a U-shape at the bottom of the windscreen to protect the pedestrian's head from hitting rigid structures like the A-pillar.

Although their safety impact, these features are mostly irreversible and hence more costly. Moreover, these mitigation systems cannot prevent the projected pedestrian while a crash from hitting the ground. This last impact with the road remains a high risk of injuries to the pedestrian. Therefore, studying active safety systems to estimate their safety potential remains a current research topic.

Different Ped-CAMS may have quite different attributes. Certainly, it appears difficult to determine the relative benefits of each attribute of these systems. In fact, these attributes operate at different level along the sequence of events preceding a crash. The forward path is analysed using image processing algorithms in real time in order to try to identify a pedestrian on the road. This image processing analysis is a logical chain of algorithms that starts from the pedestrian detection, and then tracks his motion till comes with a prediction of collision occurrence. The processing could be presented as a funnel with different levels of sieves filtering the information from detected obstacles towards a classification for distinguishing pedestrians, then "tracking" to get trajectories, until "the

prediction" of crash and "the decision" of the countermeasure. At the beginning, raw signals from the front-path of the vehicle are recorded by detection sensors. There are different types of sensors that can be classified in imaging sensors operating in visible light or Near, Mid and Far Infrared radiation (NIR, MIR, FAR), and also the "time-of-flight" sensors as RADARs and LIDARs. The most interesting characteristics for this research are essentially the field of view (FOV), the average range of detection and the update or frame rate.

Several surveys have focused on this aspect of pedestrian detection. Fang et al. (2003) have performed research on infrared image depicting the advantages and drawbacks. Gandhi and Trivedi (2007) have reviewed a range of pedestrian detection sensors outlining their strength and weakness and highlighting the problems and difficulties in identifying a pedestrian. A more recent survey done by Geronimo et al. (2010) had the same approach comparing different systems through the literature; however, a method was proposed to evaluate these systems according to the detection rate, the false positive rate and the precision. The basis of this methodology including also the average processing time of the detection algorithm was identified as the most common assessment process to determine the performance of pedestrian detection systems (Gavrila et al., 2004; Machida and Naito, 2011; Szarvas et al., 2006).

To compensate for their limited performance, sensors are combined in order to improve the detection rate by merging the data (Bertozzi et al., 2006; Meinecke et al., 2005; Scheunert et al., 2004). For example, the 2011 MY Volvo S60 with its CWAB-PD® system (Collision Warning with Full Auto Brake and Pedestrian Detection) uses both a monocular vision mounted to the car roof beside the rear view mirror and radar located in the front end of the vehicle behind the grille (Coelingh et al., 2010). Mercedes-Benz has also introduced in the latest S-Class a new generation of Ped-CAMS called Pre-Safe Brake® with Pedestrian Detection using a wide range of sensors: Short, Mid and Long Range Radar (S/M/LRR), Near and Far Infrared camera and a stereo vision (Michalke et al., 2011). After detection, the next step is predicting the trajectory of the detected pedestrians by tracking their motion in order to determine if the crash is likely. Algorithms need to trade-off speed and accuracy and none yet has reached the level of human performance (Keller et al., 2011b).

There are also other parameters influencing the efficiency of Ped-CAMS according to the actuator such as the reaction time, the strength of braking etc. After receiving command signals, the appropriate system component is triggered and accordingly executes an automatic evasive manoeuvre or support the driver by maximising braking. The performance of these components is directly related to their characteristics such as the lag time and the building rate.

Aside from the difference noticed in the performance of each attribute, Ped-CAMS vary also from a functional approach; i.e. these systems have slight different algorithms for decision-making in real configuration. Most of the algorithms start by warning the driver of a hazard then applying autonomous braking according to a time line related to criterion values associated to Time-To-Collision (TTC). This time-related measure was firstly

defined by Hayward (1972) as: "The time required for two vehicles to collide if they continue at their present speed and on the same path". Then, it was introduced as a cue for decision-making in safety manoeuvres in the early 90's with Horst and Hogema (1993). As an important representation issue, this research will also use the TTC criterion in the assessment approach of Ped-CAMS.

Although their potential appears great, Ped-CAMS have been carefully introduced in the market. There are not yet regulatory test methods and standardised assessments established to evaluate their safety benefits relatively to pedestrian crash rate and injuries (Schram et al., 2013).

Several researchers are trying to establish a standard evaluation method using test conditions developed from typical accident scenarios involving car-to-pedestrian front crashes (Eckert et al., 2013; Yuasa et al., 2013). These test scenarios are derived from a cluster analyses for identifying accident scenarios with weighting factors. For example, the European project ASPECSS has calibrated seven accident scenarios through different European accident data sources (Germany and Great Britain), relying on previous European projects including AEB Test Group and vFSS Group (Wisch et al., 2013a). These works based on synthesising accidents into common scenarios are nevertheless not representative of all the diversity encountered in the real-world accidents.

1.2. Aim and objectives

The broad aim of this present research is to develop a process to examine the response of Pedestrian Collision Avoidance and Mitigation Systems (Ped-CAMS) to challenges presented by real accident scenarios.

The basis of this current method is the development of a simulation tool for accident scenarios reconstruction and active safety systems modelling:

- accidents are reconstructed from data provided from in-depth accident investigations;
- Ped-CAMS are modelled according to their characteristics.

The modelled systems are tested through the simulation of a batch of accident scenarios.

Methods have been already developed to measure the effectiveness of pedestrian detection systems. They have been used as in-house test measures for car manufacturers (e.g. Eckert et al., 2013) and used for consumer or regulatory testing (EuroNCAP, 2016).

While other research has aimed to develop procedures for evaluation or validation of Ped-CAMS (Lenard et al., 2011; Lindman et al., 2010; Rosén et al., 2010; Wisch et al., 2013a), the present research aims differ from these works; the present aim was to provide the key parameters (such as kinematics of both vehicle and pedestrian) present in the timeline of an accident. In other words, the aim was to give information about the time and space available for an active safety system to respond before the impact. A further objective of this research was to identify the limits of Ped-CAMS by confronting them with real accident scenarios in order to point out situations that might constrain their

effectiveness. This type of information might help the automotive industry to develop new systems and define edge cases for further development of scenarios for system evaluation.

The tool developed as part of the present work is designed to examine the response of the whole active safety system according to system attributes. It was not possible to evaluate the performance of specific systems in detecting pedestrians: i.e. it was not the objective to assess whether a particular system can or cannot detect a pedestrian due to noisy signals or an algorithm not performing well. The tool was used, however, to examine how designs constraints (such as the field of view) interact with real-world environmental constraints that may affect the visibility of the pedestrian by the detection sensors (e.g. obstacles, light conditions).

The research consists of several distinct phases:

1. Design a simulation program to model accident scenarios and active safety systems.
2. Gather a sample of accidents involving vehicles with pedestrians.
3. Analyze qualitatively and quantitatively the data of the selected accidents in order to determine key parameters regarding pedestrian active safety.
4. Select active safety systems and determine their characteristics required to model them.
5. Apply the methodology on several selected systems to estimate their response.
6. Study the influence of main system parameters

The thesis ends with a simple example that demonstrates how speed reductions brought about by Ped-CAMS will translate to reduction in biomechanical injury risk.

1.3. Thesis outline

Chapter 1 introduces the topic of the research by presenting a brief overview about the pedestrian safety and fixed the objectives of the thesis.

Chapter 2 will give a state of the art in this domain. First, the in-depth crash investigations conducted by IFSTTAR-LMA and CASR will be exposed. It will define the tasks undertaken in pedestrian accident studies: seeking mechanisms of vehicle/pedestrian crashes, clustering accidents into prototypical scenarios, analyzing pedestrian kinematics at impact and examining injuries distribution data. Then, it will review the studies in the literature concerning the following subfields: the state of art of on-board pedestrian safety systems (for active and passive safety) and the existing methods to evaluate these systems.

Chapter 3 will present the simulation tool developed in this research to reconstruct real crashes. To illustrate the methodology of reconstruction, two accident cases will be detailed and processed as input data for the simulation tool. This chapter will also explain

how Ped-CAMS are modelled and implemented in numerical simulations in order to examine their response to accident scenarios.

Chapter 4 will describe the sample of 100 crashes selected for this research. A cluster analysis will be presented according to the different components of a crash: the road environment, driver, vehicle and the pedestrian. The accidents will be first classified into reference scenarios describing briefly the accident sequences. A more in-depth analysis will then focus on the pre-crash sequences and the impact configuration.

Chapter 5 will present the assessment results of existing active pedestrian safety systems by examining their effects on the 100 crash configurations described in Chapter 4. The assessment method and the simulation tool used for coupling the vehicle dynamic behaviour with the active system will be developed. The limitation of this method will be finally outlined.

From the issues highlighted in the previous chapters, Chapter 6 will introduce a generic model of active pedestrian safety system. This model will be then studied in terms of crash avoidance and speed reduction using the assessment tool developed in this research. Results will be exposed to show the potential of this model to examine the response of Ped-CAMS.

As a perspective, Chapter 7 will examine the effect of speed reduction on variations in impact conditions. The method used at this stage of the research will be presented and illustrated with an example. This chapter will be considered as an open door to future researches coupling primary and secondary safety.

Finally, a global discussion will synthesise the main results of this work and will conclude this research.

Chapter 2

Background

2.1. Accidentology: In-depth accident investigations

In order to understand the causes and consequences of traffic accidents and crashes, on-site crash investigation has long been established as the primary method for obtaining information. In such studies, researchers attend the crash scene soon after an accident occurs in order to gather relevant information from an independent perspective. Their findings often contain enough data to analyse the kinematics of the accident, likely contributing factors as well as injury mechanisms. Databases from these in-depth investigations often prove to be more useful than those maintained by national authorities such as the police, hospitals or insurance agencies because they often include more details about crashes while national databases might overlook important or critical information and contributing factors. For example, McLean et al. (1994) found that while a police crash database incorrectly suggested that almost 50 per cent of crashes are caused by inattention while car speed as a contributing factor is frequently under-reported.

Trained experts from a wide range of disciplines help to conduct crash investigations. Their goal is to collect as much pertinent information as they can, striving to address existing and potential research questions. They follow an investigation method of first observing the scene and then gathering information in order to understand what happened and why. Such methodology includes both data collection and case analyses.

Collecting data is a process that includes several activities such as taking notes and measurements, interviewing people at the scene, obtaining details about injuries from hospitals as well as taking photographs or videos. The first step in this process occurs on the scene of the crash. It involves the collection of any physical evidence before it might be lost or removed. Additionally, statements from witnesses and accident victims are obtained directly following the crash. This allows for perspectives and insights that are fresh and minimizes potential for forgetting details that could be important. Evidence that is gathered at the investigation might include the following:

- The location of debris and skid and other marks can be recorded, including also the final resting positions of crash participants
- The vehicle damage due to the crash can be separated from old damage
- The environmental conditions can be noted when attending the crash scene
- The accuracy of information obtained from crash participants and any witness can be confirmed

Because evidence at the crash site might disappear after an accident occurs, it is important for investigators to arrive quickly at the scene. Skid marks from tires, for example, are sometimes hard to detect. The presence of investigators at the site shortly after a collision occurs is of primary importance if such evidence is to be recorded. In cases where a vehicle has only been slightly damaged, the owner might leave the crash site to return home and wash the vehicle. This can remove any impact marks or tell-tale removal of road grime resulting from the accident, a point that is of particular concern regarding pedestrian accidents as the record of the impact between the pedestrian and the vehicle would normally be found on this surface. Hence, this physical record is often lost soon after the crash. Crash sites might be opened too soon for investigators to adequately research the area. Weather conditions can further complicate investigators' tasks by contributing to the deterioration or washing away of evidence. If investigators arrive before too much of this has already happened, they increase the chances of having more detailed and helpful information to understand how and why the crash occurred. Early arrival at the accident site also helps increase the odds of making contact with witnesses and victims of the crash, a point that might also make these subjects more open to follow-up interviews.

Case analysis consists of data processing and evaluation of contributing factors in collisions. After an investigation, a diagram of the scene is drawn to scale. These are helpful tools in determining the causes of an accident and also help to estimate the trajectories of vehicles and other objects involved. A diagram might include evidence from the site, such as skid marks, debris or blood as well as an estimation of the impact location, the positions of those involved in the accident and their possible trajectories during the crash. Researchers conduct a reconstruction of the accident using the conservation of linear momentum, work-energy methods and kinematics (Depriester et al., 2005). This exercise involves recreating an estimated trajectory for each vehicle in reverse order, beginning with their final positions and then applying a chain of kinematics sequences to determine their possible movements. In order to calculate the parameters, researchers use all of the evidence that has been collected on site. The most probable reconstruction is the one that is in agreement with all the indications that have been used to calculate the parameters. This reconstruction demonstrates the most likely events during the crash.

Such investigations tend to reveal a substantial number of details and facts that are helpful to the auto-industry, traffic officials, insurance companies, and policymakers. Data from these investigations has also been helpful in research on accident prevention. Discoveries of factors that contribute to accidents along with real-world input have been used in driving simulator studies while injury prevention studies have also profited from

data obtained in accident investigations as it allows researchers to study potential injuries in a range of impact scenarios. Lastly, this same data is also beneficial in the development of new products and improved safety systems.

As useful as accident investigations have proven to be, only a minority of countries, concentrated in the wealthiest and most developed, commit to consistently conducting them. Organizations in both the private and public sector take an interest in them. For example, private agencies, like Transport Research Laboratory (TRL) in the United Kingdom, are involved in accident investigations (TRL, 2016) as well as public authorities related to universities such as NCSA (The National Center for Supercomputing Applications, a unit of the University of Illinois at Urbana-Champaign) with their Special Crash Investigations (SCI) Program in the U.S. (NHTSA, 2016). In the European Union, member states have decided to create a large scale accident investigation infrastructure with the capacity to collect accident data from across the EU. The European Commission and an EU research project team have conducted a leading-edge research to harmonize in-depth crash investigation protocols and present a common methodology (for example, in the DaCoTa project (DaCoTA, 2013) and now in the iGLAD consortium (IGLAD, 2015)).

2.1.1. CASR

At the University of Adelaide in Australia, the Center for Automotive Safety Research (formerly the Road Accident Research Unit) has been conducting investigations for various studies since the 1970s. Its program is only intermittently active as it is very expensive to obtain data from a full and accurate representation of crashes. Its research is supported primarily by funds from the South Australian Government Department for Planning, Transport, and Infrastructure, and the statutory compulsory third party accident injury insurer, the Motor Accident Commission.

CASR's data derives from crashes in both rural and urban areas. Over the last 10 years, 548 crashes were investigated, of which 184 took place in rural areas and 364 in metropolitan Adelaide. Figure 2.1 illustrates the distribution of accidents in that region. Criteria for inclusion in investigations were that the crash occurred on a public road and at least one person was transported to a hospital. CASR's on-call team attends crash scenes Monday through Friday during the day and some evenings until mid-night. Team members include engineers, psychologists and health professionals. When notified about an accident, they attempt to reach the scene before the involved vehicles are removed. This is not always possible and sometimes investigations are abandoned altogether if the evidence on-site is not sufficient.

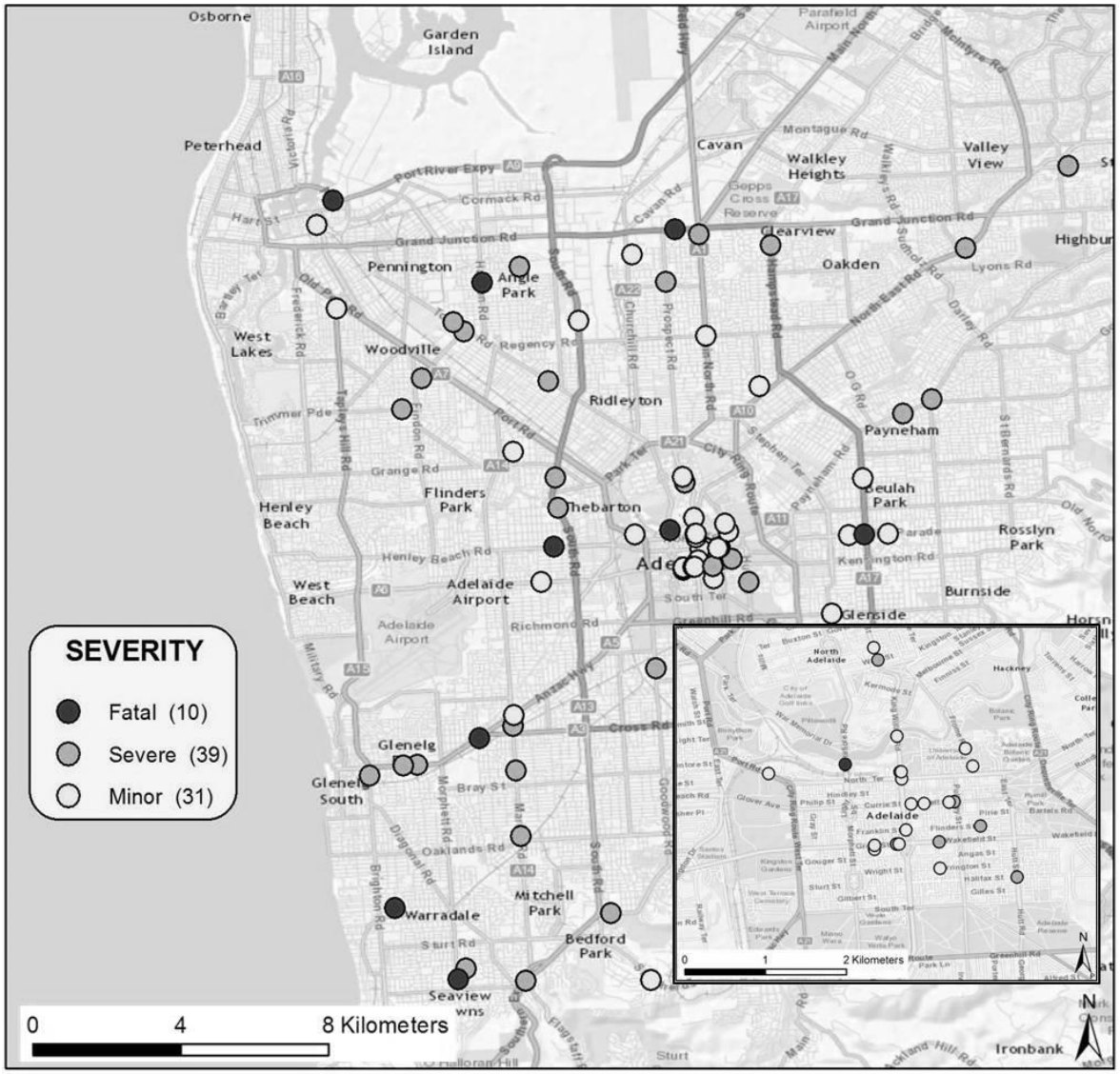

Figure 2.1. Map of pedestrian accidents investigated by CASR (2002-2005)

In terms of investigation methods, CASR teams sometimes use different approaches for dealing with fatal and non-fatal crashes. In the past, the investigation of fatal accidents usually began at the autopsy of the victim. A member of the research team visited the mortuary of the South Australian Coroner. All relevant information was noted at the autopsy, including injuries as well as the victim's height, weight and dimensions. In cases where there are no fatalities, the victims are interviewed in order to gather information about the events surrounding the collision. Interviewers also ask for consent to access medical records in order to obtain more information about the victim's injuries. If the information seems incomplete, the hospital records may sometimes be consulted as well.

In regard to site inspections, the scene of the accident is surveyed and the team records measurements of the lengths of skid-marks while also noting the precise location of the impact point, the final positions of the victims, scuff marks on the road, debris and any other relevant information. Additionally, investigators also inspect the vehicle, looking for signs of contact with the pedestrian. Evidence might include dents, scratches, and

cracks in a windscreen or the presence of hair. These contact locations would be measured and fed into a computer simulation program for verification.

Other important sources of information include police reports, engineering surveys and interviews with witnesses and victims. They each provide material that can supplement evidence investigators find on the scene. Police reports give insight on accidents from the police department's perspective while coroner's files are useful in order to verify consistency with other reports and documents. Engineering surveys, available from road authorities, offer facts and figures about road geometry, vegetation and line-markings. Lastly, interviews play a crucial role in understanding the events surrounding a crash. Physical evidence, in itself, does not explain human behaviour and decision-making in a crash scenario, and so interviews are helpful to understanding cognitive processes. However, the success of the interview depends on the interviewer's capacity to elicit information along with the interviewee's memory and willingness to communicate.

Once all necessary information is collected, CASR's staff conducts a review of each case. They identify factors that contributed to the accidents and injuries. Their method is influenced by ethical considerations with respect to the confidentiality of witnesses and participant statements.

2.1.2. IFSTTAR-LMA

The Laboratory of accident mechanism analysis (“Laboratoire Mécanismes d’Accidents” –LMA–) is a research unit of the French institute of science and technology for transport, development and networks (IFSTTAR). It has been involved in accident investigations since the early 1980s. Over the last 10 years, LMA has analysed around 500 cases. This attempt is supported by sustaining funds from public authorities.

LMA’s investigation teams involve technicians (specialized in infrastructure and vehicles) and psychologists. They usually attend accident scenes during business hours, but every third week they conduct investigations 24 hours a day, allowing them to collect information about evening crashes. Its teams investigate collision scenes in a geographical range that covers 600km² around Salon-de-Provence including the city of Aix-en-Provence (since 2000). This range covers a variety of road infrastructures which include motorways, major and minor roads, a few winding roads and urban areas. Figure 2.2 illustrates the areas covered with mention of accident sites that involved pedestrians.

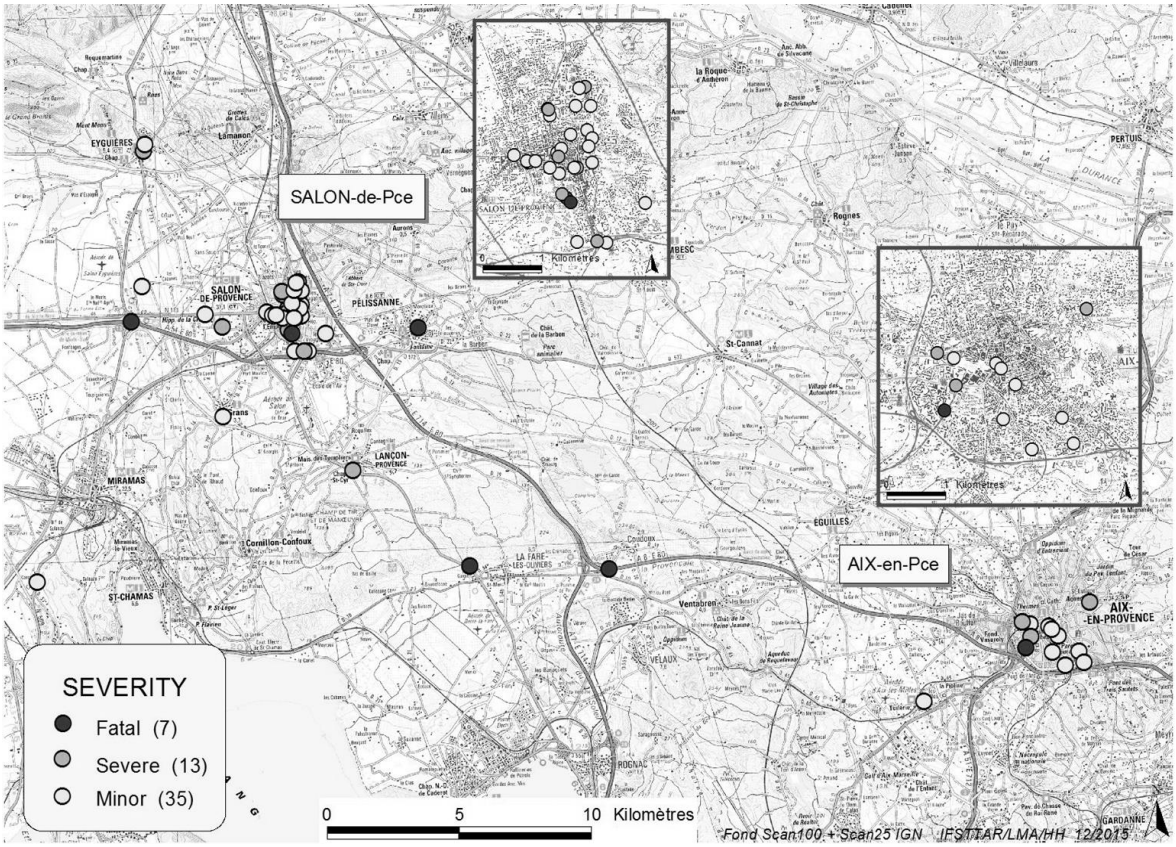

Figure 2.2. Map of accidents investigated by IFSTTAR-LMA (1999-2011)

The goal of LMA's research is to identify the processes behind accidents and the dysfunctions of the driver-vehicle-infrastructure system. Investigation quality is constantly monitored by researchers involved in the laboratory and their approaches derive from multidisciplinary research fields, a point that has encouraged improvement in data collection protocols. Its research strives to respond to current and future needs in the community it serves.

LMA's investigation procedures occur in phases. The first takes place at the scene of the accident. When the team receives notice of a crash, it arrives on the scene as soon as possible, usually within 15 minutes of notification. They receive this alert through a short message system from the central computer of the rescue service. Once on the scene, team members record as much relevant evidence as possible before it vanishes. Such evidence might include locations of any objects involved in the crash, the point of impact, or skid marks. The team also films the crash site and takes measurements that they later use to draw a diagram of the scene which reflects any evidence and its location along with the final positions of vehicles and pedestrians, estimated impact locations, and estimated trajectories during the crash.

Interviews provide another source of data input. Psychologists on the LMA teams conduct and record interviews with both victims and witnesses either at the crash scene or in the hospital emergency room. This task is a delicate one and requires a high degree of skill. The interviewer should make the subject comfortable and allow them to freely recall

the event with little or no interruption. The interviewer might ask a series of questions to begin to help establish the scene of the crash in order to help the subject recall the events. He or she can then proceed to additional information about minute details or clarifications if necessary.

In the second phase of the investigation, all collected data is pooled together in an attempt to reconstruct the accident scenario. The investigators then conduct a second round of data collection guided by assumptions made during the accident reconstruction. Data might include noting the descriptive characteristics of individuals involve, their driving history, or their trajectory that day and their familiarity with that particular route or road passage. Supplemental information about their injuries is acquired from the emergency service at the hospital in Salon-de-Provence.

The final phase of the investigation is the creation of a global synthesis of the accident which tells its entire story, from the beginning of the itinerary of all involved subjects. This includes the sequence of events before the crash took place which is calculated using kinematics methods (Lechner and Ferrandez, 1990) and verified against the collected data. Contributing factors are listed and broken down into interactions between the User, the Vehicle, and the Environment.

2.2.Pedestrian safety

2.2.1. Mechanism of an accident

In-depth investigation studies have shown the complexity, the dynamic character and the significance of the time dimension throughout an accident sequence. Ferrandez et al. (1995) proposed a structure for the accident process by identifying various phases (Figure 2.3).

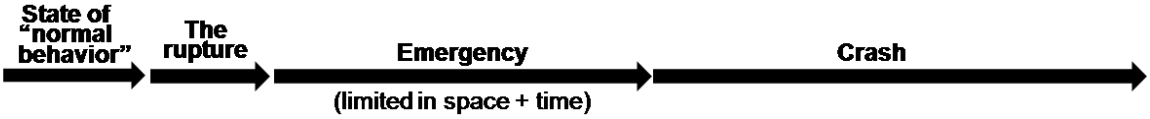

Figure 2.3. Diagram illustrating the sequence of events (timeline) of an accident

The structure shown in Figure 2.3 breaks down an accident's time sequence into four parts based on information from data collected during investigations. The "state of 'normal behavior'" is the User's usual driving situation in which things unfold as expected and nothing out of the ordinary occurs. The driving scenario follows predictable patterns and no unexpected demands are required of the User. There is, then, a balance between demands of driving and the User's response to them.

In an accident scenario, the "state of 'normal behavior'" is broken by an unexpected occurrence that disturbs this balance and threatens the system (e.g. an unexpected subject or object comes into the vehicle's path). In a moment of "rupture" or "conflict", the demands on the User or the system suddenly become excessive to effectively respond. Note that "unexpected" does not necessarily mean "unpredictable", and the factors that make an event "unexpected" must also be considered.

The emergency phase of an accident includes the moment between rupture and impact. During the moment of rupture, a problem presents itself to the driver. During "emergency", the driver has a limited time in which to react or solve the problem. The options available to him or her depend on the environment in terms of potential obstacles or space available to avoid an impact. The vehicle's efficiency in performing the manoeuvre in question depends on several factors, including its state of repair and design as well as the conditions of the road environment.

The crash and its consequences constitute the phase from the impact to the final resting position of the crash involved. Its severity is judged by material and bodily harm. The events during and after a crash phase are determined by what has happened beforehand, during the other phases of the scenario, which can be understood as the interaction between User-Vehicle-Environment.

The description of the initial system status, the identification of the triggering event and the reconstruction of the emergency situation allows to reconstruct the accident scenario and to identify the mechanisms that contribute to the production of this sequence of events preceding the crash.

2.2.2. Prototypical accident scenarios

In road accident research, a prototypical accident scenario is a concept that defines general accident processes covering a set of accidents with overall similarities (chain of facts and causal relationships). These prototypical scenarios serve to generalize, compare and combine information provided by accident case studies including in-depth investigations and police reports. Data from area-specific investigations can be paired with data from other sources or even regions and countries while also offering a means of grouping similarities between different accidents. The analyses that these scenarios ultimately provide are important to the design of new safety systems and are used in computer and driving simulations as well as track testing.

In order to develop prototypical scenarios, researchers establish different categories of accidents and cluster real-world accident cases accordingly to possible prevention measures. There are diverse approaches to determining accident types and how they should be categorized. One methodology entails grouping accidents according guided by specific research needs, such as accidents that have injured child pedestrians (Schofer et al., 1995). Others might choose to emphasize significant events that took place before an accident, highlighting in particular their factual sequences (Ebner et al., 2011; Huang et al., 2008; Matsui et al., 2013). Still another means of categorizing accidents is to consider causal relationships (e.g. parked vehicles hiding pedestrians), or recurring circumstances across cases studied (Brenac et al., 2004; Lenard et al., 2014; Wisch et al., 2013b).

A common technique used to cluster accidents consists of data mining, a technique that can automatically classify accidents. Similarities between accident cases are identified mathematically. The criteria must be coded and weighted in order to permit such a system to easily identify and categorize information. The chosen variables must further be presented in generic form in order to enable the system to perform this task. For example,

Lenard et al. (2011) developed this technique to identify typical pedestrian accident scenarios. The criteria for the cluster analysis were selected for their relevance to physical testing for autonomous emergency braking systems.

Another approach to developing these prototypical scenarios is the Human Functional Failure model (HFF). This model considers people as information processing systems. Fleury and Brenac (2001) developed a method for cluster analysis of accident cases based on the aforementioned model. It consists of gathering accidents based on general similarities in their processes. It requires that each accident case is individually examined while also taking into account criteria such as human failure (e.g. misjudgement, not noticing an oncoming vehicle or pedestrian). Using this model, Brenac et al. (2004) presented a cluster analysis of pedestrian accidents corresponding with prevention possibilities.

2.2.3. Pedestrian kinematics at impact

This section deals with how a pedestrian's body behaves in a collision, from its first impact with a vehicle to its final impact with the ground. The first impact usually occurs with the front of the vehicle, sometimes with either of its corners, thereby pushing pedestrian to the side (projection called fender vault). Instances of partial contact are less common than instances of full contact. The pedestrian kinematics after a full contact with the vehicle front is mainly the “Forward” (34.4%) and “Wrap” (45.2%) projections (Simms et al., 2004). Two other collision types include “Roof vault” and “somersault” (see Figure 2.4).

Many contributing factors lead to the trajectories depicted in Figure 2.4, including speed, the vehicle's front structure and pedestrian height (Daniel, 1982; Liu et al., 2002; Roudsari et al., 2005). If the pedestrian's centre of gravity falls below the edge of the bonnet but above the bumper level, a “Forward” projection would likely occur (see Figure 2.4). This is the case when a passenger vehicle hits a child or when a high-fronted vehicle hits an adult. The pedestrian is pushed horizontally but still maintains foot contact with the ground while the head and shoulders might turn and impact the upper surface of the bonnet edge. In the case of a “Wrap” collision, the pedestrian rotates or wraps over the vehicle's front surface. Unlike a “Forward” collision, these typically involve collisions between adult pedestrians and passenger cars as the centre of gravity is usually higher than the bonnet's leading edge.

Pedestrians often suffer multiple impacts with a vehicle during a collision. The first impact is usually between the car bumper and pedestrian's legs, after which follow impacts between the upper thigh or pelvis and leading edge of the bonnet, which could also strike the abdomen or chest. The pedestrian's head and upper torso might then strike against the top surface of the bonnet or windscreen. The final impact usually occurs 100ms after the initial leg contact. Several researchers have outlined the chronology of such impacts during a pedestrian-vehicle collision (Crandall et al., 2002; Masson et al., 2005). The pedestrian's final impact in a collision is usually with the ground. From the first to final impact, the duration is about one second.

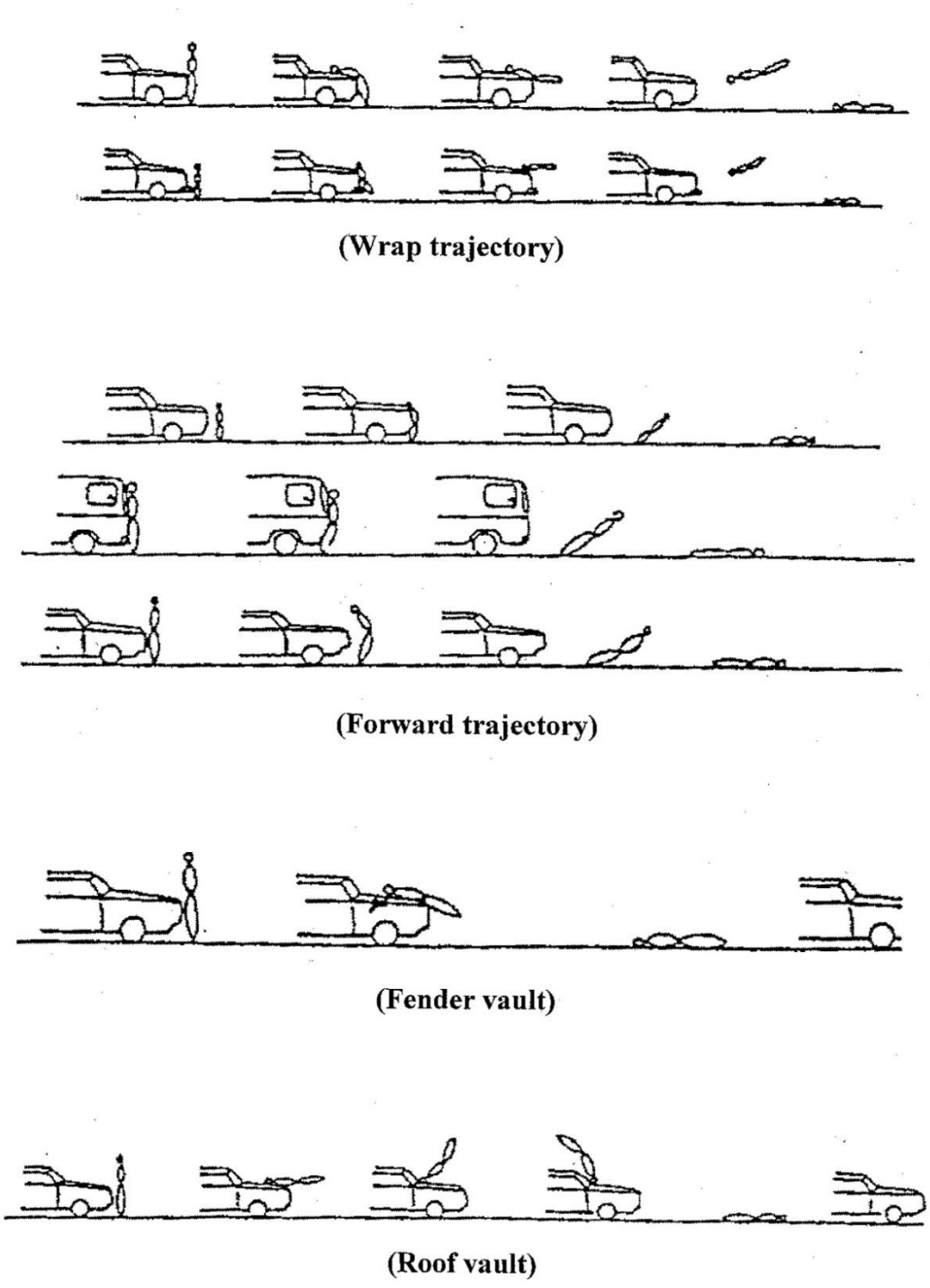

Figure 2.4. Pedestrian kinematics at impact (Eubanks and Haight, 1992)

The speed of the impact plays a key role in determining the projection of the pedestrian and how the body moves during the collision. Different models have been developed to demonstrate the relationship between impact speed and its effect on the pedestrian's body including the thrown distance (or distance of projection). These models are derived from fundamental mechanics equations and 2D kinematics modelling (Han and Brach, 2002; Searle and Searle, 1983; Wood, 1988).

2.2.4. Injury patterns

Pedestrian injuries provide data concerning injury patterns, risk factors and causes. This information is valuable to automotive industry in terms of improving vehicle design and reassessing systems to protect pedestrians. Researchers classify injuries by their severity using AIS[1] (Abbreviated Injury Scale) as a parameter. For purposes of classification, they often choose MAIS (maximum AIS of all injuries sustained by a body) or 'AIS code+' (e.g. AIS3+, all injuries registered starting from serious injuries –coded 3–) as a factor for their reviews.

The International Harmonized Research Activities Pedestrian Safety Working Group (IHRA/PS-WG) gathered data from Japan, Germany, the United States and Australia to analyse pedestrian injuries (Mizuno, 2005). Table 2.1 summarizes their findings, demonstrating that components of vehicles are the biggest contributing factor to pedestrian injuries (see also (Crandall et al., 2002; Otte et al., 2012)). The most frequent locations of injuries include the head and lower extremities, respectively 31.4% and 32.6%. In general, lower extremity injuries (including the hip and upper leg) are caused by impact with the bumper and leading edge of the vehicle. For the head, the source of injury was mainly the windscreen, the A-pillar and also the bonnet (which is commonly the source of head injuries for children).

At higher AIS levels, the injury distribution by body region changes with an increase in torso injuries (Helmer et al., 2010). Hu and Klinich (2012) plotted the distribution of the occurrence of injuries by body segment according to a range of severities (Figure 2.5). Head and torso injuries are more likely to induce casualties consistent with their rate for AIS4+.

Table 2.1.
Sources of IHRA pedestrian AIS 2+ injuries by body region for all ages (Mizuno, 2005)

Injured body region	Vehicle body part involved
Head (71%)	windscreen, A-pillar, bonnet top surface
Pelvis (61%), abdomen (69%), Chest (54%)	bonnet leading edge, bonnet
Lower-extremity (61%)	Bumper

[1] Abbreviated Injury Scale is a standard system to measure the severity of single injuries (AAAM, 2008).

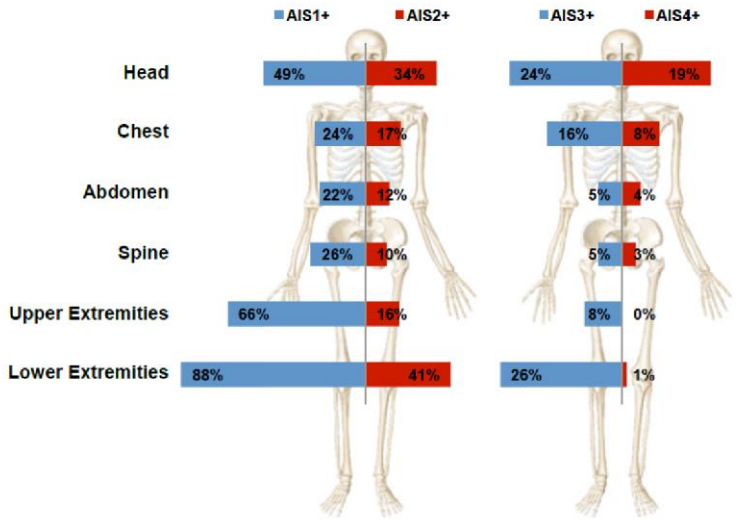

Figure 2.5. Distribution of injuries by body segment according to a range of severities (Helmer et al. 2010, quoted by Hu and Klinich, 2012)

2.2.5. Safety solutions for pedestrian protection

Pedestrian safety can be improved at different stages of the accident process. Figure 2.6 illustrates a diagram of the safety needs for each phase of an accident process involving a vehicle and a pedestrian.

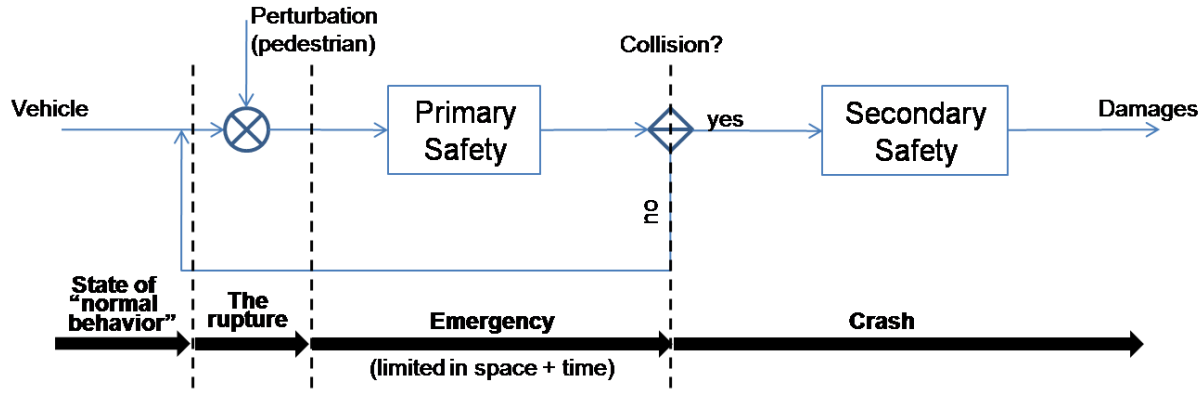

Figure 2.6. Diagram of the safety needs for each phase of an accident

Primary safety consists of systems responding to detection of hazards (pedestrians) and prevents accidents by assisting the driver reaction or triggering autonomous emergency manoeuvres. These systems interfere during the emergency phase of the accidents which is limited in time and space. This stage concerns crash avoidance.

In the case where an accident cannot be avoided, collision mitigation systems are deployed to reduce the impact speed and consequently, the injury outcomes.

At the impact, secondary safety takes over the continuing emergency. It encompasses safety designs added to the front-end structures of vehicles for cushioning the impact energy. In addition to pedestrian friendly design containing energy absorbing materials (Hu and Klinich, 2014), deployable devices are implemented in the vehicle such as active bonnets (pop-up bonnets) and windscreen airbags (Volvocars, 2012).

Beside primary and secondary safety, there is a tertiary safety that has not been presented in the diagram above. It concerns the Automatic Crash Notification (ACN) that alerts emergency services, and provides protection and assistance after an accident (e.g. Toyota-global, 2016). This section gives an overview on pedestrian safety solutions. The two following sections will discuss in detail primary and secondary safety (active safety systems) including the existing assessment.

2.3.Primary or active Safety systems

2.3.1. Architecture of a system

In this section, attention is drawn to vehicle on-board systems based on pedestrian detection and collision prediction. These active safety systems interfere with the road environment and potentially prevent from hazards or reduce the severity of crashes. The forward path of the vehicle is analysed using image processing algorithms in real time in order to try to identify a pedestrian on the road. This image processing analysis is a logical chain of algorithms that starts from the pedestrian detection, and then tracks his motion till comes with a prediction of collision occurrence. As a countermeasure to avoid or mitigate an imminent crash, these systems deploy autonomous emergency manoeuvre or reinforce avoidance actions initiated by the driver. According to its functioning, primary safety systems are comprised of the three following modules: sensors for detection, a unit for processing and actuators for triggering an emergency manoeuvre (see Figure 2.7).

Figure 2.7. Components of a Pedestrian-CAM system (Eckert et al., 2013)

2.3.1.1. **Sensors**

Sensors are technologies for environmental perception. They are mounted into vehicles in order to monitor the forward path over time. They cover an operational area where obstacles like pedestrians can be detected. This area of coverage is defined by a field of view (or angle of sight) and a range. The capability of providing accurate measurements depends on the resolution of these technologies. The robustness of measurements is also consistent with the measurement rate (update rate or frame rate).

There are different types of sensors configuring an active safety system. Gandhi and Trivedi (2007) classified these sensors in two categories: "time-of-flight" sensors (RADAR, LIDAR) and imaging sensors operating in visible light or Near, Mid and Far Infrared radiation (NIR, MIR, FAR). Each of these detection sensors has their strengths and weaknesses.

The "time-of-flight" sensors are designed to provide accurate information about the distance from the obstacle. This distance is measured based on the phase shift (Doppler frequency shift) analysis between the emitted and received signal after being reflected back by the surrounding background.

There are two kinds of "time-of-flight" sensors:
- Radars operating with radio waves;
- LIDARs which are laser scanner devices (scanning horizontally the forward scene at different azimuth angle).

The advantage of "time-of-flight" sensors is the ability of operating in day/night conditions with a considerable measurement rate (in general, about 50 Hz). Besides, radars are more likely to detect obstacles in any weather condition (heavy rain, snow, fog). However, "time-of-flight" sensors have a limited resolution and are not able to give information pavement markings and curbs (Gandhi and Trivedi, 2007). This lack of information can lead to a wrong system response. A pedestrian standing in front of the vehicle may be detected as a hazard while he/she is located on the curb (Broggi et al., 2009).

Concerning imaging sensors, they are composed of electric light devices like APS (Active-Pixel Sensors also known as CMOS sensors) capable of capturing a forward scene with a high-resolution. However, the captured scene is limited to a 2-D map and information about the forward distance of the targets (or obstacles) is lost. To recover the depth sensing, there are the stereo vision cameras (made from two or more overlapping lenses) which can locate in 3-D the obstacles by analysing the disparity between the images captured by the different lenses (Figure 2.8). With this technology, it is less complicated to separate the obstacles from background comparing to mono vision cameras (Gandhi and Trivedi, 2007).

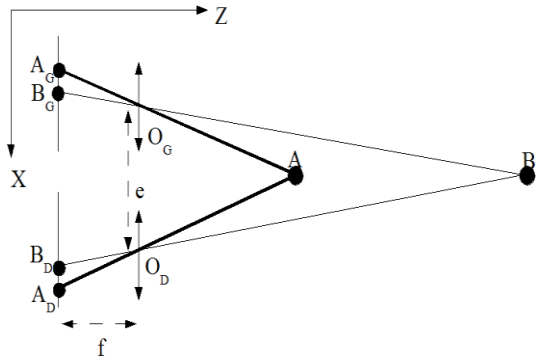

Figure 2.8. A stereo sensor configuration (Suard, 2006)

Image sensors are able to detect pedestrians during the day as well as in nighttime depending on the technology used:

- visible light based sensors sensitive to ambient light;
- infrared sensors which measure the intensity of infrared energy radiated from the surrounding background. It produces images with various brightness intensities.

In a study of Fang et al. (2003), these two technologies were compared by addressing their strengths and weaknesses. It was state that temperature homogeneity among people (and also for a whole body) was an advantage in the pedestrian detection process. The pedestrian radiate more hit than the static background (road, pavement, etc). Therefore, in infrared images, pedestrians are easily remarkable represented with different non-uniform brightness like the body trunk region that is darker than the head regions (due to the clothes and their transmissivity). The detection of pedestrians is then guided by the small region of interest where there is remarkable intensity. In contrary, it was reported that the images from visible light based sensors are more complex to process since their intensity varies significantly considering the multitude of appearance of pedestrians according to their clothes. However, visible light based sensors provide images with a high resolution and the contrast between the foreground and background is clear, while the infrared images have a poor resolution and are blurrier especially in hot daytime.

Near infrared sensors (NIR) are designed to take advantages of visible light based sensors with the ability of detecting in nighttime. These sensors are accompanied with illuminators. Besides the appearance of pedestrian and its recognition in the images, NIR sensors provide other information such as the lane markings, the pavement, etc. Luo et al. (2010) demonstrated that NIR sensors are not affected by dazzling lights as IR sensors (Figure 2.9), yet their images have a high visual clutter inducing a longer time to process images.

Figure 2.9. Same scene captured using an FIR-NVS (Left) and an NIR-NVS (Right) (Luo et al., 2010)

A pedestrian detection system can use a combination of multiple sensors in order to overcome the limited performance of each sensor. For example, Mercedes-Benz has introduced in the 2013 MY S-Class a Ped-CAM system called Pre-Safe Brake® with Pedestrian Detection using a wide range of sensors: Short, Mid and Long Range Radar (S/M/LRR), Near and Far Infrared camera and a stereo vision. The use of multiple sensors is likely to imply more robust pedestrian detection. Besides the high-value of information collected from the different sensors, data redundancy may prevent the system from false detection (Michalke et al., 2011).

2.3.1.2. **Processing unit**

The processing could be presented as a funnel with different levels of sieves filtering the information (Figure 2.10). It starts from the detection of obstacles towards a classification for distinguishing pedestrians, then "tracking" to get trajectories, until "the prediction" of crash and "the decision" of the countermeasure. At the beginning, data from the front-path of the vehicle are recorded by detection sensors.

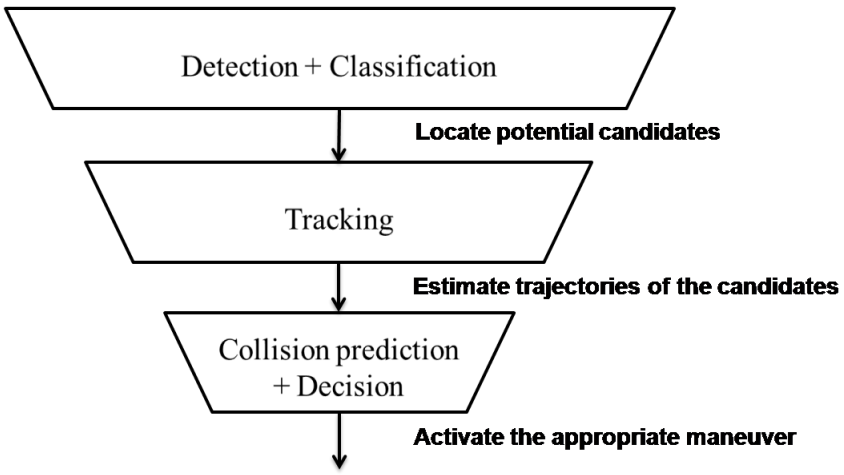

Figure 2.10. Data flow diagram of a pedestrian detection system

Pedestrian detection process starts with a first phase of segmentation consisting in extracting obstacles from the background. The selected obstacles are then classified into pedestrians or non-pedestrians candidates. Several methods were developed to accomplish this function. A state of the art of these methods were presented through surveys (Gandhi and Trivedi, 2007; Geronimo et al., 2010).

Multiple sensor systems may raise an issue of managing data acquisition process. In these systems, each sensor is working independently and in an asynchronous way. To merge the collected data, there are two types of configurations: sequential or parallel (Gandhi and Trivedi, 2007). These two configurations can be also combined in a multi-level fusion system (Tons et al., 2004).

Potential hazards are tracked analysing frame-by-frame. This technique differs from a system to another with possibilities of combining this step with the classification or detection phase (Keller et al., 2011a).

The last and main task in the process unit is the collision prediction and decision-making. Collision avoidance is the primary objective of the system. Data are generated in real time by the system and compared to threshold to predict an imminent accident. A widely used measure is the time-to-collision (TTC). It was firstly defined by Hayward (1972, quoted by Horst and Hogema, 1993) as: "The time required for two vehicles to collide if they continue at their present speed and on the same path". Then, it was introduced as a cue for decision-making in safety manoeuvres in the early 90's (Horst and Hogema, 1993). Since then, different alternatives in decision-making algorithms were developed (Brannstrom et al., 2010; Ferguson et al., 2008; Kaempchen et al., 2009; Tamke et al., 2011). These algorithms are based on what is called time-to-react (TTR). It corresponds to the last moment to engage an emergency manoeuvre to avert an accident. Tamke et al. (2011) categorized the TTR regarding the specific manoeuvre:

- time-to-brake (TTB);
- time-to-steer (TTS);
- time-to-kickdown (TTK).

These measures are computed using specific manoeuvre models including the vehicle dynamics (Hayashi et al., 2012; Keller et al., 2011a).

Decision-making algorithms incorporate also driver's behaviour through feedback of the vehicle control (Keller et al., 2011a). Hence, the Ped-CAM system may support the driver in evasive driving manoeuvres or trigger an autonomous action.

2.3.1.3. **Actuators**

After receiving command signals from the processing unit, the appropriate system component is triggered. Different actuators intervene at different times preceding the crash depending on the decision-making algorithms. Usually, it starts with alarm signals (visual and/or sound signals) which are emitted to warn the driver. Then, an autonomous

emergency manoeuvre is executed unless the driver reacts to the warning by initiating a manoeuvre reinforced by the safety system.

For autonomous control manoeuvres, there are two devoted systems: Autonomous Emergency Braking (AEB) and Autonomous Emergency Steering (AES). Depending on the emergency situation, these two systems can be both activated or solely one of them (Hayashi et al., 2012).

The performance of these autonomous systems is directly related to their intrinsic characteristics: the system lag, the build-up time and the limit.

For current AEB systems, the maximum brake jerk is limited to 20 m/s^3 (Eckert et al., 2013; Rodarius et al., 2012). There are already systems been designed and tested with a better brake force gradient of 66m/s^3 (Broggi et al., 2009). However, there is a concern about the impact of these high gradients on the safety of the vehicle occupants. Observations have been conducted on the kinematic of the vehicle occupants while emergency manoeuvres (Huber et al., 2014; Kirschbichler et al., 2014). Future AEB systems will eventually improve building rate.

For the deceleration amplitude, it can actually reach a maximum value of 10 m/s^2. Through a brake test realized by the engineers of CASR (Centre for Automotive Safety Research), it was observed that, for a vehicle equipped with an AEB system, the recorded deceleration profile had peaks at 10 m/s^2. Yet, this value of deceleration is limited by the dynamic properties of the tire.

Concerning AES systems, the steering wheel angle rate is limited to 400°/s (Brannstrom et al., 2010; Seiniger et al., 2013). This parameter determines the severity of the manoeuvre and should be acceptable for the driver. The steering ratio relating the steering wheel angle to the steering angle is constant (N=16.25) in most of the vehicles. There is also steering systems that have a speed-dependent steering ratio (Brannstrom et al., 2010).

Severe steering manoeuvres are also associated to the lateral acceleration. AES systems are commonly limited to a maximal lateral acceleration of 5m/s^2 (Isermann et al., 2008; Keller et al., 2011a). But, the steering manoeuvre can reach higher lateral acceleration up to 7m/s^2 (Brannstrom et al., 2010).

Another factor constraining the steering manoeuvre is the available clearance enabling a safe evasive action. This factor might need the use of additional sensors. Consequently, emergency steering is a complicated manoeuvre even though it occurs at low speed.

2.3.2. Assessment of primary safety systems

Primary safety systems act within a complex and dynamic traffic environment. These systems are expected to reduce the pedestrian deaths and injuries. These systems need to be evaluated in terms of detection and safety assessment performance.

2.3.2.1. **Detection performance**

The responses of a detection system can be presented in the form of four possibilities as described in the ASPECSS project (Seiniger et al., 2014):

- True positives (TP) which correspond to correct detection of pedestrians at risk;
- True negatives (TN) which are the correct non-detection cases where pedestrians were not at risk;
- False negatives (FN) are the non-detection cases of pedestrians at risk;
- False positives (FP) are the detection of pedestrians who were not at risk.

The two first responses (TP and TN) are intended to be achieved by the detection system. However, the two last responses (FN and FP) are adverse effects that represent system failures.

Detection performance is addressed by examining two criteria: the sensitivity and the precision (Keller et al., 2011a). Sensitivity corresponds to the rate of true detection of a system (i.e. the rate of pedestrian detection to the number of pedestrians at risk). Precision concerns the rate of correct detection of the system (i.e. the rate of true pedestrian detection to the number of false detection).

Detection performance can be presented in the form of curves named received operating curves (ROCs). These curves represent the distribution of detection rate according to false detections. In Figure 2.11 the different reaction patterns of a sensor response are represented.

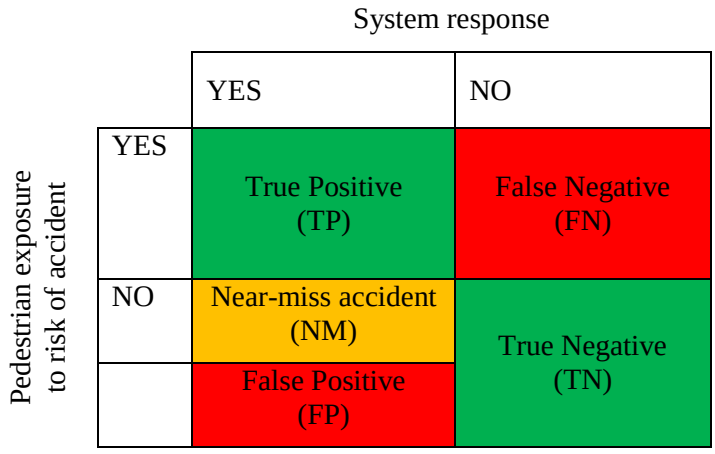

Figure 2.11. Patterns of a sensor response (Seiniger et al., 2014)

2.3.2.2. **Overall performance**

Before being introduced to the market, new on-board technologies (Ped-CAMS) are validated attested by large-scale testing procedures named Field Operational Tests (FOTs). These tests provide feedback on the efficiency of these systems and also an assessment of driver acceptance (FOT-Net, 2014).
FOTs are generally realized on closed test tracks with a limited number of test drivers (FOT-Net, 2014).

In Europe, several research projects under collaboration of private and public stakeholders developed objective tests to assess the overall performance of AEB systems (Ped-CAMSs triggering only emergency braking manoeuvres). Theses research project were devoted to draw proposals on their assessment methods for Euro NCAP test protocol (AEB Group, vFFS, ASPECSS project). These projects started first by analysing pedestrian accidents to identify reference scenarios that comply with the system functioning (i.e. system intended to operate in the event of frontal collisions).

Advanced Emergency Brake Group (AEB Group) established three scenarios from a cluster analysis of two databases of accidents in Great Britain. These scenarios take into account the trajectory of the vehicle (straightforward or turning) and its average speed, the trajectory of the pedestrian (crossing, walking along with traffic or stationary in the road) and its pace (walking or running) and the light conditions (daylight or night-time) (Lenard et al., 2011).

Advanced Forward-Looking Safety Systems (vFSS) identified six reference scenarios from different accident databases in Germany. For test purposes, only four scenarios were kept removing scenarios with turning (because these scenarios were considered similar to those with pedestrian masked by an obstacle while a vehicle travelling straightforward). The four tests scenarios developed were varying some parameters such as pedestrian speed but not the vehicle speed (Niewöhner et al., 2011).

ASPECSS project has identified preliminary seven generic test scenarios based on previous research and derived from the analysis of several crash databases (from Germany, Great Britain and France). Five test scenarios were finally selected and developed for a range of vehicle speeds (Table 2.2).

Table 2.2.
ASPECSS test scenario Protocol (Lubbe and Kullgren, 2015)

	Walking adult	Running adult	Walking adult	Walking adult	Walking child obstructed
Scenario number	**1**	**2**	**3**	**4**	**5**
Weight	**12.5%**	**3.4%**	**9.8%**	**4.9%**	**0.9%**
Pedestrian speed	**3 km/h**	**8 km/h**	**5 km/h**	**5 km/h**	**5 km/h**
Dummy type	**Adult**	**Adult**	**Adult**	**Adult**	**Child**
Dummy initial position	**Far side**	**Far side**	**Near side**	**Near side**	**Near side**
Vehicle test speeds	**20-60 km/h**	**20-60 km/h**	**10-50 km/h**	**10-50 km/h**	**20-60 km/h**
Obstruction	**No**	**No**	**No**	**No**	**Yes**
Impact point	**50% (Centre)**	**50% (Centre)**	**25% (Near side)**	**75% (Far side)**	**50% (Centre)**

In line with Euro NCAP test protocol established for vehicle-vehicle AEB systems (Schram et al., 2013), ASPECSS project proposed an assessment methodology generating a score. This score is a unified result of a test suite taking into account factors weighting not only scenarios but also individual test speeds within scenarios (Figure 2.12).

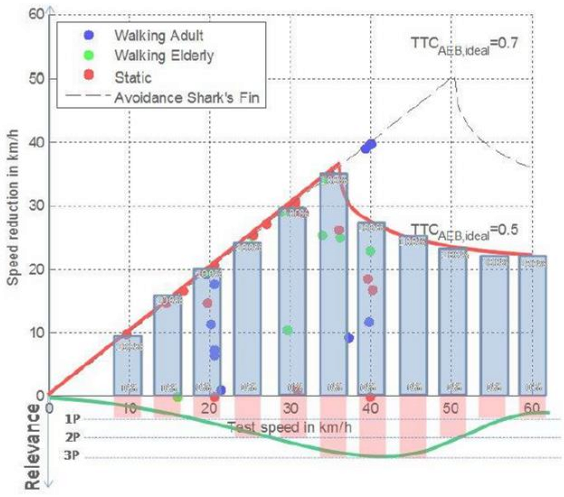

Figure 2.12. Scoring method assessing Ped-AEB system established in the ASPECSS project (Seiniger et al., 2014)

2.4.Passive safety

2.4.1. Understanding injury mechanisms

In pedestrian accidents, the most injured body segments are the head and lower extremities. Injuries to these regions are generally caused by the vehicle (Crandall et al., 2002; Otte et al., 2012).

Head injuries to pedestrians mainly result from an impact with the hood or windscreen (Fredriksson et al., 2010; McLean et al., 1996; Roudsari et al., 2005). The impact location of the head depends mainly on the size of the pedestrian, the front shape of the vehicle and its speed (Okamoto et al., 2003). A relationship between the size of the pedestrian and the Wrap Around Distance (WAD - corresponds to the distance between the head impact and the floor along the front end of the car) have been established (Mizuno, 1998).

Head injury mechanisms for pedestrians are different from vehicle occupants since the impact conditions are not similar (Yang, 2003). There is a direct loading of vehicle structures coupled with a rotational acceleration of the pedestrian head induced by the impact kinematics (Yao et al., 2008). Moreover, the impacts are generally located on the posterior or lateral area of the head for pedestrians (McLean et al., 1996).

Head impact kinematics is characterized by two main parameters (Mizuno and Kajzer, 2000): the head impact velocity and the head angle. For head injury risk assessment, the Head Injury Criterion (HIC) is used.

Pedestrian lower-extremity injuries results from direct contact with the bumper. Cadaver tests have highlighted two injury patterns to the lower extremity: bone fractures and knee injuries (Arnoux et al., 2005; Kajzer et al., 1999). Bone fractures are related to direct loading and knee injuries are a direct consequence of the bending and shearing (Cesari et al., 2007). The lower-extremity injuries of the knee are more related to the loading distribution and location on the bumper (Arnoux et al., 2005; Masson and Brunet, 2006). In fact, if the bumper hits the tibia directly, it results bone fractures, while an impact at a knee level causes a combination of shear displacements and bending which can injure knee ligaments.

Several studies have shown that as a threshold of injury risk, the knee rotation should be less than 20° while the knee shear displacements should be less than 15 mm and the tibia acceleration should be less than 150 g (Cesari et al., 2007).

2.4.2. Enhancing passive safety

Pedestrian injury mitigation can be realised by reducing the impact speed as a first step and absorbing the impact energy with deformable contact structures on the vehicle (Crandall et al., 2002; Hu and Klinich, 2014).

Pedestrian injury risk is related to the vehicle front shape. For example, the load sustained by the head depends on the impact angle on the vehicle structure (windscreen, bonnet…). Indeed, more severe injuries are observed if the head struck perpendicularly the vehicle structure as it is the case with flat front shapes (Tanno et al., 2000). It is then possible to design the vehicle front shape in order to avoid a direct impact with stiff vehicle structures and to promote a sliding motion of the pedestrian head (Masson et al., 2007; Serre et al., 2007).

To enhance pedestrian safety, the focus for many studies was designing pedestrian-friendly vehicle by improving the front-end geometry of the vehicle and reducing the stiffness of its structures that can be in contact with the pedestrian body at impact. Further passive safety systems have been introduced in the market. These systems are also known as crash-active protection systems since they are triggered by contact-sensors located in the bumper. These sensors can differentiate impacts with pedestrians from other objects (Evrard, 2011). These systems offer deployable safety features such as pop-up bonnets and windscreen airbags.

Pop-up bonnets are deployable structures that, once actuated, lift the bonnet to provide additional clearance over rigid components. Deflection of the bonnet is then used for a better absorption of the impact energy. Many car manufacturers (e.g. 2006 MY Citroen C6, Mercedes-Benz E-Class 2009) have developed vehicles with pop-up bonnets.

Windscreen airbags are crash-active protection systems. They are deployed in a U-shape at the bottom of the windscreen to protect the pedestrian's head from hitting rigid structures like the A-pillar. The shape of the airbag was designed to minimize the obstruction of the driver's view. These pedestrian airbags has been lately introduced in

the Volvo V40. More sophisticated airbags are being under development to reduce head injuries even at high impact speeds (Fredriksson and Rosén, 2014).

2.4.3. Assessment of passive safety systems

Organizations including the European Enhanced Vehicle Safety Committee (EEVC), the International Organization for Standardization (ISO), the International Harmonized Research Activities (IHRA), and the New Car Assessment Programme (NCAP) have developed test programs to assess pedestrian secondary safety (i.e. evaluate the protection at impact). All these programs are based on component tests (or sub-system tests). These tests reproduce separately impacts of different body regions including:
- Lower legform modelling the impact of lower extremity with the bumper;
- Upper legform for impact of pelvis with the bonnet leading edge;
- Headform to represent the impact of the head with the bonnet or windscreen.

These components are designed based on pedestrian injury data (EEVC, 1998).

As an example, Figure 2.13 shows the differences between experimental protocols of the EuroNCAP and the European Directive 2003/102/EC phase 2.

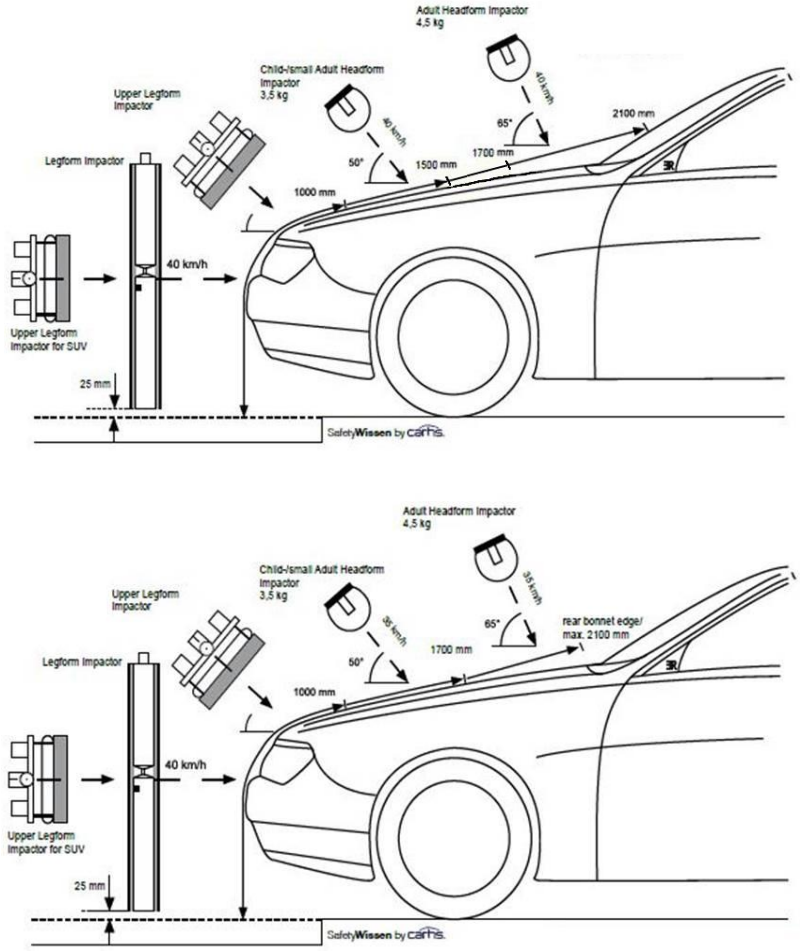

Figure 2.13. Pedestrian protection test procedures according to Euro NCAP (top) and to European directive (bottom) (Carhs, 2012)

The objective of component tests concerns the modelling of an impact between a pedestrian and a vehicle structure in order to estimate the injury risk. Compared to full-scale dummy tests, component tests are repeatable especially for the head impact (Fredriksson, 2011).

According to EEVC, the HIC calculated from head sub-system tests should not exceed 1000. Over this value, head impacts are considered severe (Anderson et al., 2003). According to EuroNCAP, this HIC value has been considered as a lower limit while the upper limit is 1350.

2.5. Integrated Safety

Integrated safety assessment combines the evaluation of active and passive safety to measure the overall pedestrian protection. The performance of passive safety is in fact dependent on the consequences of active safety deployment. There is not yet standard assessment. But, several methods have been developed using numerical approach (Kompass, 2012) or experimental testing (Hamacher et al., 2013) or a combination of these two last aforementioned approaches (Kuehn et al., 2005).

The effectiveness of combined active and passive safety was firstly measured through risk reduction at a level of injury severity (Fredriksson and Rosén, 2012). This study analyse the combined effect of an AEB and secondary safety system (active bonnet and pedestrian airbag) on AIS3+ injuries. Further method based on HARM metric was used to estimate the benefit through analysing the cost value calculated on all injuries (Edwards et al., 2015). This last method integrates passive safety tests (Euro NCAP protocol test using impactors) with active safety assessment.

2.6. Synthesis

Pedestrian safety can be decomposed into two main approaches: primary safety which aims to trigger an active system before the impact in order to avoid the crash, and secondary safety which aims to protect the pedestrian during the crash in order to mitigate injuries. This thesis will focus on primary safety. The systems to be considered are on-board active safety systems that have been developed to detect pedestrians at risk of coming into a collision with the vehicle. These systems have specific characteristics especially in terms of detection algorithm, identification of pedestrian, decision making, triggering emergency manoeuvers and efficiency which will affect their performance in actual crashes.

It appears important to examine these systems to evaluate the potential of such systems to respond to real conditions, and the factors that are likely to place limits on the ability of such systems to respond.

Current methods for pedestrian active safety assessments are conducted as track testing. These methods measure the effectiveness of systems to reduce impact speed in pre-defined collision scenarios (Ebner et al., 2011; Lenard et al., 2011; Niewöhner et al., 2011; Wisch et al., 2013a). In consumer or regulatory tests, a scoring system was established according to a desired profile of speed reduction (Euro NCAP, 2015). The main problem of this assessment is that it is limited to certain number of configurations (see Table 2.2).

A substitutive method of track testing is to assess systems based on a simulation approach. The advantage of this method is its modularity since it is faster and cheaper to add scenario tests compared to the first described method. Two different approaches have been introduced in the assessment of systems through simulation. The first approach is based on accident reconstruction which consists of drawing the kinematics of both vehicle and pedestrian (Lindman et al., 2010; Rosén et al., 2010). The second approach is a stochastic method (Monte Carlo method) creating traffic simulation from accident data (Helmer, 2015).

For the simulation approach, the key issues are to replicate real accident scenarios. Two crash databases with potential use in respect of examining real accident scenarios were presented in this chapter: the CASR and the IFSTTAR/LMA in-depth crash databases. The use of these in-depth crash databases, including a considerable number of details, is an alternative to achieve robust reconstructions of accidents. Indeed, it is considered that the accident reconstruction is robust when it is in agreement with all the real data collected on scene.

Chapter 3

Method testing the response of Ped-CAMS

The aim of the research in this chapter is to develop a method to examine the response of Pedestrian Collision Avoidance and Mitigation Systems (Ped-CAMS) on preventing crashes involving pedestrians.
The methodology is based on computer simulation. The procedure is to confront the safety systems with real-world accident configurations involving pedestrians. The intent is to replicate real-world pre-crash events, and see whether the technology helps to avoid or mitigate these crashes. The accidents are drawn from in-depth crash databases since there is a need to have relevant data in order to have a robust reconstruction and simulation of the crash scenarios.

3.1. General presentation of the methodology

The response of defined Ped-CAMS will be tested numerically in real accident configurations drawn from in-depth crash databases.

As an initial step, it is necessary to select crash cases and reconstruct them numerically in order to obtain a "virtual crash population". The method consists then of modelling different components of each crash: crash environment, driver, vehicle and pedestrian. Each component is modelled regarding the data provided from in-depth crash investigation database. The objective is to reproduce the crash sequences displaying the interaction between the four components.

The next step aims to take into account in the simulation the functioning of a Ped-CAM system. It consists of coupling the safety systems with the vehicle pre-crash kinematics. It is then necessary to model these systems in order to implement them in the crash

simulation process. A preliminary survey on these systems and their characteristics was conducted (see Chapter 2, Section 2.3) in order to understand their functioning.

Running the simulations with these systems provides data for estimating their potential response at specific events (detection of the pedestrian, triggering an emergency manoeuvre). However, the simulation outcomes cannot be used directly to estimate what difference the technology would make to the real world crash population.

The methodology described above was realized using a program coded in MATLAB® (Matlab, 2008). The software consists of three major modules: the pre-processor, the runtime system and post-processor module. The pre-processor module encompasses steps required to compute the input data for the simulation of the effect of the Ped-CAMS. The post-processor module takes the output data from the simulations to present statistical data about the response of the Ped-CAMS. Figure 3.1 shows a simplified representation of the building blocks (modules and sub-modules) of the software.

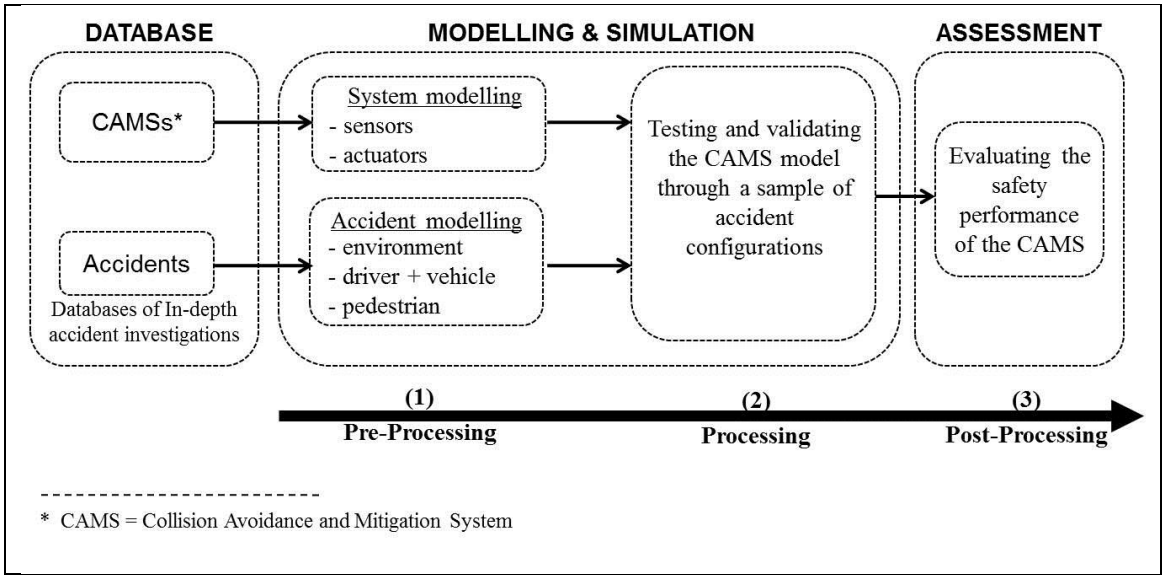

Figure 3.1. The method Framework

3.2. Accident modelling

To enable a reconstruction of an accident, four components of the crash were considered: the environment, the vehicle, the driver and the pedestrian.

Regarding the complexity of an accident, its analysis was structured by identifying various phases in its process as defined by Ferrandez et al. (1995):

- The "normal" situation: which describes the movements of the units involved in the accident (the vehicle and pedestrian) leading to the accident site, their status and behaviour;
- The "rupture" phase is induced by an unexpected event shifting towards a critical situation;

- The emergency situation that is limited in time and space to allow possible manoeuvres to prevent collision;
- The collision which includes the impact and its consequences.

The description of the initial and boundary conditions of the system comprising user (driver and pedestrian), vehicle and environment, and the identification of the detection of an imminent collision, allow the reconstruction of the pre-crash and crash phases of the scenario. This analysis leads to an identification of the mechanisms contributing to the sequence of events preceding the collision.

3.2.1. Modelling the crash environment

Modelling the crash environment consists of loading the site diagram of an accident (a 2D jpeg image). This site diagram is used as a background for the crash simulation. This site diagram is drawn to scale by engineers to record road geometry, the location of roadside objects and any other relevant information such as line marking. It also includes relevant information like the marks observed on the scene (skid, debris, blood, etc.), the estimated impact location, the final position and the trajectories of the different subjects involved in the crash.

The site diagram of the accident is also used to extract relevant information. The scale of the diagram expressed in pixels/meter is extracted and saved as a variable. This variable allows getting from the diagram any data with the appropriate dimensions identical to their counterparts in the real world. For example, the width of the road where the accident occurred is extracted from the site diagram.

Other parameters related to the road are saved as variables for the simulation. Some of these variables are directly extracted from the site diagram (the offset or distance between the impact location and the road boundaries) and others are extracted from the corresponding in-depth accident database (the slope of the road, the coefficient of tyre/road friction).

Road environment factors that may have influenced the driver's perception of the pedestrian are considered as variables as well. These factors are on one hand the light and weather conditions and on the other hand obstacles. The light and weather conditions are likely to limit the efficiency of on-board imaging sensor systems. It is used qualitatively in the simulation process based on a general estimation of the relevance of these light and weather conditions (darkness, heavy rain…). Obstacles are included when they obstructed the line of sight between the driver and the pedestrian prior to a collision. They are taken into account in the modelling process of the crash environment. Three coordinates are sufficient to define an obstacle on the scaled accident diagram. The influence of obstacles can be included as they are related to the trajectories of the vehicle and the pedestrian.

3.2.2. Modelling the kinematics of the vehicle

Retracing the trajectory of the vehicle is achieved by applying a chain of three kinematics sequences: a normal driving sequence, a brake sequence if the driver reacts, and a crash sequence. The reconstruction method consists of going back in time; i.e. considering first the crash, then the brake and finally the normal driving sequences.

For each sequence, the kinematics parameters are determined by taking into account all signs or indications collected on the scene of the accident: skid marks on the road, the throw distance of the pedestrian, the vehicle speed stated by the witnesses and/or the involved persons, the location and damages on the vehicle, etc.

Crash reconstruction methods use principles related to the conservation of linear and angular momentum, work-energy methods and general kinematics (Depriester et al., 2005). These methods are used to estimate the impact speed of the vehicle.

The travelling speed of the vehicle is related to the estimated impact speed and have to take into account the driver behaviour (or reaction) prior to the impact.

For cases with no reaction from the driver, the vehicle speed is assumed to be constant, equal to the estimated impact speed as described by Equation 3.2 (noted [E3.2]) in Figure 2.2. If skid marks were observed on the site diagram of the accident, it is assumed that the driver reacts with a full brake. The vehicle kinematics goes through different phases: a first phase presumed to have a constant speed, a second phase which is a transition to the third phase which is a uniform deceleration before collision (Figure 3.2). Each phase is represented by the appropriate equation of motion (Equations E3.1-E3.9). The parameters of these equations are retrieved from the estimated impact speed of the vehicle, the length of any skid marks, the time for the braking system to lock the wheels and time interval of the simulation. The time to lock the wheels is the time elapsed for the vehicle to travel from the application of the brakes to the wheels locking and producing visible skid marks. This time interval depends on the braking system of the vehicle: for Brake Assist Systems or equivalent, this time characteristic is assumed to be 0.35 seconds, and for normal brakes, it is 0.5 seconds as defined by Reed and Keskin (1989). During this time interval, it is assumed (based on experiments detailed in Reed and Keskin (1989)) that there is a loss of kinetic energy of 20%. If the driver has declared braking before impact but no skid marks were observed, the accident case was not considered.

In the subject collision reconstructions, the impact location is first picked from the site diagram as a reference point. Using this pre-defined reference point, it enables locating and drawing the vehicle on the scaled accident diagram at the impact. An estimate of the vehicle trajectory is extracted from the scaled accident diagram and converted from pixel coordinates (2D) to curvilinear distances or travel distances in meters (1D).

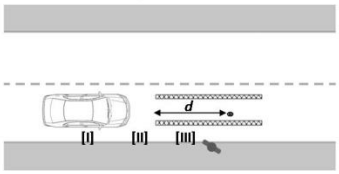

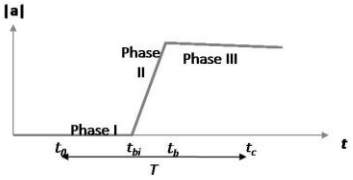

Phase [I] : Normal driving phase ($t \le t_{bi}$)

$$S(t) = v_I.t + s_I \quad [E3.1]$$

$$V(t) = V(t = t_{bi}) \quad [E3.2]$$

$$a(t) = 0 \quad [E3.3]$$

- $t = t_0 = 0$

$$\begin{cases} V(t_0) = V(t = t_{bi}) \\ S(t_0) = 0 \end{cases}$$

Phase [II] : Brake initiation phase ($t_{bi} \le t \le t_b$)

$$S(t) = \frac{1}{6}\gamma_{II}.t^3 + \frac{1}{2}a_{II}.t^2 + v_{II}.t + s_{II} \quad [E3.4]$$

$$V(t) = \frac{1}{2}\gamma_{II}.t^2 + a_{II}.t + v_{II} \quad [E3.5]$$

$$a(t) = \gamma_{II}.t + a_{II} \quad [E3.6]$$

- $t = t_b$

$$t_b = T - \frac{-V_{impact} + \sqrt{V_{impact}^2 + 2\mu.g.d}}{\mu g}$$

$$\begin{cases} V(t = t_b) = \sqrt{V_{impact}^2 + 2\mu.g.d} \\ a(t = t_b) = \mu.g \end{cases}$$

- $t = t_{bi} = T - t_b - 0.5$

$$\begin{cases} V(t = t_{bi}) = \dfrac{V(t = t_b)}{\sqrt{1 - L}} \\ a(t = t_{bi}) = 0 \end{cases}$$

Phase [III] : Full brake phase ($t_b \le t \le t_c$)

$$S(t) = \frac{1}{2}a_{III}.t^2 + v_{III}.t + s_{III} \quad [E3.7]$$

$$V(t) = a_{III}.t + v_{III} \quad [E3.8]$$

$$a(t) = \mu.g \quad [E3.9]$$

- $t = t_c = T$

$$V(t_c) = V_{impact}$$

t_0	beginning of crash sequence (s)	a	deceleration of the vehicle (m/s²)
t_{bi}	time at the beginning of braking (s)	V	speed of the vehicle (m/s)
t_b	time at full braking (s)	S	travel distance of the vehicle (m)
t_c	time of collision (s)	γ	jerk due to the deceleration (m/s^3)
T	time interval of the simulation (s)	μ	coefficient of tire/road friction
d	distance from start of skid marks to point of impact (m)	g	acceleration due to gravity (m/s²)
		L	percentage of kinematic energy loss prior to full braking
V_{impact}	impact speed of the vehicle (m/s)		

Figure 3.2. Brake model for the crash reconstruction

3.2.3. Modelling the kinematics of the pedestrian

Modelling the kinematics of the pedestrian is similar in terms of procedure to the method for the vehicle kinematics. However, it was assumed that the pedestrian has a rectilinear trajectory with a constant speed. The speed of pedestrians was estimated based on the work of Huang et al. (2008). This speed is associated with the pace and age of the pedestrians (Figure 3.3). The speed values used in the crash reconstruction correspond to the speeds of the 50th percentile as shown in Table 3.1.

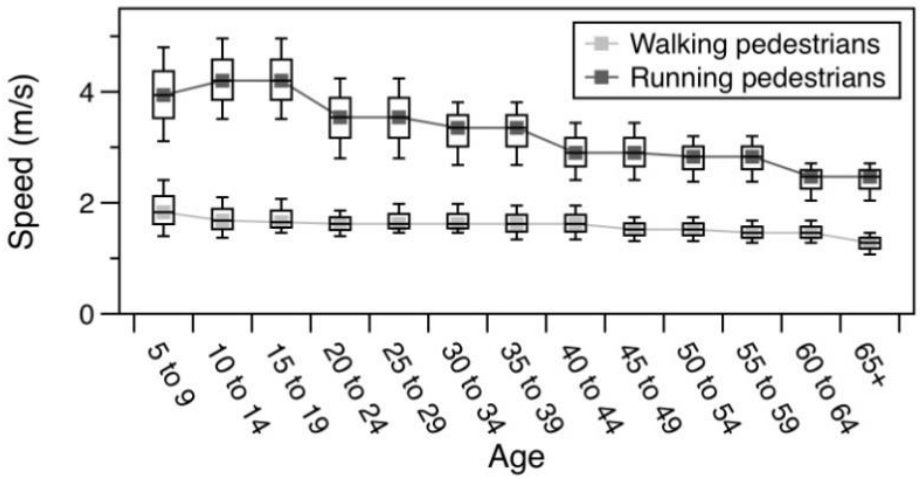

Figure 3.3. Pedestrian speed relative to its age and pace
From Huang et al. (2008)

Table 3.1. Pedestrian speed estimation

Age	50% speed (m/s)	
	Walking	Running
5-9	1.83	3.94
10-14	1.68	4.20
15-19	1.65	4.20
20-29	1.62	3.54
30-39	1.62	3.35
40-44	1.62	2.90
45-49	1.52	2.90
50-54	1.52	2.83
55-59	1.46	2.83
60-64	1.46	2.47
65+	1.28	2.47

3.2.4. Validating the reconstruction of the accident

The simulation reproduces the kinematics of both the vehicle and the pedestrian starting from some initial set of conditions until the crash. At each time step, the remaining distance before impact $S_i(t)$ was calculated. Then, this distance is identified within the

trajectory already defined (noted $S_i(X)$) in order to shift from a time domain to space coordinates. This procedure is applied for both vehicle and pedestrian (Figure 3.4). Any obstacles that may obscure the visibility of the pedestrian are taken into account. The interaction is finally obtained between the different components of the accident (users-vehicle-environment) and the pedestrian motion over the time is displayed relative to the vehicle taking into account the blind spots due the obstacles.

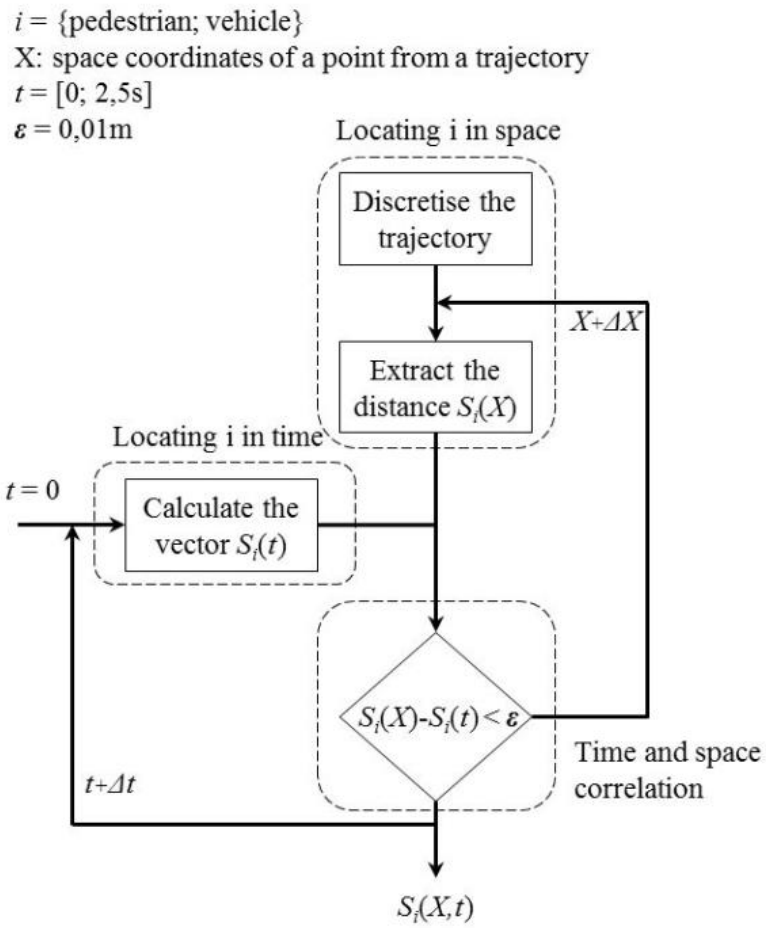

Figure 3.4. Overview of the time and space reconstruction of an accident

When the reconstruction is in agreement with all the data from in-depth database, the parameters modelling the accident are saved in a file that can be read for simulation in MATLAB. Other data are also recorded in this file like the tire/road friction coefficient or complementary information such as light conditions. This last parameter cannot be represented in a simulation approach but its effect can be estimated by adjusting the performance of a pedestrian detection system.

Table 3.2 summarizes the required parameters for the simulation of a crash. The parameters are classified according to the three components of the accident: the crash environment, vehicle and the pedestrian.

Table 3.2. Components properties required for modelling a pre-crash scenario

Class	Variable name	Purpose
Control system	Time interval analysis (sec.)	Computing dynamic variables
	Timer (sec.)	
Crash Environment	Site diagram (scaled image)	Extracting data as the impact location
	Scale	Converting distance of pixels to meters
	Tyre/road Friction	Validating braking manoeuvre for the vehicle
	Slope of the road (rad.)	
	Width of the road* (m)	Validating steering manoeuvre for the vehicle
	Traffic density (Boolean)	
	Number of obstacles	Retrieving blind spots
	Location of obstacles (m)	
	Obstacles' cross section (m)	
Vehicle	X&Y-coordinates (m)	Positioning in space relative to the site diagram
	Curvilinear coordinates (m)	Positioning in space relative to the trajectory
	Relative position (m)	Positioning in time
	Relative speed (m/sec.)	Determining the speed in time
	Pointer 1	Matching the position in time with the coordinates relative to the site diagram
Pedestrian	X&Y-coordinates (m)	Positioning in space relative to the site diagram
	Curvilinear coordinates (m)	Positioning in space relative to the trajectory
	Relative position (m)	Positioning in time
	Relative speed (m/sec.)	Determining the velocity in time
	Pointer 2	Matching the position in time with the coordinates relative to the site diagram

* It is the distance between the centre of vehicle and the road boundary. It is withdrawn and scaled from the site diagram.

3.3. Examples of accident reconstruction

Two examples of accident cases are presented in the following section to illustrate the method of accident reconstruction previously described. The two selected accident cases show how late detection due to poor visibility caused the collision. These kinds of

situations are known to be a challenge for Collision Avoidance and Mitigation Systems (Yuasa et al., 2013).

3.3.1. Example 1: Accident case in a curve

The accident occurred in an urban area at the exit of a roundabout between a 5-door hatchback and two children running to cross the road. The investigation of the accident was conducted by a technician specialized in collecting "on-scene" data relative to the infrastructure and the vehicle involved in the crash. On the spot, one of the pedestrians and the driver were both interviewed separately by the psychologist (from the in-depth investigation team) to get information about the crash. Then, a second interview was undertaken several days after the accident (8 days) to complete the missing information to reconstruct the pre-crash scenario.

3.3.1.1. **"On-scene" data collection**

- Road environment

The accident site was at the entrance of the town of Salon-de-Provence, France (urban area). It happened at the exit of a roundabout, a road with two lanes in each direction separated by a central median strip. The crash occurred at the start of school in the morning. At that time, the traffic was busy and the weather was overcast with heavy rain.

The investigators assessed the possibility that a sign giving directions may have hidden the pedestrians while they were crossing through the median strip. The sign was 2.4m long and 0.5m height. Other details of the road are assessed such as the pavement width including the central median strip, the curve radius of the roundabout and its exit, the width of the pedestrian crossing, etc. These details allowed drawing to scale the site diagram of the accident (Figure 3.5).

- Vehicle

The vehicle was a Citroën C3 1.4i, a 5-door hatchback first registered in February 2004. It was a brand new car with no defects observed.
There was no damage on the vehicle indicating the impact locations of the two pedestrians. These impact locations were retrieved through the statements of the different parts involved in the accident and confirmed by the reconstruction of the accident scenario.

- Driver

There was only the driver in the vehicle. He was an elderly man aged 78. He was not injured. He was familiar with the route undertaken on the day of the accident. He estimated he was driving at a speed between 20 and 30 km/h. He states he didn't see the pedestrians crossing due to the heavy rain and so, didn't apply the brakes. He didn't stop the vehicle until he arrived at his destination (1 km after the accident spot). He declared he didn't notice that an impact occurred.

- Pedestrian

Two brothers were involved in the crash: 6 and 10 years old boys. They were going to school. They were holding hands a step back from the pedestrian crossing waiting for a gap in traffic. They started to run after a car stopped to let them cross. They kept on running across the opposing lane without looking at the oncoming traffic.

The older brother was slightly injured. He was thrown about 4 m ahead of the middle of the pedestrian crossing. Concerning the other child, after been thrown forward into the path of the vehicle, he found himself trapped underneath the vehicle and was dragged for approximately 1km. He suffered from multiple lacerations. He was admitted to hospital.

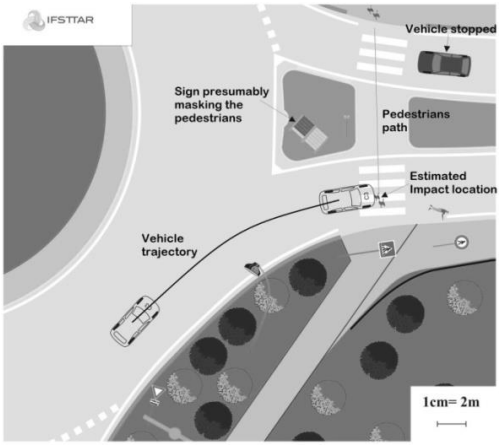

Environment	Vehicle	Pedestrians
Impact location estimated at the middle of the walkway; No skid marks *Infrastructure* lane width from impact: 2.75m One driving lane; Urban area Speed limit: 50km/h *Masking obstacles* Type: sign Width: 2.4m Height: 0.5m *Weather and light conditions* Day time Heavy rain Wet road : tire/road friction coefficient of 0.6	C3 Citroen (2004 MY): B-segment or subcompact hatchback *Dimensions* Length: 3.85m Width: 1.66m Distance Gravity Center /front-end of the vehicle: 1.85m Action: turning right (first exit of a roundabout) No emergency maneuver First impact on the vehicle Distance from the center : 0m	2 kids: 6 and 10 years old Struck on their right side Action: crossing on a walkway without looking at the oncoming vehicles Pace: running Pedestrian 1 (6 years old) Impact: center of the vehicle Projection: forward trajectory Severe injuries, MAIS: 3 Pedestrian 2 (10 years old) Impact: right front-end corner Projection: thrown off to the right-hand side Minor injuries
Vehicle turning; Masked pedestrians; Inclement weather; Frontal impact; No deaths, MAIS : 3		

Figure 3.5. Accident data of a case collected from the database of IFSTTAR-LMA

3.3.1.2. **Data from reconstruction**

- Road environment

The road surface was wet; it was assumed that maximum the coefficient of friction between the road and tyre was reduced, limiting the amount of longitudinal deceleration to -6 m/s².
According to the statements of witnesses, the collision occurs in the middle of the lane; the distance measured from the impact location to the lateral boundary (the central median strip) was 2.7 m.

A road sign located on the central median strip was considered to be an obstacle that may have masked the pedestrians from the driver. The shortest offset of this obstacle measured from the side of the vehicle is 2.9 m.

- Vehicle

The driver did not react. There was no evidence of pre-impact or post-impact brake, so the travelling and impact speeds of the vehicle were considered to be the same. This speed was estimated to be 30 km/h from the throw distance of the pedestrian, which was estimated at 4m. This speed was also consistent with the measured speed of the vehicles driving through that section of the road.

- Pedestrian

Regarding the statements of the witnesses and the involved persons, the location of the impact with the first pedestrian was assessed to be in the centre of the front-end of the vehicle, while the impact with the second pedestrian was with the right front edge of the vehicle.

The pedestrians were running prior to the impact at a speed that was inferred to be about 3.5 m/s. This speed is slightly under the one corresponding to the age of the pedestrians since it is constrained by the fact that the two brothers were holding their hands.

3.3.1.3. **Summary of the crash**

- Driving phase

On a rainy day in the morning of November 2011, a 2004 MY Citroen C3 took the first exit at a roundabout travelling at an average speed of 25 km/h. At the pedestrian crossing near the roundabout, two brothers aged 6 and 10 were holding their hands while waiting to cross the road.

- Discontinuity phase

After a vehicle stopped to give them way to cross, the pedestrians run across the road without paying attention to the oncoming vehicles.

- Emergency phase

Although there was a central median strip separating the lanes of each direction, the visibility of the pedestrians was masked by a sign of 2.4 m wide but with low height. Additionally, at 1 second before the impact, the pedestrians were located at 4 m far from the point of impact.

The driver of the Citroen C3 declared that he didn't see the children crossing due to the heavy rain. He did not react.

- Crash phase

The youngest child was struck approximately in the centre of the vehicle and has been forwarded straight ahead, while the other child was hit by the right front edge of the vehicle and thrown about 4m ahead on the right side of the road. The driver did not stop the vehicle and continued his itinerary as he didn't notice that a collision occurred (according to the driver's statement).

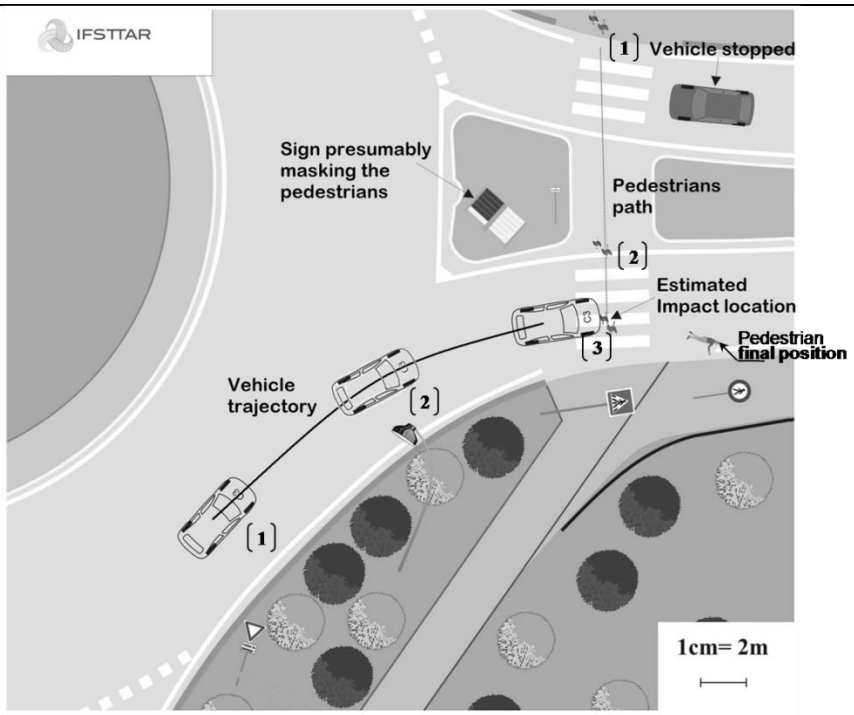

	[1]	[2]	[3]
Time-To-Collision (s)	2.5	1.0	0
Vehicle speed (km/h)	30	30	30
Distance to impact for the vehicle (m)	20.8	8.5	0
Pedestrian speed (m/s)	3.5	3.5	3.5
Distance to impact for the pedestrian (m)	9.7	3.7	0

Figure 3.6. Data from crash reconstruction of the accident case n°1

3.3.2. Example 2: Accident case with masked pedestrian

The accident occurred in a metropolitan area of Adelaide on a 3-lane highway between a mid-sized sedan and an elderly pedestrian crossing between vehicles that had stopped due to traffic. This case has a detailed report on pedestrian injuries provided by the Royal Adelaide Hospital records. Also, clues have been observed on the spot of the accident such as skid marks and blood stains.

3.3.2.1. **"On-scene" data collection**

- Road environment

The accident site was on a 3 lane highway in the metropolitan area of Adelaide (urban area). The left lane was empty while the two other lanes contained stationary queued vehicles. The crash occurs at day time in the afternoon and the weather was dry.

From the tyre marks left on the dry road, the total lengths measured were 9.6 (left mark) and 13.3 m (right mark). There was a discontinuity observed in the skid marks at the impact point. The throw distance was measured from that point to the location of the final position of the pedestrian.

The investigators review the site design to draw to scale the scheme of the accident (Figure 3.7).

- Vehicle

The vehicle was a 2002 model year Toyota Corolla Ascent, a mid-sized sedan. No defect was noticed in its characteristics. It had been owned by the driver for one year before the crash and was first registered three years before the collision.

The vehicle was inspected in order to identify damage due to the impact with the pedestrian. A scratch was found on the right side of the bumper and measured at 705 mm from the middle of the vehicle. A dent was noted on the right upper side of the bonnet which can be associated to the head impact.

- Driver

The driver was a 17 year old male. There were two other people in the vehicle. No one in the vehicle was injured.
The driver applied the brakes after he saw the pedestrian coming out from the right lane in front of a dark van stopped due to traffic.
The driver declared that he was familiar with the road and knew the speed limit was 50 km/h. He stated he was driving at 40 km/h and struck the pedestrian at 20 km/h.

- Pedestrian

The pedestrian was a 58 year old woman. She was carrying a handbag and was wearing dark clothes. She was walking through the traffic. She was struck on her left side by the vehicle. A witness stated that she lost consciousness for less than 1 minute.

The pedestrian was admitted to the hospital for 2 days. Her injuries included a laceration and haematoma to the occipital region of the scalp, a comminuted fracture of the right clavicle with a contusion and a fracture to the right fibula head/neck.

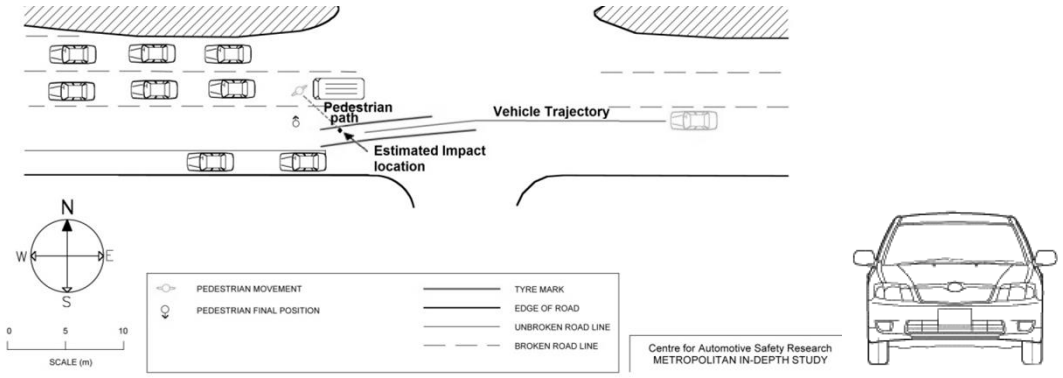

Environment	Vehicle	Pedestrians
skid marks: 9.6 and 13.28m pre-impact skid: 11m *Infrastructure* lane width : 2.5m driving lanes: 3 Traffic flow: busy *Masking obstacles* A van Distance from the vehicle side: 1.8m *Weather and light conditions* Day time Dry weather Dry road : tire/road friction coefficient of 0.72	Toyota Corolla (2002 MY): B-segment or subcompact sedan *Dimensions* Length: 4.18m Width: 1.71m Distance Gravity Center/front-end of the vehicle: 2.1m Action: driving straight Emergency maneuver: Braking and steering First impact on the vehicle Distance from the center : 0.7m	Female: 58 years old struck on the left side Action: crossing through stationary traffic Pace: walking *Injuries* head: laceration + hematoma thorax: right clavicle fracture lower leg: fibular head fracture 2 days hospital No death MAIS: 2
Masked pedestrian; Impact with the right-front of the vehicle ; No deaths, MAIS : 2		

Figure 3.7. Accident data of a case collected from the database of CASR

3.3.2.2. **Data from reconstruction**

- Road environment

The road surface was dry: the coefficient of friction of road/tyre was assumed to be 0.72. The post impact skid marks was measured to be 2.25 m long, and the throw distance of the pedestrian was about 3 m. The distance measured from the impact location to the road boundaries was 1.5 (left to the vehicle) and 2.3m (right to the vehicle).

- Vehicle

From the skid marks left on the dry road (9.6 and 13.3 m long), the travelling speed of the vehicle was estimated to be 55 km/h. The impact point was assessed based on the discontinuity in the pattern of the skid marks, and also consistent with results of the impact speed from the formula of Searle and Searle (1983) and the equation of a uniform vehicle deceleration. Accordingly, the impact speed was estimated at 20 km/h.

- Pedestrian

Regarding the statements of the witness and the marks found on the vehicle, the pedestrian kinematics during the collision could be described as a wrap projection. It was possible to relate the injured body regions of the pedestrian with the correspondent parts of the vehicle. The contusion over the right knee and the fracture to the right fibular head and neck was caused by the bumper of the vehicle. The comminute fracture mid-shaft of the right clavicle with the right chest contusions was resulted from the impact with the bonnet. It was assumed that her pre-impact walking speed could be estimated from her age; hence her walking speed was assumed to be 1.4 m/s.

3.3.2.3. **Summary of the crash**

- Driving phase

On a clear day, a Toyota Corolla® (Sedan MY2002) was heading west in left lane of a 3 lane highway at an average speed of 55 km/h. The lane where the vehicle was driven through was empty while the two other lanes were full of queued vehicles stopped due to traffic.

A 58 years old pedestrian was crossing (jaywalking) the highway, walking between stopped vehicles, just in front of a van.

- Discontinuity phase

The driver of the Toyota saw the pedestrian coming out in front of the stationary van.

- Emergency phase

The driver of the Toyota applied the brakes locking them up. He started to swerve to the left.
The pedestrian continue to cross the road taking an angular direction towards the vehicle.

- Crash phase

The impact occurred at a speed of 20 km/h. The pedestrian struck on her left side the right front of the vehicle. Her body got wrapped along the front of the vehicle then projected 3.2 m away.

The driver was maintaining the brakes until the vehicle stopped leaving post-impact skid marks on the road of 2.25 m long.

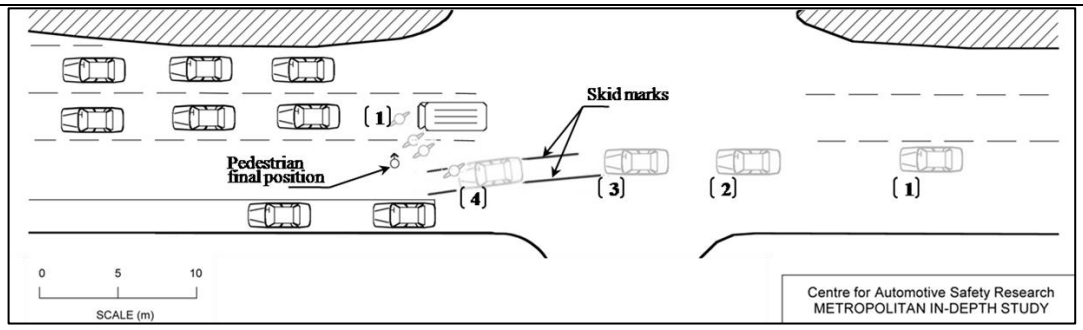

	[1]	[2]	[3]	[4]
Time-To-Collision (s)	2.5	1.75	1.1	0
Vehicle speed (km/h)	55	55	50	20
Distance to impact for the vehicle (m)	31.4	20	11.7	0
Pedestrian speed (m/s)	1.4	1.4	1.4	1.4
Distance to impact for the pedestrian (m)	3.6	2.5	1.7	0

Figure 3.8. Data from crash reconstruction of the accident case n°2

3.4. CAMS modelling

In this section, the method of modelling collision avoidance and mitigation systems will be described. The structure of CAMS modelling sub-module is divided in 2 blocks: detection sensor and system actuation and each of these will be described below.

3.4.1. Detection sensor modelling

The first block defines the parameters of vehicle-mounted sensors designed for detecting pedestrian as well as any other obstacle on the road (Table 3.3). These parameters are directly extracted from the description of systems developed in Section 2.3.1 and Section 5.1.1.

Most of the pedestrian active safety systems processed in this survey are systems that use multiple detection sensors. Instead of testing different sensor combination, the program structure was designed to assess detection by each sensor individually without considering the fusion of the sensor data. The fusion of the sensor data was then considered separately (see Chapter 5).

3.4.2. Modelling the system actuation

The second block of this sub-module concerns modelling the decision to deploy the countermeasure (braking or steering). The relevant variables are described in Table 3.3. Assumptions were established simplifying the motion of the vehicle. For example, steering manoeuvres were characterised as uniform circular motion, so the velocity of the vehicle was held constant during the entire emergency trajectory. For braking, it was assumed that, before reaching the defined brake force, a transient state occurred corresponding to the system lag and was approximated by a linear ramp of a fixed duration.

Table 3.3. Components properties required for CAMS modelling

Class	Variable name	Purpose
Sensor modelling	X&Y-coordinates (m)	Positioning the sensor
	Field of View (rad)	Validating the pedestrian detection by the system
	Range (m)	
	Update frequency (sec.)	
Actuator modelling	Activating time before impact (sec.)	triggering policy
	Brake system lag (sec.)	validating braking manoeuvre
	Brake power (m/s²)	
	Steer system lag (sec.)	validating steering manoeuvre

3.5. Simulation of the accident with the CAMS interaction

Each simulation describes the motion of the vehicle and pedestrian in time and space. It is then possible to determine the position of the pedestrian relative to the vehicle and to follow its evolution for each time step of the simulation. At each time step of the simulation, the remaining time (respectively distance) before impact called time-to-collision (respectively distance-to-collision) and noted *TTC* (respectively (d_{TTC}) is computed.

By coupling the CAMS modelling with the trajectory of the vehicle, the interaction of the data from each sensor can then be evaluated by applying it to each accident configurations and the feasibility of an autonomous intervention is assessed (see Figure 2.9). The simulation therefore consists of two steps:

- The potential detection of the pedestrian by the sensors
- The feasibility of triggering an autonomous emergency manoeuvre.

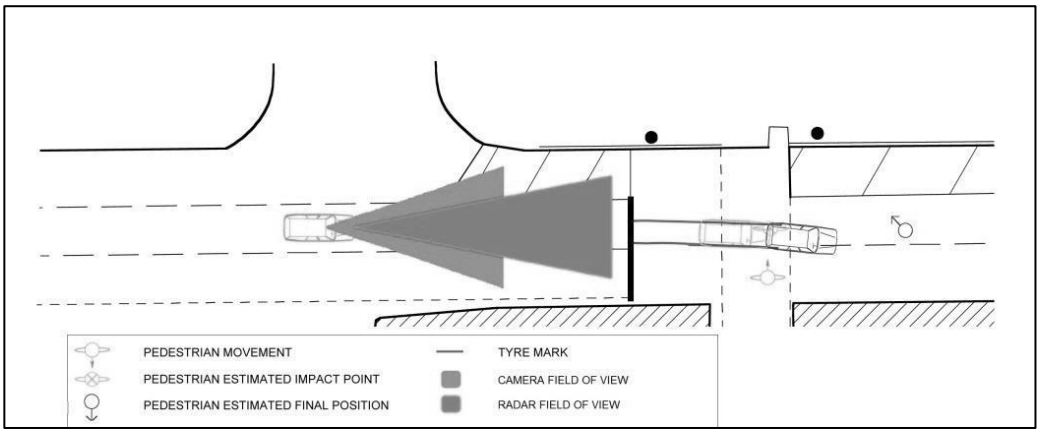

Figure 3.9. Scheme illustrating a crash representation including an example of CAMS

The first step in the simulation process is to calculate when the pedestrians would be detected by each sensor (as they are modelled in the software) and to compute their position relative to vehicles (in longitudinal and lateral)

The next step is to verify the feasibility of triggering an autonomous emergency manoeuvre. Two possible manoeuvres were considered: braking and steering. The configuration of these two emergency manoeuvres will be presented in detail.

The last step is to examine the response of the detection system and autonomous intervention. In the simulation, the deployment of an emergency manoeuvre will change the outcome of an accident scenario. There will be either no impact (avoided accident) or an impact with changed conditions (mitigated accident). There will be also cases where there is no opportunity for a Ped-CAM system to detect a pedestrian or deploy an emergency manoeuvre (late detection).

3.5.1. Time frame for the simulation

To simulate the sequence of events preceding the collision, an appropriate time interval preceding the collision needs to be defined. Brannstrom et al. (2010) used a time horizon of 3s in their model-based algorithm for avoiding arbitrary objects (other vehicle, pedestrian, etc.). The resolution of the timing of events was 50 ms.

In this present research, the objective is to establish a simulation model of accidents involving a vehicle with a pedestrian. Pre-crash scenarios were modelled using a time interval corresponding to an initial distance-to-collision suitable to study pedestrian detection. As it was assumed that sensors used in active safety system are limited to detect up to about 40 m (Meinecke et al., 2003), it was not considered necessary to simulate accident scenarios for distances above this value. As most (90%) of the pedestrian accidents occur at vehicle speeds lower than 60 km/h (Schaller et al., 2012), it appears relevant to simulate the chronology of the accident for speed up to this threshold. Considering the distance travelled by a vehicle at different speeds during a given time period, a duration of 2.5 s of simulation appears sufficient.

The time step for the simulation was 10 ms which corresponds to a measurement frequency of 100 Hz. This resolution is above the measurement frequency of pedestrian detection sensors found on the market.

3.5.2. Pedestrian detection

In the simulation of a crash scenario, a test is conducted every time step to determine if the pedestrian is potentially detectable by the sensors of a system. Detectable means that the pedestrian is located within the field of view (FOV) of the sensor. In order to do this, the position of the pedestrian is expressed in the local coordinate system of each sensor in polar coordinates: r(t) and θ(t) (Figure 3.10). At each time step, the polar coordinates of the pedestrian's position was checked to determine whether it was within the boundaries of the detection area of the sensor (R: the range; φ: the FOV).

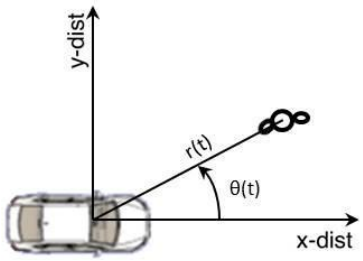

Figure 3.10. Pedestrian position relative to the vehicle

The line of sight from the vehicle can be obstructed by obstacles on the road side. These obstacles are considered in the simulation process. They were represented by their cross section: i.e. diagonals of a rectangle covering the obstacle position (Figure 3.11).

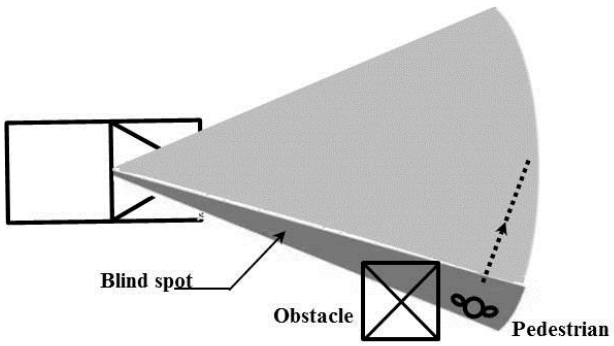

Figure 3.11. Illustration of an obstacle masking an on-board sensor's line of sight

Pedestrians are considered detected only if they remain continuously visible to the sensors (located within the detection area) during a time period that represents the processing time of the detection system. It is assumed that this processing time corresponds to 10 consecutive update measurements of each sensor (see Section 3.4.1).

3.5.3. Actuation of autonomous emergency manoeuvres

Once the pedestrian is detected by a system, the following steps in the simulation compute the feasibility and effects on autonomous interventions. The feasibility is evaluated at the instant (noted TTC_{trig}) that the system would trigger an autonomous manouevre. At this time TTC_{trig}, the remaining distance to travel before reaching the impact location (noted d_{trig}) is assessed for validating the feasibility of the autonomous intervention.

Two types of advanced driver assistance systems are considered in this research: Autonomous Emergency Braking (AEB) and Autonomous Emergency Steering (AES) systems.

3.5.3.1. **Braking manoeuvre**

For validating the feasibility of the emergency braking, there are two possibilities. The first condition is to determine if there is enough distance to stop the vehicle before impact. The braking distance is calculated at a time step of the simulation using Equation 10:

$$d_{stop} = \frac{v^2}{2 \cdot |a|} + d_{L\_offset} \qquad \text{(Equation 3.10)}$$

Where v is the approach speed of the vehicle, a is the deceleration that depends on the road conditions, d_{L_offset} is the safety distance between vehicle longitudinal clearance set at 0.8 m.

The calculated braking distance (d_{stop}) is then compared to the d_{trig}. To consider the accident avoided, d_{trig} has to be longer than d_{stop}.

If this first condition is not satisfied, the next step is to determine if the pedestrian would be able to clear the path before the arrival of the vehicle. It is assumed here that the pedestrian would continue crossing the path of the vehicle at a constant speed. Because of the deceleration, the time (noted t_{brake}) spent for a vehicle to travel the remaining distance before the impact (noted d_{trig}) is increased (compared with no or delayed braking) according to Equation 11. The difference between braking time and the time-to-collision is calculated using Equation 12. If this time difference (noted δt_{travel}) is longer than the time required for the pedestrian to clear the vehicle's path and to reach a safe distance (half meter away from the vehicle's path), then the accident is considered avoided.

$$t_{brake} = \frac{v - \sqrt{v^2 - 2 \cdot |a| \cdot d_{trig}}}{|a|} \qquad \text{(Equation 3.11)}$$

$$\delta t_{travel} = t_{brake} - TTC_{trig} \qquad \text{(Equation 3.12)}$$

3.5.3.2. **Steering manoeuvre**

Several conditions are necessary for an autonomous emergency steering manoeuvre to be feasible. The conditions are related to 1) the traffic situation, 2) the feasibility of the emergency trajectory according to the dynamic characteristics of the Ped-CAMS and 3) the space availability for manoeuvring.

The first condition identify whether there are other vehicles in the vicinity of the subject vehicle. Information about traffic is provided from the in-depth investigation conducted on the accident scene (see Section 3.2.4). If there is no other traffic then this first condition is satisfied. If there was other traffic then the authorisation for deployment is denied.

To check the second and third conditions, it is necessary to model the emergency steering trajectory. It is assumed that the trajectory is represented by two arcs of same radius which are centrally symmetric about a point (Figure 3.12). In the simulation, this last point of the trajectory is located at a fixed distance from the pedestrian (an offset of 1 meter plus the half width of the vehicle, noted d_{offset}). Regarding the vehicle dynamics, the lateral acceleration (noted a_y) is assumed constant and limited to 5 m.s^{-2} (Isermann et al., 2008; Keller et al., 2011a). As a result of the described model, the characteristics of the steering trajectory can be determined. The radius of steering (noted R_{steer}) is calculated by dividing the square of the vehicle approach speed by the lateral acceleration limit. The steering angle (noted θ_{steer}) and the steering angle rate (noted $\dot{\theta}_{steer}$) are then computed as follow:

$$\theta_{steer} = \sin^{-1}\left(\frac{d_{trig}}{R_{steer} + d_{offset}}\right) \quad \text{(Equation 3.13)}$$

$$\dot{\theta}_{steer} = \frac{v}{R_{steer}} \quad \text{(Equation 3.14)}$$

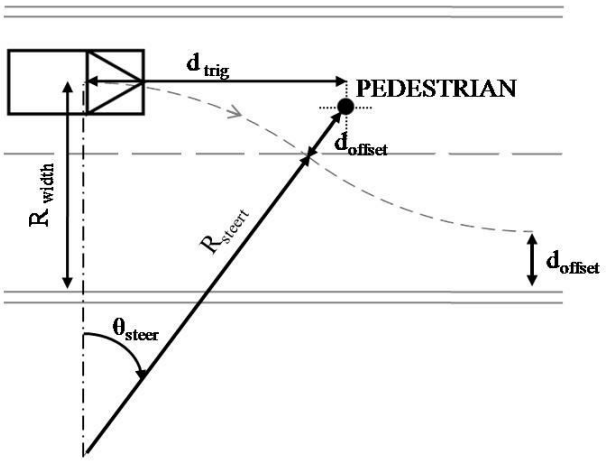

Figure 3.12. Modelling of the emergency steering trajectory

Once the emergency steering trajectory is modelled, the computed parameters are compared to the maximum steering angle and the steering angle rate allowed by the steering system. If the condition is not satisfied, the steering manoeuvre is then disallowed.

The third condition to verify is the space availability for steering. The vehicle must have enough lateral space to realize the evasive manoeuvre. The lateral displacement travelled by the vehicle during a possibly steering manoeuvre is compared to the distance between the centre of vehicle and the road boundary. This distance (noted R_{width}) is withdrawn and scaled from the site diagram (see Section 3.2.4). Finally, the lateral displacement of the vehicle should be lower than the distance from the road boundary (Inequality 1).

$$R_{width} > 2 \cdot R_{steer} \cdot (1 - \cos\theta_{steer}) + d_{offset} \qquad \text{(Inequality 3.1)}$$

3.5.4. Estimation of system response

The response of each system was estimated in the following steps:

- determine the number of cases in which the pedestrian was detectable in time to deploy an emergency manoeuvre;
- In the cases where there was likely to have been an emergency manoeuvre, determine the number of cases in which the pedestrian was avoided;
- In the remaining cases, determine the reduction in impact speed caused by the emergency manoeuvre.

The outcomes of an accident scenario will change with the deployment of the emergency manoeuvre. The procedure employed was to first evaluate the braking manoeuvre and then the steering manoeuvre. As explained in Section 3.5.3, a list of conditions has to be validated in order to consider the accident avoided.

In cases where an autonomous intervention was unable to prevent a collision, impact may be expected to occur but with modified conditions. The impact speed and the location of interaction between the vehicle and the pedestrian will be altered. The impact speed will be reduced by the time the vehicle will reach the pedestrian path.

The modified impact speed (noted u) is calculated in the simulation using Equation 15.

$$u = \sqrt{v^2 - 2 \cdot |a| \cdot d_{trig}} \qquad \text{(Equation 3.15)}$$

Where v is the approach speed of the vehicle, a is the deceleration that fluctuates depending on the road conditions of the reconstructed accidents, d_{trig} is the remaining distance between the vehicle and the pedestrian before impact.

The location of the first impact configuration (the original accident configuration without the autonomous intervention) will be displaced since the pedestrian is assumed to continue walking while the impact is delayed. The delay is estimated using Equation 3.12 and 3.13 developed in Section 3.5.3. The displacement of the impact location is then determined multiplying the delay and the pedestrian speed.

3.6.Synthesis

The methodology described in this chapter is the use of simulation to test the response of Ped-CAMS to real accident scenarios. The simulation models the Ped-CAMSs and the accidents. Then, a Ped-CAM system can be coupled to the trajectory of the vehicle in order to emulate the effects of a system on the accident outcome. There is a two steps test in the simulation (Figure 3.13). The first step consists in determining if the system can detect or not the pedestrian. The second step is to identify whether the accident can be avoided or mitigated (i.e. with speed reduction) or unaffected by the system.

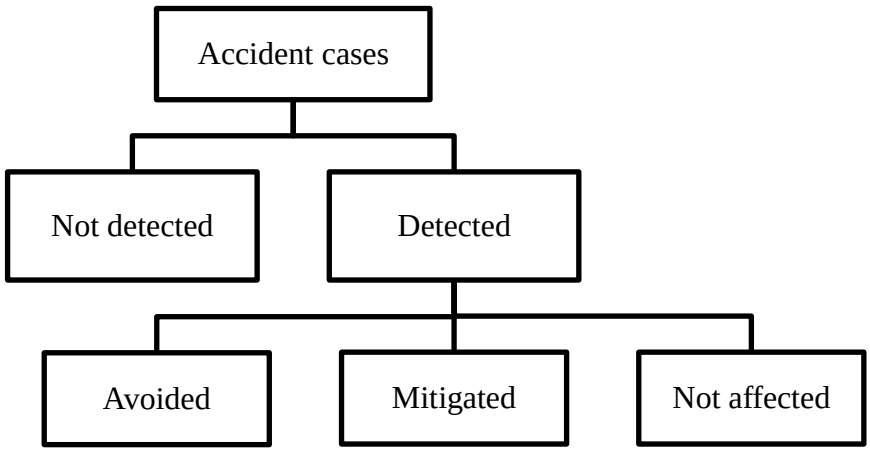

Figure 3.13. Diagram of the different Ped-CAMS responses

The method relies on robust accident reconstructions in order to obtain a realistic simulation of accident scenarios. Two examples of accident reconstructions are presented to illustrate how accidents were modelled. The accidents are drawn from in-depth crash databases. In these databases, the level of details is important as explained in the previous chapter. However, it has to be noted that some data were inevitably missing such as pedestrian speed. As a consequence, assumptions were established.

The accident reconstruction method presents random errors such as the trajectories and speeds of vehicles and pedestrians. A sensitivity study has been made on the both speeds of pedestrian and vehicle. Results show that a variation of +/- 10% of these speeds can lead to a variation of the pedestrian position relative to the vehicle (and also for the remaining vehicle travelling distance before impact) of about +/- 20%. Concerning the time-based measures, the TTC can vary of +/- 10%. Same results can be observed with a deceleration variance analysis.

Ped-CAMSs were modelled according to their characteristics. In chapter 5, there will be a discussion on the limitation about this system modelling. Detection was considered if the pedestrian was entirely located in the coverage area of the detection system and for successive iterations. In this method, issues related to sensor technologies such as resolutions and accuracies (in term of positions and dynamics) are not taken into account. The detection difficulties cannot be assessed by the developed method.

Chapter 4

Analysis of the accident database

The accident reconstruction method described in Chapter 3 was applied to a sample of pedestrian crashes that had been investigated at the scene. This sample was from two sources providing accidents investigated in local areas (around the township of Salon-de-Provence and in the Adelaide metropolitan area). The methodology used to collect these cases is described in Chapter 2.

A qualitative and quantitative analysis was conducted on the data of the selected accidents. Its objective was to describe the conditions under which the pre-crash events occurred. A first step was to describe the situation and conditions at the moment of the accidents. Parameters were gathered into fields: factors related to the road environment and condition, the involved vehicle and pedestrian. The second task was to describe the accident outcome in term of severity and injuries sustained by the pedestrians. The last step was to analyse the configuration of the impacts.

Finally, through the simulation of the accidents, the kinematic of the pedestrian relative to the vehicle was analysed in time and space.

4.1. Method for establishing the accident database

The sample of accidents for the research was selected from two sources: the accident databases of IFSTTAR-LMA and CASR. As described in Chapter 2, these two databases include accident data from in-depth investigations.

Case selection was based on specific criteria. The first concerned filtering accidents involving pedestrians with passenger vehicles; accidents with heavy vehicles, two powered wheelers, cyclists and other vulnerable road users were excluded.

A second criterion in the selection method was the availability of the data that were required for the accident reconstruction. It was, for instance, crucial to know not only the impact location on the vehicle body but also on the roadway (locating the accident on the site diagram). It was important to get the actions (including their trajectory) of both the pedestrian and vehicle. In addition, the impact speed should be reliably assessed from standard crash reconstruction techniques. In some cases, the impact speed was known but it was difficult to recover the vehicle travelling speed. For example, if a driver stated having triggered the brakes before the collision, it is difficult for the investigators to estimate the level of deceleration unless skid marks are observed. As described in Chapter 3 (section 3.2.1), it was assumed that full braking was applied if skid marks were found on the site of an accident. These cases of full braking were then considered in the accident selection; otherwise, the other cases of braking were rejected.

Injury severity of the accidents was not taken into account among the selection criteria. It is worth noting that accidents included in the two database sources were systematically involving pedestrians sustaining at least minor injuries. Hence, the sample of accidents did not only include severe and fatal cases.

The accidents selected in this research were provided from two sources: The French accident data source IFSTTAR-LMA and the Australian data source at CASR. These sources included accidents provided from in-depth investigations. Because in-depth studies are time-consuming and costly exercises, the number of accident cases in these two databases were limited (55 cases for IFSTTAR-LMA and 138 cases for CASR). In addition, the potential number of cases relevant for the research was a subset of all cases because the current study is focussed on pedestrian accidents with passenger vehicles.
One hundred cases satisfied the sampling criteria: 40 cases from IFSTTAR-LMA and 60 cases from CASR.

The selected accidents were classified into scenarios for the purpose of simulation based assessment. This classification method considered specific factors challenging the visibility of the pedestrian by the driver and even on-board detection systems. Five reference scenarios were defined as follow:
- Scenario 1: pedestrian obscured due to poor visibility conditions (e.g. nighttime, heavy rain…).
- Scenario 2: pedestrian crossing through or after a turn (intersection, exit of roundabouts, bends).
- Scenario 3: pedestrian obscured by an obstacle (e.g. parked or vehicles stopped due to traffic, road furniture).
- Scenario 4: pedestrian starting crossing from the sidewalk or nearby (from the right of the vehicle in France, from the left in Australia).
- Scenario 5: pedestrian crossing from the far side of the roadway (from the left of the vehicle in France, from the right in Australia).

For scenarios of vehicles turning in intersections, it is possible to classify them into sub-classes according to the type of turns: Near and Far turn (i.e. the vehicle should cross the road while turning).

This classification allows gathering accident cases from the different databases although the traffic rules are different between countries (driving right in France and left in Australia) as illustrated in Figure 4.1.

Types of turns	In France	In Australia
• Near turns	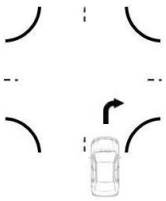	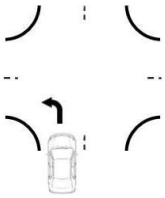
• Far turns	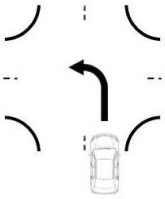	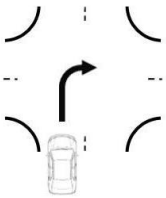

Figure 4.1. Turning configurations

4.2.Description of the sample

4.2.1. Crash period

Figure 4.2 shows the distribution of the selected accidents over the period they occurred. The cases from IFSTTAR-LMA cover a wide period from 1995 to 2011, while the CASR cases occurred in the period April 2002 to October 2005. More than two third of the selected accidents in this study were consequently accidents occurring between 2003 and 2005.

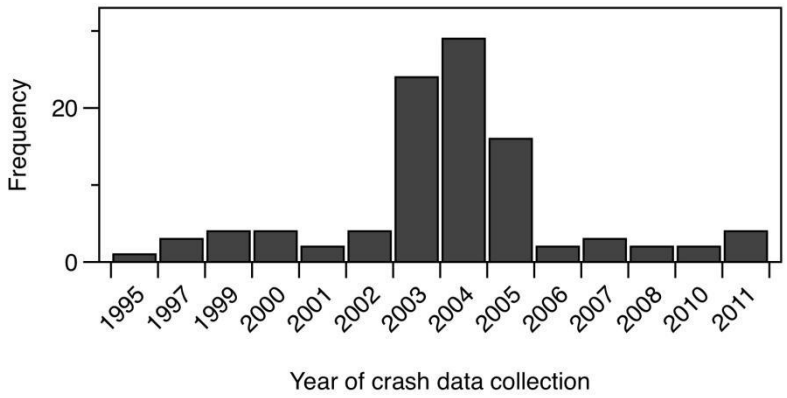

Figure 4.2. Distribution of the crash period

4.2.2. Road environment and conditions

The majority of the accident cases happened during the day (83%). Among these cases, some drivers declared not seeing the pedestrian due to inclement weather (heavy rain, 4%) or bad light conditions: (dazzling light, 7%). The proportions are likely to be affected by the choice of data-sets. As the collection was made around Salon de Provence and Adelaide, it might be expected that poor weather could be under-represented in this data-set.

Most of the accidents involving pedestrians occur in urban areas. They represent in our database 96% of the cases which is similar to the figures recorded in France for example.

53% of cases happened on midblock section with a quarter of these occurring on a pedestrian crossing. Accidents at intersections were coded according to the intersection types. Forty seven percent of accidents at intersections occurred at 4-way intersections. Accidents at T-junctions and Y-junctions represented 34% and 6% of all intersection accidents. The remaining 13% occurred at the exit of roundabouts.

Thirty eight percent of accidents at intersections (18% of all the accident set) occurred while the vehicle was turning. In the database, among the accidents occurring in turns, there were 72% that occurred in far turns (configuration b and d as described in Figure 4.1).

In the crash set selected for the research, 22% were accidents where pedestrians were masked by obstacles. These obstacles are mainly:

- parked vehicles: 11 cases
- stopped vehicle due to traffic: 7 cases
- urban furniture: tree (2 cases), rubbish bin (1), traffic signs (1)

Figure 4.3 gives the cumulative frequency of the lateral distance between the vehicle and the pedestrian at the moment that the pedestrian was detectable.
In 80% of cases where the pedestrians were masked, the lateral distance between vehicles involved in crashes and obstacles was greater than 1 m. 50% of pedestrians were visible less than 1.5 m laterally from the vehicle. All the pedestrians are unobstructed when they were located at half a meter from the side of the vehicle.

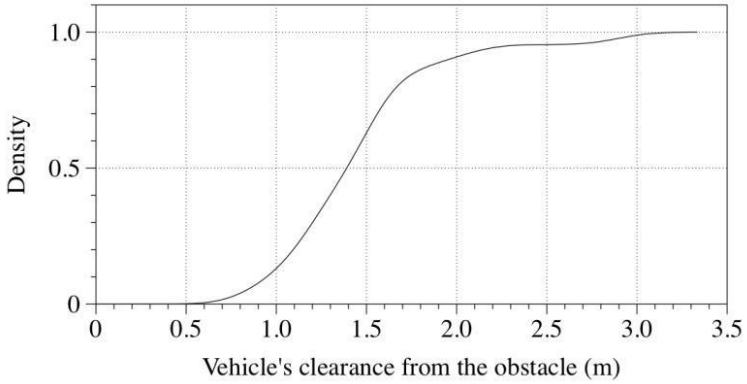

Figure 4.3. Cumulative distribution function of the vehicle's clearance from obstacles

4.2.3. Vehicle types

Table 4.1 shows the distribution of the vehicles involved in the crash database according to Euro NCAP classification. Twenty four percent of the crashes involved light truck Vehicles (LTVs which includes pickup trucks or utilities, Multi-Purpose Vehicles, vans, and SUVs) or Truck Vehicles (buses, Light Commercial Vehicles LCVs, and Large Goods Vehicles LGVs). Most of the passenger vehicles are Executive (23% and mostly from the Australian cases) and Supermini cars (24% and mostly from the French cases).

Table 4.1.
Distribution of vehicle type for the French, Australian and all cases of the database

Vehicle type	French cases (N=40)	Australian cases (N=60)	All cases (N=100)
Sports car	0	3%	2%
Supermini car	45%	10%	24%
Small family car	15%	12%	13%
Large family car	17%	12%	14%
Executive car	7%	33%	23%
LTV’s	8%	22%	16%
TV’s	8%	8%	8%

4.2.4. Vehicle speeds

Figure 4.4 shows the distribution of both travel and impact speeds. 95% of the travel speeds of vehicles were under 60 km/h and 50% of the travel speeds are under 40 km/h, while the impact speeds are under 30 km/h.

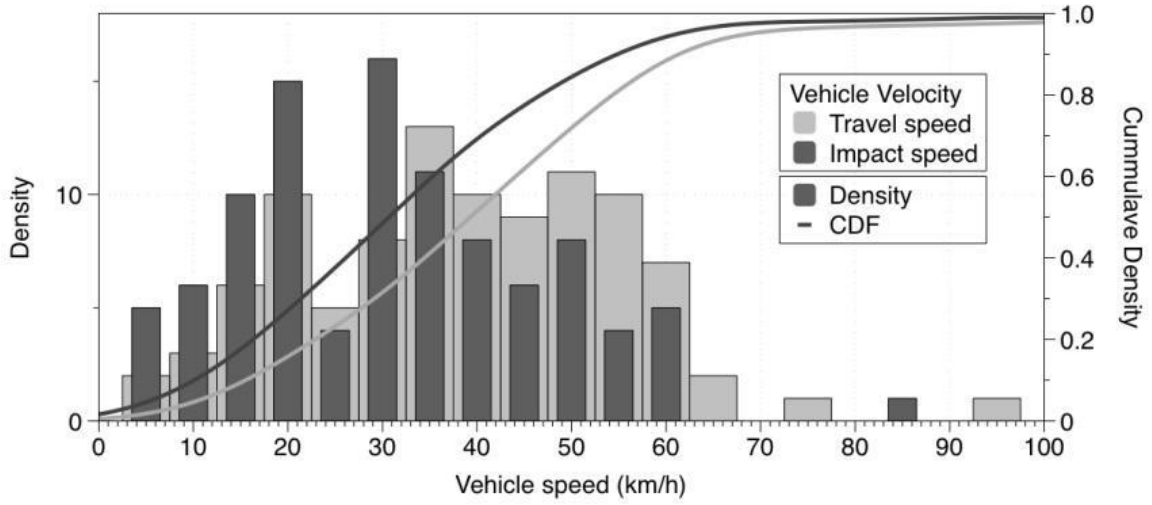

Figure 4.4. Vehicle speed distribution

Twelve percent of vehicles were exceeding the posted speed limit at the time of the accident (Figure 4.5). One third of these vehicles were exceeding the speed limit by more than 20 km/h (i.e. 4 cases among the accident sample). The remaining two thirds were within 10% of the speed limit.

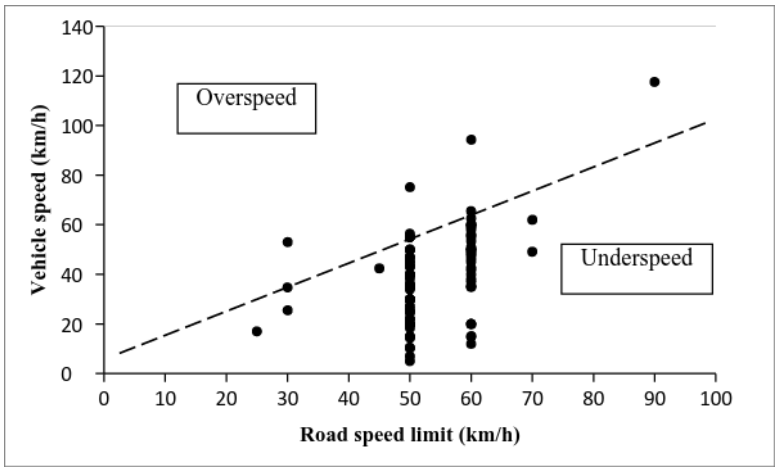

Figure 4.5. Comparison between travel speeds and the speed limits

4.2.5. Pedestrian age and speed

Figure 4.6 displays the distributions of pedestrian age according to the reported pace of the pedestrian. The distribution of pedestrian ages displays a U-shape form, as children (under 15 years old) and elderly pedestrians (over 65 years old) are over-represented. This distribution is similar to those reported in other studies (Martin et al., 2011; Mizuno, 2005).

It was observed that elderly pedestrians are mostly walking (72%). For running pedestrians, children are the largest group representing 15%.

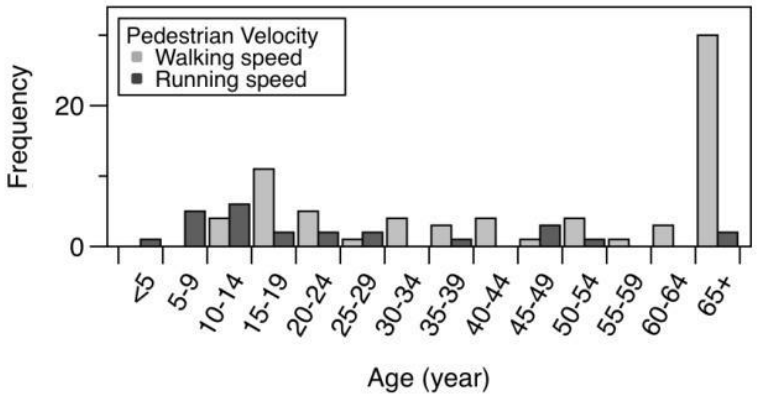

Figure 4.6. Pedestrian age distribution according to the pace

Knowing the age and pace of the pedestrian, it is possible to estimate a distribution of their speed as explained in Chapter 3 section 3.3. Figure 4.7 presents the cumulative frequency distribution of the estimated pedestrian speed for walking (N=72 cases), running (N=25 cases) and all cases (N=100 cases; the distribution includes three cases in the sample in which the pedestrian was static).

Most of the pedestrians were walking normally with an average speed of 1.4 m/s (~ 5km/h). This average speed is related to the rate of elderly pedestrians in our database. The average speed of running pedestrians is 3.7m/s (~13km/h). This last group concerns mainly pedestrians aged less than 20 years old and their speeds can appear high.

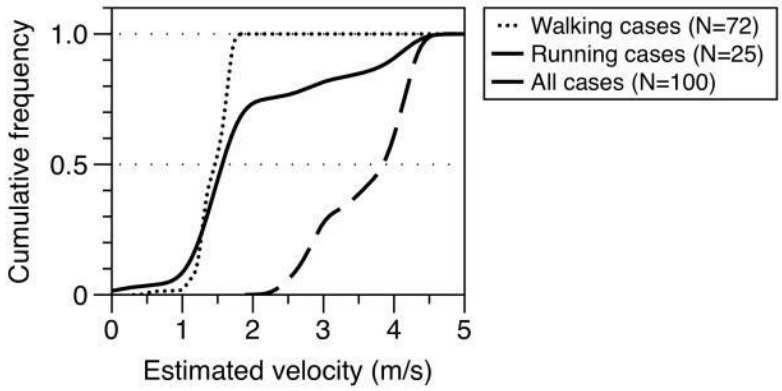

Figure 4.7. Pedestrian speed distribution according to the pace

4.2.6. Injury characteristics

Since the focus in this research is based essentially on primary safety, the priority in accident selection was given to data required for reconstruction of the pre-crash phase. Not all the selected cases in our database have information on pedestrian injuries. 83 out of 100 cases (30 French cases and 53 Australian cases) had injury data.

The head and lower extremities are the most injured body parts (respectively 26.9% and 29.6%) representing more than 50% of all injuries when injuries of all seventies are considered (Figure 4.8).

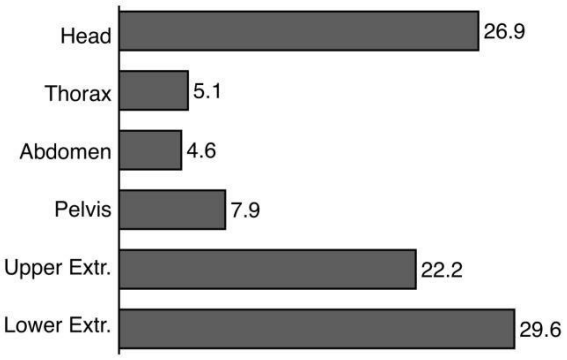

Figure 4.8. Frequency of injured body regions for pedestrians

Table 4.2 shows the distribution of AIS2+ injuries in the data. Data are given separately for French (noted IFSTTAR-LMA cases) and Australian cases (noted CASR cases). For the two databases, a common general shape of the distribution can be observed with high frequencies of AIS2+injuries to the head and the lower extremities.

Table 4.2. Distribution of AIS2+ injuries according to body regions

Body segment	French cases (N=30)	Australian cases (N=53)	All cases (N=83)
Head	31%	32.8%	32.6%
Thorax	3.4%	3%	2.1%
Abdomen	3.4%	3%	3.2%
Spine	6.9%	4.5%	5.3%
Pelvis	6.9%	19.4%	15.8%
Upper Extremities	17.2%	13.4%	14.7%
Lower extremities	31%	23.9%	26.3%

A difference was observed in the frequency of injuries sustained by the pelvis. In the Australian data, pelvis injuries are more frequent (19.4% versus 6.9% in the French data).

Another classification coding the severity of the accident cases was also used in this research. In this study, the injury severity was coded according to the following scheme:

- Pedestrians who died from traffic accident-related injuries are considered fatally injured (F);
- Pedestrians admitted to hospital for more than 24 hours were coded as being seriously injured (S);
- Pedestrians who did not require surveillance at hospital for more than 24 hours were coded as being lightly injured (L).

Figure 4.9 shows the distribution of the injury severity according to the age of the pedestrians involved in the accidents of the database. It is noted that the fatalities of pedestrians over 70 years old represent 30% of all the fatal cases. Moreover, the fatal and serious injuries represent ¾ of all injuries sustained by this age category of pedestrians.

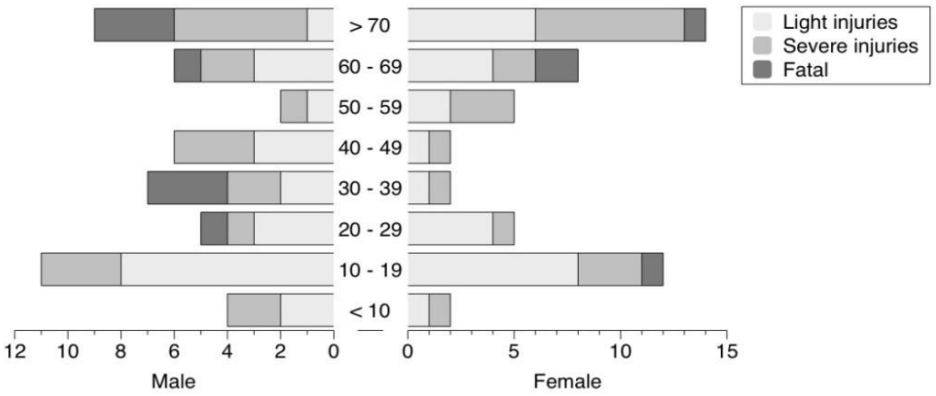

Figure 4.9. Distribution of the injury severity according to the pedestrian age

4.2.7. Impact configurations

The crashes were categorised according to whether the collision happened at the first front corner, centre or last corner of the vehicle (considering the direction from which the pedestrian crossed), and also whether the pedestrian crossed from the curb (near side) or from the other side of the road (offside). 6 configurations are established from these combinations (Figure 4.10). Cases in which the pedestrian struck the first front corner include those that were struck by the side of front fender panel of the vehicle (16%).

There are as many cases of pedestrians coming from the near side (the curb) as those crossing a lane. The remaining 2% were static pedestrians. The most frequent configuration representing a quarter of the sample was where the pedestrian was struck immediately after stepping from the curb.

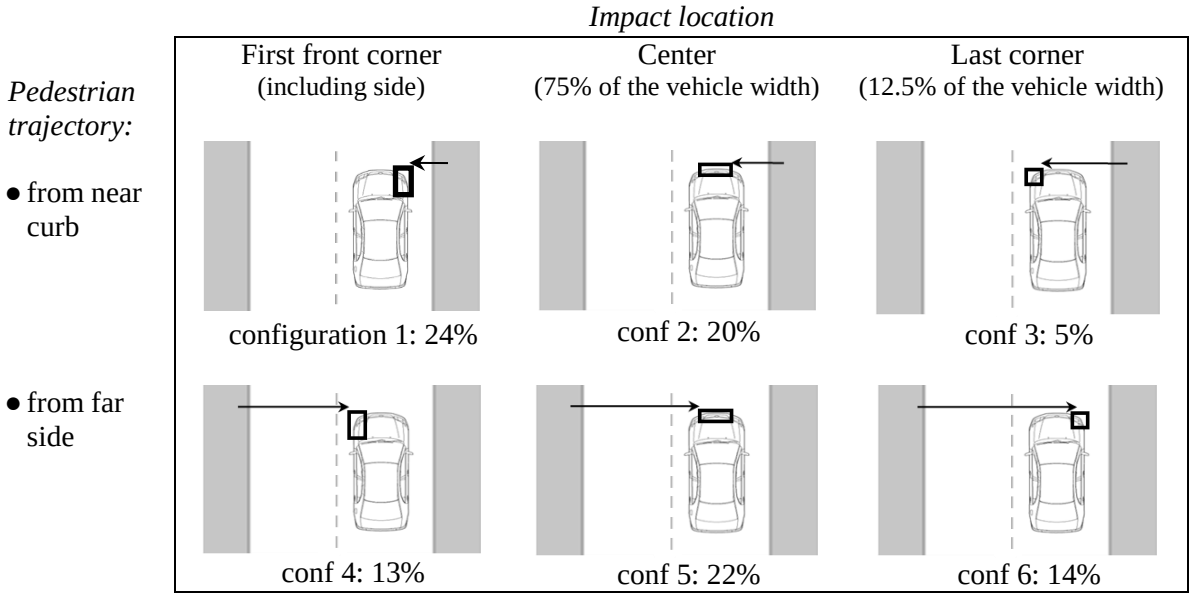

Figure 4.10. Description of the configuration of the crash dataset

4.2.8. Pedestrian kinematics relative to that of the vehicle

The simulations of all accidents were used to examine the position of the pedestrian relative to the vehicle at times-to-collision (TTC) of 2.5 s, 2.0 s, 1.5 s, 1.0 s and 0.5 s before impact. Figure 4.11 shows the cumulative frequencies of the pedestrian positions in longitudinal (x-axis) and lateral (y-axis) for each TTC. It may be observed that, at 2.5 s, 90% of the pedestrians are located within the 40 m of the front of the vehicle. This longitudinal distance decreases over time to be less than 20 m when the TTC is 1.0 s. The lateral distance is displayed in Figure 4.11 (bottom) as the distance from the centre of the vehicle. At 2.5 s before impact, most of the pedestrians are located in a lateral distance not exceeding 10 m. This distance drops to 4 m at 1.0 s, with half located 1 m to the side of the vehicles (considering that the mean width of a passenger car is 1.7m).

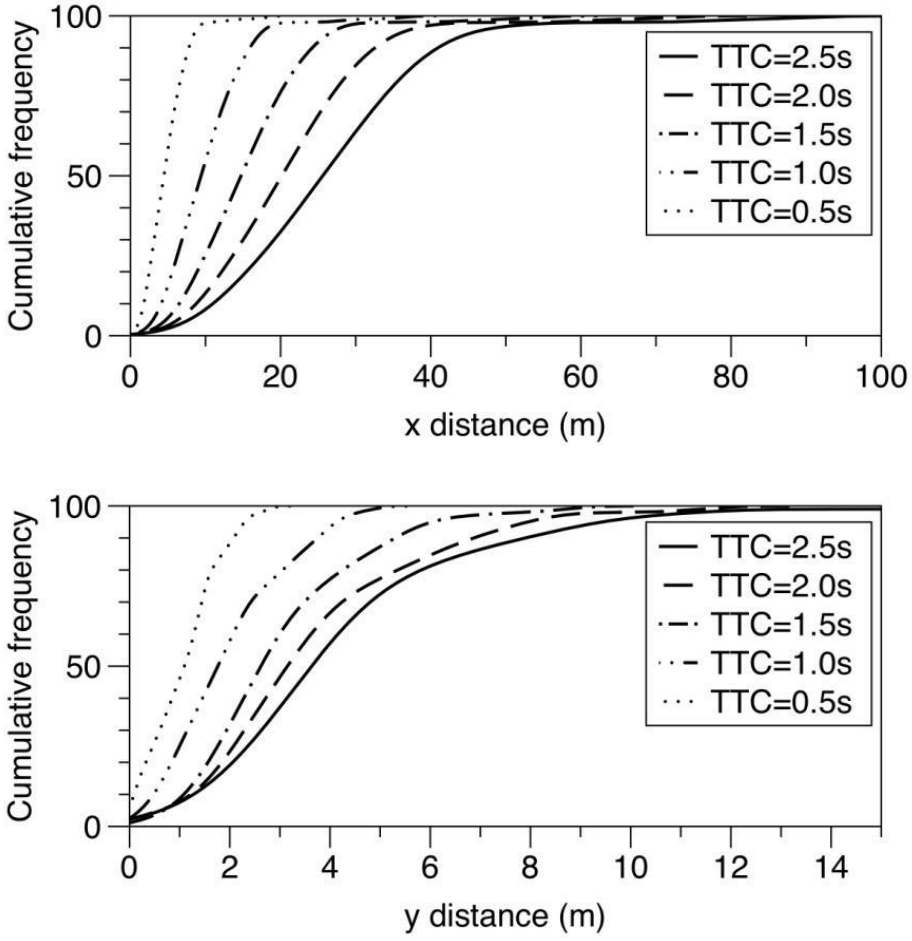

Figure 4.11. Distribution of pedestrian position in longitudinal (Top) and lateral (Bottom)

Figure 4.12 shows the pedestrian position relatively to the vehicle position at 2.5s, 2s, 1.5s, 1s and 0.5s before the impact. This figure highlights in particular that before a TTC of 1.5s, the positions of the pedestrians relative to the vehicle are still scattered, and would have been unlikely to invoke any response from an autonomous system. Then between 1.5s and 0.5s, the positions of the pedestrians are gathered toward the front of the vehicle. This period between 1.5 s and 0.5 s TTC would appear to be critical for the timely response of an autonomous system.

Moreover, the results show that the lateral position of the pedestrian a short time before collision appears to be very important because at 1s before the impact, it can be observed that most of the pedestrians are located within 3m of the side of the vehicle but many are still outside the forward path of the vehicle.

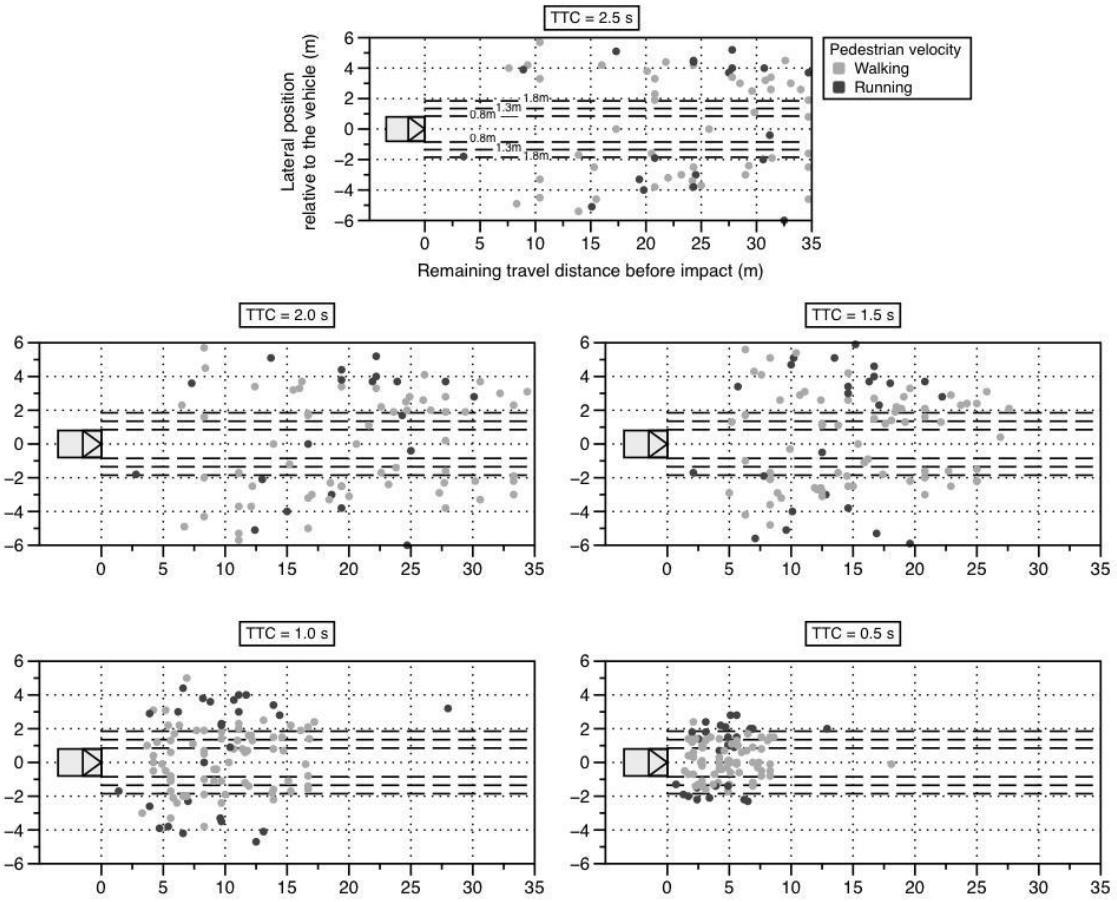

Figure 4.12. Pedestrian position relatively to the vehicle at different TTC

4.3.Discussion

4.3.1. Representativeness

- Road environment and conditions

Among the accidents selected in this research, 17% occurred during hours of darkness. In comparison, in France, night-time accidents account for 27% of the crashes involving pedestrians (ONISR, 2013). Hence, night-time crashes are underrepresented; note that the in-depth investigations were mostly conducted during normal working hours.

There are only 4 accident cases where there was heavy rain. The proportions are likely to be affected by the choice of data-sets. As the collection was made around Salon de Provence and Adelaide, it was expected that poor weather could be under-represented in this data-set.

Most of the accidents involving pedestrians occur in urban areas. They represent in our database 96% of the cases, which is similar to the figures recorded in France for example. It is true that the accident cases from our database occurred inside delimited areas, since they were provided by in-depth investigations operating within prescribed geographical boundaries. Yet, the IFSTTAR-LMA investigation team has the particularity to intervene in various types of roads. Although the investigations have this characteristic, the number of pedestrian crashes outside urban areas is low. Consequently, the travel and impact speeds of vehicles reflect mainly crashes occurring in urban areas.

Thirty eight percent of accidents at intersections (18% of all the accident set) occurred while the vehicle was turning. The curvature of the road (or road alignment) is presumably challenging for sensor systems designed to detect pedestrians. Since the accidents of our database happened in France and Australia, it would be meaningless to give figures on the whole set about right and left turns. These two countries have different traffic rules (driving right in France and left in Australia). What is considered here is the radius of curvature of the turns. A near turn (small curve radius) is assigned to left turns in Australia and right turns in France (Figure 4.1). In the database, among the accidents occurring in turns, there were 72% that occurred in far turns (configuration b and d as described in Figure 4.1). It could be explained by the fact that drivers are distracted paying attention to the incoming traffic while they have to cross a road.

- Vehicle speed

The vehicle speed distribution of this study was similar to another distribution found in a survey of the GIDAS database (Schaller et al., 2012). It is possible that the similarity arises because the accidents in each dataset mostly occurred in urban areas.

When the travelling speed is reliably estimated according to the accident reconstruction method (Chapter 3, section 3.2.2), it has been compared to the road speed limit. It appears that most of the accidents occurred at speeds below the road speed limits (88%).

- Pedestrian velocity

Most of the pedestrians were walking normally with an average speed of 1,4 m/s (~ 5km/h). This average speed is related to the rate of elderly pedestrians in our database. The average speed of running pedestrians is 3.7m/s (~13km/h). This last group concerns mainly pedestrians aged less than 20 years old and their speed can appears high. Nevertheless, these average speeds comply with other research findings (Montufar et al., 2007; Zębala et al., 2012; Zhang et al., 2013).

- Pedestrian injury data

Regarding pedestrian injury data provided by the databases used in this research, the distribution clearly showed that the head and lower extremities were the most injured body parts representing more than 50% of all injuries (respectively 26.9% and 29.6%). This distribution was consistent with the results found in the literature review (Cesari et

al., 2007; Mizuno, 2005). This result, often seen in other studies, was the reason for the focus on head injury, pelvic injury and lower extremity injury that was embodied in the protocols of sub-system tests conducted by EuroNCAP to evaluate pedestrian passive safety (Euro NCAP, 2009).

Comparing the injury data from the two databases (IFSTTAR-LMA and CASR), a common general shape of the distribution can be observed with high frequencies of injuries for the head and the lower extremities. These results are similar to the injury distributions reported by Martin et al. (2011) and Mizuno (2005). However, a difference was observed in the frequency of injuries sustained by the pelvis. In the Australian data, pelvis injuries are more frequent (19,4% for the Australian data while 6,9% for the French data). It could be interesting to evaluate if the significant difference in the distribution of the vehicle fleet between the two countries (higher proportion of larger vehicles like SUV's in Australia than in France) would have an influence on the pedestrian injury pattern.

Pedestrian age has a large influence on the injury severity outcome, beside the collision speed and the impacted part of the vehicle (Demetriades et al., 2004; Peng and Bongard, 1999). The sample of the selected accidents shows that the older (over 65 years-old) and younger (under 15 years-old) pedestrians trends to be more injured. The younger age group was found to be involved in traffic accidents mainly due to the lack of attention from the persons accompanying them (Hillman et al., 1990). For elderly pedestrians, they were more exposed to the risk of injury, specifically severe injuries due to morphological and physiological properties (Kent et al., 2009).

4.3.2. Challenges in pedestrian primary safety

- Road environment and conditions

Detection of pedestrians is challenged by light conditions. Visible light sensors are less effective during night-time (e.g. Gandhi and Trivedi, 2007).

There are other factors during daytime that can influence the detection of pedestrians. Heavy rain and fog limit the visibility of the forward path of the vehicle. These factors are pointed as they are a constraint not only for drivers but also for camera sensors (Wisch et al., 2013b). In the in-depth data such factors were usually reported by the involved driver during the interview with the investigator of the accident.

Another constraint during daytime for camera sensors is the presence of sun glare. Although the cameras adjust automatically the exposure as the image brightness changes, this adjustment can affect a late detection of the hazard located in the field of view of the camera (Figure 4.13).

Figure 4.13. Image illustrating the effect of sun glare

In the literature, one of the most studied factors from the road environment factors consists of the effect of roadside obstacles on hazard perception (Yuasa et al., 2013). Roadside obstacles can lead to the late detection of the pedestrian and thus, constrains the safety system to react in limited time and space. It is then important to consider this factor particularly since it is not complicated to model it in the crash simulation. These obstacles can be differentiated and classified into different crash scenarios as described by Brenac et al. (2004).

Other factors from the road environment have also an influence (on the performance of the response of the system) in the situation analysis and decision making relative to active safety systems fitted in vehicles. These systems employ emergency braking and some may possibly employ emergency steering as a countermeasure to avoid an imminent crash (Hayashi et al., 2012). Braking as well as steering depends on the road state expressed through the tire/road friction model. Moreover, steering manoeuvres are restricted by a considerable number of additional factors such as the traffic situation and it is parameterized according to the road boundaries (road width) and other features related to the vehicle.

- Vehicle speed

Vehicle speed is also an important factor interfering in the situation analysis and crash prediction. High speed reduces the time available for the driver to react. Speed has the same influence on the pedestrian detection systems giving them a shorter time to analyse the situation and to trigger an emergency manoeuvre.

- Pedestrian velocity

One strategy that Ped-CAMS can use to detect a potential accident with pedestrians is to estimate their trajectory in order to evaluate the probability of a collision. An important variable to consider is the velocity of the pedestrian. This parameter was not always available although data of the accident cases provided from in-depth investigation were fairly comprehensive. The velocity was then estimated according to the age of the pedestrian and the pace estimated from the statements of the persons involved in the accidents and/or the witnesses (see Chapter 3, Section 3.2.3 and Figure 4.6). Consequently, results concerning pedestrian speed are driven largely by the speeds assigned to “running” and “walking”.

- Kinematics

The crash configuration analysis combined the trajectory of the pedestrian with the impact location on the vehicle according to the timeline of the crash. The objective was on one hand to determine if the collision happened at the beginning, mid or end of the pedestrian move (given that the beginning and end of crossing corresponding to an overlapping of less than 12.5%, and over 87.5% of the vehicle width). On the other hand, it was to identify if the pedestrian was coming straight from the curb or already crossing from off-side the road (Figure 4.10).

Through the simulation of the accidents, the kinematic of the pedestrian relative to the vehicle was analysed in time and space. From the simulation, frames were captured to freeze the motion of the pedestrian at different times corresponding to times-to-collision (TTC) of 2.5 s, 2.0 s, 1.5 s, 1.0 s and 0.5 s before impact. For each selected time window, the data from the simulation of the 100 accident cases was merged in order to plot the cumulative frequency of the pedestrian positions in longitudinal (x-axis) and lateral (y-axis).

Based on the accident classification mentioned in Chapter 2 (Section 2.2.2), accidents were gathered into scenarios. These scenarios highlight the challenges in pedestrian safety. This approach could be used to evaluate the representativeness of the accident sample relatively to a wider crash population (e.g. a national scale). Simple analytical methods can be used to estimate a global probability estimates to assess the safety performances of Ped-CAMSs (Burgett et al., 2008; Ference et al., 2006).

4.3.3. Limitations

In the selection process, it was decided to rely on the amount of data and level of details provided by the accident databases. It was important to ensure as insofar as possible that the required data for the accident reconstruction was available. A list of data was checked including the impact location on the vehicle and on the roadway, the trajectories and the actions of both pedestrians and drivers prior to the collision, etc. Concerning actions prior to impact, it was assumed that finding skid marks on the accident site attested that the driver reacted by a full braking. In this case, it was easier to reconstruct the accident by assuming a constant braking deceleration according to the road surface condition (i.e. the deceleration is assumed to be -8m/s² for dry conditions and -6m/s² for wet conditions). For cases without physical evidence of braking, it was not possible to nominate the timing or the strength of the reported braking. Such cases were considered unsuitable for analysis in this study.

As a result of the selection criteria, the sample of accidents was reduced to 100 cases (40 from IFSTTAR and 60 from CASR). A previous study performed by IFSTTAR on clustering accidents into prototypical scenarios (or reference scenarios as described in Chapter 2, section 2.2.2) showed that a sample of one hundred crashes can cover the whole set of scenarios (Brenac and Megherbi, 1996). The sample size of the selected accidents can be then considered acceptable.

The use of accident databases of two different countries (France and Australia) was not aimed to conduct a comparison between the two countries. Additionally, the sample size cannot enable a comparison between the French and Australian accident cases. To do so, it requires a larger sample like in the study performed by Ebner et al. (2011). Indeed, they found in their study similar results in the calculation of the reference scenarios starting from databases of two different countries: US and Germany. Although the difference between these countries is present, the authors assumed that the causes of the accidents remain comparable.

Chapter 5

Estimating the response of CAM systems

The methodology described in Chapter 3 is applied to six pedestrian collision avoidance and mitigation systems. By simulating their effects on the accident scenarios contained in the database (described in Chapter 4), these systems were tested to estimate their relevance in avoiding crashes or reducing impact speeds. The intention here is not to compare systems but to determine characteristics which are important to effectiveness.

The six systems have been selected in order to be representative of the state-of-the-art and because sufficient information was available about their technical characteristics. These characteristics included the field of view of the different sensors comprising a system, their range, the update frequency, etc. Two of the selected systems were prototypes at the time of the study, while others were already introduced in the market. The systems vary in the type of sensors used and their configurations (the position where they are mounted in the vehicle).

As described in chapter 3, the accidents were reconstructed providing realistic crash scenarios describing the kinematics of the pedestrian and the vehicle prior to the collision. In order to estimate the performance of these Ped-CAMS, specific events of a crash sequence were identified. These events were relevant to the ability of a system to detect pedestrians and to trigger an autonomous emergency manoeuvre in order to avoid the crash. In particular, the time available between the pedestrian detection and the last time to brake was evaluated.

In the simulation, detection is considered when the pedestrian located entirely within the sensor field of view during a period of time (processing time). Concerning autonomous emergency manoeuvres, only braking is considered for reasons outlined in Chapter 3. The response of systems is measured by examining their potential ability to avoid the crash or reduce the impact speed.

5.1. Assessment method

5.1.1. Description of the selected Ped-CAM systems

Six different Ped-CAM systems were considered in this study. The models are idealized representations of Ped-CAM systems already in the market. The choice of the six systems was made due to the knowledge of their characteristics and their descriptions were based on existing information in the literature. Each of them is briefly described hereafter but references are given for more details about the systems.

S1. CWAB-PD® is a pedestrian detection system developed by Volvo Cars and launched in the Volvo S60 MY2011. This third-generation system is composed of a Forward-Looking Camera (FLC) mounted near the rear view mirror (a 48° Field of view –FoV– and 60 m range) and a Forward-Looking Radar (FLR) mounted in the vehicle grille (a 60° FoV, e.g. range) (Coelingh et al., 2010).

S2. The Artificial Vision and Intelligent Systems Laboratory (VisLab), University of Parma has developed a system based on a laser scanner (with a scanning angle of 100°, up-to-80 m range) and a near-IR camera for night-time capabilities achieved with an NIR light-diode headlight mounted in the front end of the vehicle (having an aperture of about 25°) (Broggi et al., 2009).

S3. The EyeSight® 2.0 system designed by Subaru uses a stereo camera: twin overlapping lenses mounted on the top edge of the windscreen (a 25° FoV for each lens) (Subaru Australia, 2014).

S4. The system developed by Continental A.G. within the project Proreta 3 also uses a stereo camera for pedestrian detection but the lenses have a wide field of view of 44° (Eckert et al., 2013).

S5. The PRE-SAFE® system developed by Daimler uses a near-IR camera located near the rear view mirror in addition to a stereo camera (with a 45° FoV). A combination of different range levels of radar is mounted in the front end of the vehicles (Michalke et al., 2011).

S6. Toyota Motors preferred to fit to the new Lexus models a system using a stereo vision based on twin near-IR cameras (Hayashi et al., 2013).

The 6 selected systems presented in the previous part are summarized in Table 5.1. As described in the chapter 3, only main parameters of these systems were taken into account in the accident simulation process.

Table 5.1. **Characteristics of Pedestrian Detection Systems**

	System	Sensor (Detection)		
		Type	FOV	Range (m)
S1	Volvocars (CWAB-PD®)	Mono camera (FLC)	48°	60
		Radar (FLR)	60°	200
S2	University of Parma	NIR camera	25°	30
		Laser Scanner	100°	100
S3	Subaru (EyeSight®)	Stereo camera	25°	50
S4	Continental (ContiGuard®)	Stereo camera	44°	60
		Laser Scanner	22,5°	200
S5	Daimler Chrysler (PRE-SAFE®)	Stereo camera	45°	50
		NIR/FIR camera	20°	160
		Mid-Range Radar	60°	60
		Short Range Radar	80°	30
S6	Toyota Motors (Lexus)	NIR Stereo camera	30°	25
		Radar	60°	200

5.1.2. Factors relating to detection

Once the selected Ped-CAMS were modelled, their effects were simulated over the sample of 100 accident cases. In the simulation process, two conditions were required in order to consider the pedestrian detected by a sensor. The first one was that the pedestrian was entirely located within the coverage area of the sensor (within the range and the field of view). The second requirement was that the first condition was met continuously over a period corresponding to the processing time of the system. It was assumed that a pedestrian would not be registered by any system unless it was detected for a continuous period of 10 cycles of the sensor update rate.

Fusion of sensor data was also taken into account in the detection assessment. Detection was considered to have occurred if the pedestrian would have been in the coverage area overlapped by a camera and one other sensor.

The detection rate was first calculated for each sensor composing a system starting with the camera. Then, a global detection rate was estimated taking into consideration the fusion process: the detection rate of the camera was supplemented with the cases detected by the other sensors in poor light conditions.

In the simulation process, factors which can affect the visibility and/or detection of the pedestrians were taken into account. These factors correspond to obstacles (masking the pedestrian from the line of sight of the detection sensors) and poor visibility due to the light condition (darkness, dazzling sunlight, heavy rain).

The assumption of the ability of detecting pedestrian under poor light conditions can be considered as optimistic. Therefore, the number of pedestrians detected is estimated as follow:

- A lower extremity considered as 'pessimistic' view presenting the results without including the cases under poor light conditions possibly detected;
- An upper extremity considered as 'optimistic' view including in the results the cases detected in poor light conditions.

Algorithms that describe detection and AEB activation were coupled with the accident simulations. These coupled simulations were used to estimate the effect of the systems. Systems were evaluated by counting the number of pedestrian detections among the sample. The detection rate of each studied system was computed at different times before impact: at 2.5s and 1s before the impact. A number of maximum pedestrian detections for the whole sample was also estimated by running the entire simulation of each accident case.

5.1.3. Brake actuation

The ability of an AEB system to assist in complete collision avoidance is evaluated with reference to a time in the crash sequence: the last time-to-brake (LTTB). This particular moment is the time-to-collision related to a necessary distance to activate an emergency braking and to stop the vehicle before a safety clearance with the pedestrian. The LTTB is then retrieved by determining the corresponding braking distance with the following equations:

$$d_{stop} = v \cdot t_{tr} + \frac{v^2}{2 \cdot |a|} + d_{L\_offset} \qquad \text{(Equation 5.1)}$$

$$LTTB = \frac{d_{stop}}{v} \qquad \text{(Equation 5.2)}$$

Where: v is the approach speed of the vehicle given in m/s, t_{tr} is the brake lag (assumed to be equal to 0.2s), a is the deceleration that depends on the road conditions of the reconstructed accidents (m/s²), d_{L_offset} is the longitudinal clearance between the vehicle and the pedestrian set at 0.8 m.

The model of braking used in Equation 4.1 is similar to the model described in Chapter 3. It takes into account the intervention of the Brake Assist that improves the actuation phase. The braking lag phase has been modelled in order to represent the global behaviour of the Ped-CAMS (t_{tr} = 0.2s).

At LTTB, an estimation of the avoidance rate of collisions is established for each system. It is calculated by establishing whether the pedestrian is detected before this time.

The most relevant parameter which will be taken into account is the lateral position of the pedestrian relative to the vehicle trajectory. This parameter will be studied as it is assumed as a criterion for brake actuation. The position of the pedestrian is measured in Cartesian coordinates with the reference placed at the front end of the vehicle. The x-axis for computing the longitudinal distance of the pedestrian is aligned to the centreline axis of the vehicle (Figure 5.1). For the lateral position of the pedestrian, the y-axis is considered positive towards the left direction of the driver.

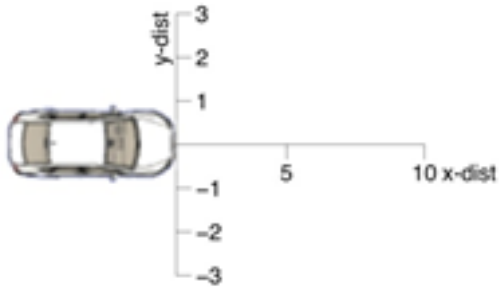

Figure 5.1. Space coordinate reference related to vehicle

5.1.4. Estimation of system response

The effects of each of the six pedestrian AEB systems were examined across the 100 reconstructed accidents. It was assumed that the autonomous intervention would be deployed under two conditions:

- at one second before impact;
- The pedestrian is located in the forward path of the vehicle.

It was assumed that the autonomous intervention would be deployed at one second before impact; hence, in each case, the position of the pedestrian at this time was determined.

The estimation of system response is presented in sets representing the possible outcomes of the simulation. For each accident analysed, there are three possible outcomes: avoided accidents, mitigated impact speeds, and no effect.

5.2.Results of the simulations

5.2.1. Position of the pedestrian 2.5 s before the impact

The crash scenarios were reconstructed over the 2.5 seconds before the impact. A map of the location of the pedestrians relative to the corresponding vehicles is drawn in Figure 5.2.

At 2.5 s before impact, it can be observed that all pedestrians masked by obstacles are located at a distance greater than 12 m ahead of the vehicles. Additionally, night-time cases, representing 17% of all cases, are also located at a distance greater than 12 m.

Table 5.2 gives the visibility of the pedestrians by the different sensors of each system. For example, the system S1 fitted with a camera and radar is likely to detect 66 pedestrians at 2.5 s before impact. The camera of the system is assumed to detect 43 pedestrians and increases the number of detections to 66 (43+23) with the help of the radar in the processing of cases under poor light conditions.

Additionally, it may be observed that, 2.5 s before the impact, approximately half of the pedestrians were potentially detectable by the majority of the systems. Among these cases, most of the pedestrians are located outside the forward path of the vehicle and only 4 of them are inside (see Figure 5.2).

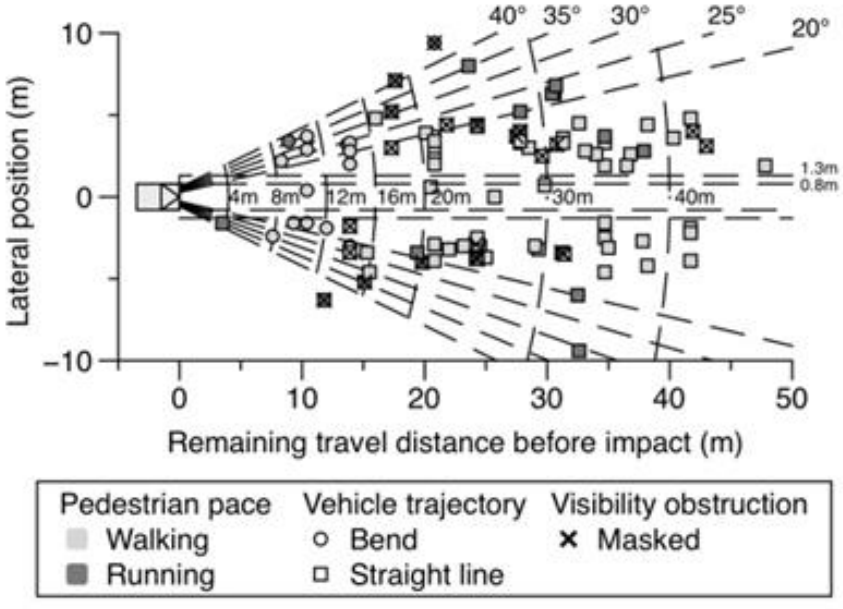

Figure 5.2. Pedestrian location at 2.5s before impact

Table 5.2. Detection rate at 2.5 sec before impact

		In FOV			Out FOV	Fusion	
System	Sensors	Good light	Poor light	Obstacle		Pessimistic Detected (Not detected)	Optimistic Detected (Not detected)
S1	Camera (48°)	43	23	19	15	43 (57)	66 (34)
	Radar (60°)	46	23	19	12		
S2	NIR cam. (25°)	40	8	15	37	47 (53)	55 (45)
	LIDAR (100°)	46	24	19	11		
S3	Stereo (25°)	37	16	16	31	37 (63)	37 (63)
S4	Stereo (44°)	41	21	19	19	41 (59)	57 (43)
	Lidar (22,5°)	37	16	15	32		
S5	Stereo (45°)	41	21	19	19	45 (55)	62 (38)
	NIR cam. (20°)	40	7	14	39		
	SRR (80°)	46	24	19	11		
S6	NIR stereo (25°)	37	16	16	31	37 (63)	43 (47)
	Radar (60°)	46	23	19	12		

5.2.2. Position of the pedestrian 1s before the impact

The crash set is described at a TTC of 1s. Before 1 s TTC, note that about a quarter of the drivers did react and trigger the brakes. So no response of AEB systems is assumed in these cases.

Figure 5.3 shows the position of the pedestrian relative to the vehicle at TTC=1s. 14 of the 100 pedestrians are located in the forward path within the width of the vehicle. This number rises to 25 pedestrians if the path is broadened to include an additional half a meter on both sides of the vehicle. Among this set, there are 10 pedestrians that were involved in accidents during night-time (Scenario 1) and 7 others that were involved in accidents at intersections involving vehicles turning (Scenario 3). The remaining set are pedestrians coming from the near and far side (Scenarios 4 and 5).

Regarding the pace, walking pedestrians are located laterally up to 2.5 m from the centreline of the vehicle with a mean of 0.6m (SD = 0.69m). The lateral position of running pedestrians relative to the vehicle ranges from 1.6 to 4.5 m with a mean of 2.6 m (SD = 0.78m).

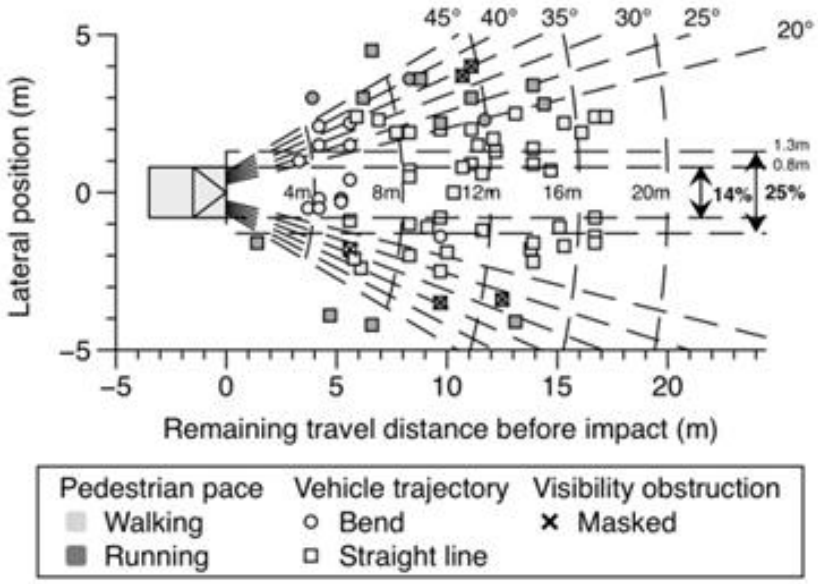

Figure 5.3. Pedestrian location at 1s before impact

The detection rate at 1s before impact is shown in Table 5.3. The systems can detect three quarters of the pedestrians (excepting for system S3). For example, the system S4 fitted with a stereo camera (44° FoV) and lidar (22.5° FoV) can detect 73 pedestrians at 1s TTC. The camera of the system can detect by itself 59 pedestrians plus 14 cases (among the 23 cases detectable under poor light conditions) detected by the combination of the camera coupled with the lidar.

Table 5.3. Detection rate at 1sec before impact

		In FOV			Out FOV	Fusion	
System	Sensors	Good light	Poor light	Obstacle		Pessimistic Detected (Not detected)	Optimistic Detected (Not detected)
S1	Camera (48°)	59	23	2	16	59 (41)	82 (18)
	Radar (60°)	57	25	2	16		
S2	NIR cam. (25°)	57	9	0	34	57 (43)	66 (34)
	LIDAR (100°)	57	25	2	16		
S3	Stereo (25°)	37	16	15	32	48 (52)	48 (52)
S4	Stereo (44°)	59	23	2	16	59 (41)	75 (25)
	Lidar (22,5°)	37	16	0	32		
S5	Stereo (45°)	59	23	2	16	59 (41)	82 (18)
	NIR cam. (20°)	57	9	0	34		
	SRR (80°)	57	25	2	16		
S6	NIR stereo (25°)	37	16	15	32	48 (52)	68 (32)
	Radar (60°)	57	25	2	16		

5.2.3. Maximum detection rate

The maximum detection rate is defined as in Table 5.4. The table distinguishes the reasons for pedestrian non detection: either out of FOV and/or poor light conditions. These are the basis for the pessimistic estimate of detection.

From the sample of reconstructed accidents, most of the systems would be able to detect about 90% of the pedestrians. According to the results of each sensor considered separately, it seems that the detection with camera alone is limited and could be substantially improved by combining with other sensors. Indeed, cameras appear as constrained in particular by the bad light conditions. Moreover, NIR cameras (with capabilities of night detection) have better detection rate than "basic" cameras (visible light cameras) even if these technologies have a smaller field of view.

Table 5.4. Maximum detection rate

		In FOV		Out FOV	Fusion	
System	Sensors	Good light	Poor light		Pessimistic Detected (Not detected)	Optimistic Detected (Not detected)
S1	Camera (48°)	65	28	7	65 (35)	93 (7)
	Radar (60°)	66	28	6		
S2	NIR cam. (25°)	56	28	16	56 (44)	84 (16)
	LIDAR (100°)	66	28	6		
S3	Stereo (25°)	54	28	18	54 (46)	54 (46)
S4	Stereo (44°)	65	28	7	65 (35)	93 (7)
	Lidar (22,5°)	48	28	24		
S5	Stereo (45°)	65	28	7	65 (35)	93 (7)
	NIR cam. (20°)	54	28	18		
	SRR (80°)	66	28	6		
S6	NIR stereo (25°)	54	28	18	54 (46)	82 (18)
	Radar (60°)	66	28	6		

The average travel speed of the vehicles was about 40 km/h (~11 m/s) (see Figure 4.4). Consequently, the necessary distance to activate an emergency braking and to stop the vehicle (including a safety clearance) from this speed is approximately 10.6 m. This value is composed as follows:

- 2.2 m to activate the brakes (brake lag of 0.2 s, see Section 2.5.3)
- 7.6 m to stop the vehicle (with a deceleration of -8 m/s²)
- 0.8 m of safety clearance with the pedestrian (see Section 2.5.3)

Finally, from this calculated distance, the average Last-Time-To-Brake (LTTB) is approximately 0.97s (S.D. 0.42s).

In order to estimate if the impact could have been avoided by each system, the pedestrian location was first displayed at this LTTB time (Figure 5.4). Considering a lateral offset of approximately 0.8m (which correspond to half of the vehicle width), it can be observed that 26% of the pedestrians are in front of the car. If this lateral distance is extended by half a meter, the number of cases rises to 39%. Beyond a lateral distance of 2.5 m from the centreline of the vehicle, all the pedestrians were running. Therefore, it appears that unless a system can distinguish running from walking pedestrians, AEB systems may not be able to avoid collisions with running pedestrians.

The longitudinal distance between the vehicle and the pedestrian at LTTB is linked to the travel speed of the vehicle. For example, pedestrians located within 2 m in front of the vehicle correspond to cases with very low speed (e.g. vehicle just starting at an intersection). It was also noticed that pedestrians located less than 4 m from the vehicle at LTTB correspond mostly to cases where the vehicles are turning (Scenario 3).

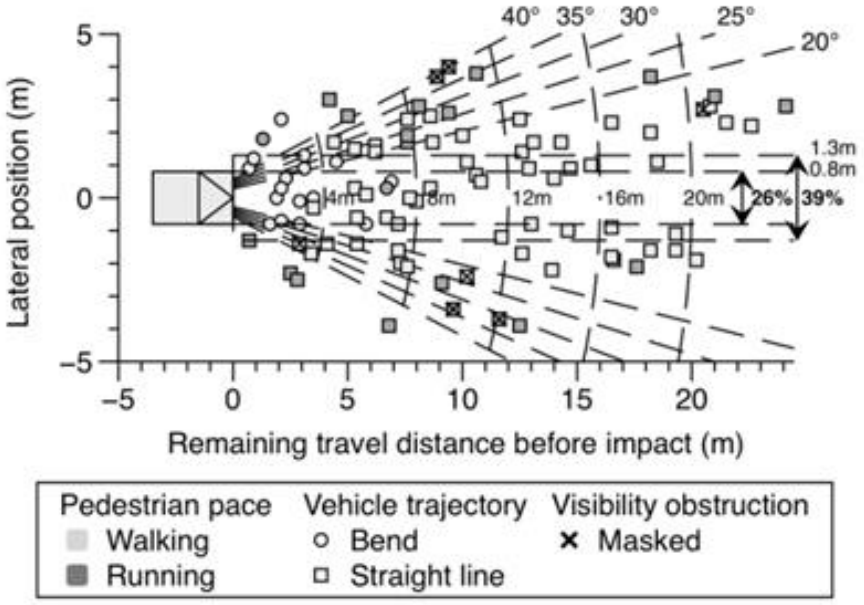

Figure 5.4. Pedestrian location at the Last Time-To-Brake

At the LTTB, the detection rate is estimated for the six Ped-CAMS (Table 5.5). From the sample of reconstructed accidents, there are two systems that could detect pedestrians early enough to avoid about 80% of the pedestrians (50% without cases under poor light conditions) if their AEB system were triggered. These systems have cameras with wide fields of view (45° and 48° FOV) combined with radar (also with a wide FOV). These systems appear to be able to detect pedestrians located far from the side of the vehicle (over 2.5 m from the centreline of the vehicle regarding Figure 5.4). Such pedestrians are typically running. An important consideration is then whether such systems can be designed with the sensitivity and specificity required to accurately respond to such pedestrians located so far laterally from the forward path of the vehicle.

Table 5.5. Detection rate at LTTB

		In FOV			Out FOV	Fusion	
System	Sensors	Good light	Poor light	Obstacle		Pessimistic Detected (Not detected)	Optimistic Detected (Not detected)
S1	Camera (48°)	54	28	6	12	54 (46)	82 (18)
	Radar (60°)	55	28	6	11		
S2	NIR cam. (25°)	50	11	1	38	50 (50)	61 (39)
	LIDAR (100°)	55	28	6	11		
S3	Stereo (25°)	41	23	1	35	41 (59)	41 (59)
S4	Stereo (44°)	59	23	5	13	59 (41)	72 (28)
	Lidar (22,5°)	35	13	1	51		
S5	Stereo (45°)	59	23	5	13	59 (41)	82 (18)
	NIR cam. (20°)	50	11	1	38		
	SRR (80°)	55	28	6	11		
S6	NIR stereo (25°)	41	23	1	35	41 (59)	64 (36)
	Radar (60°)	55	28	6	11		

Following this result, it is possible to estimate how many impacts have the potential to be avoided if autonomous braking were to be activated on a vehicle using one of the six Ped-CAMS at the earliest opportunity. Figure 5.5 shows for each system the distribution in boxes with whiskers of the elapsed time between detection (i.e. location of the pedestrians within the sensor's field of view) and LTTB. This time characteristic is called Time-To-Brake (TTB).

The boxes and whiskers represent the distribution of TTB values above 0.5sec. The remaining sets of TTB (values below 0.5sec) are plotted in black dots as outliers.

For each system, the proportion of accident cases included in the box plot is displayed next to the box. Accordingly, it may be noted that more than 50% of pedestrian crashes could be avoided if systems don't need to include additional criteria for triggering the brakes such as a criterion requiring the pedestrian to be within the forward path or a criterion that the TTC should be below 1s before intervening.

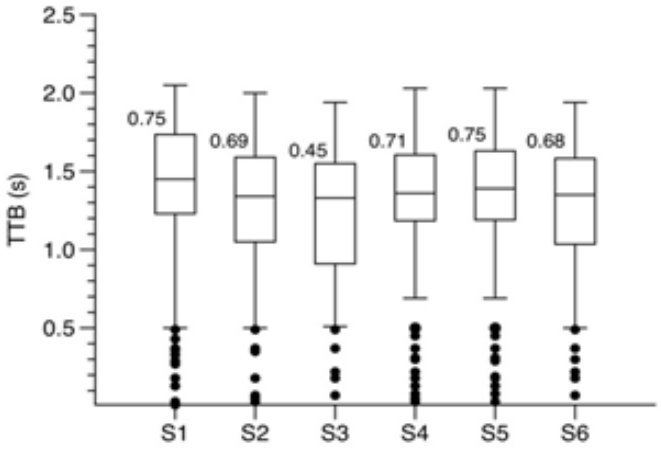

Figure 5.5. Distribution of TTB for the six pedestrian AEB systems

5.2.4. Estimation of speed reduction

The potential response of six Ped-CAM systems is displayed in Figure 4.6 according to the following conditions (see Section 5.1.4):

- the trigger of an AEB system is performed at 1s before the impact,
- the pedestrian is detected in the forward path defined as the vehicle width (1.8 m).

Three sets of cases are defined: avoided, mitigated and unaffected crashes. The system S3 has the lowest avoidance rate since it was considered unable to detect in bad light conditions (28% of the selected cases). For systems with multiple sensors, the systems S1 and S5 were assessed to presumably avoid 24% of pedestrians and mitigate 38% of the crashes.

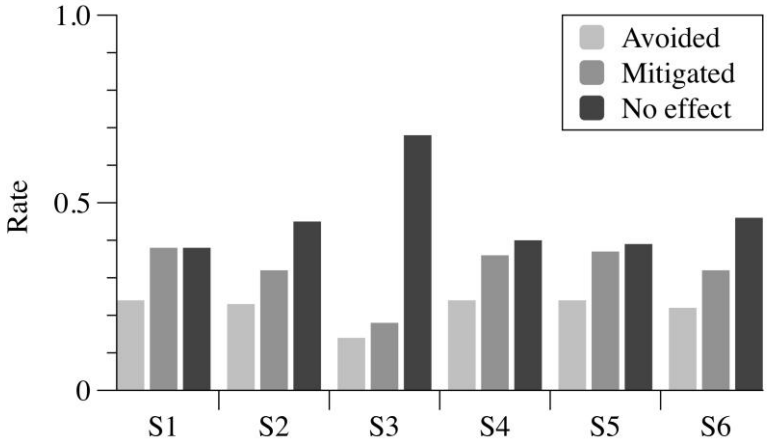

Figure 5.6. Responses of the six pedestrian AEB systems

In the cases the pedestrians are detected but the accidents are not avoided, if the brakes are autonomously applied before the collision occurs, the assessed impact speed is reduced. Consequently, the injury risk may be mitigated.

Figure 5.7 shows for each system the distribution of the impact speed (with the effect of autonomous braking activated). These distributions encompass all the cases: avoided, mitigated and unaffected. They are compared to the impact speed of the original set of accidents.

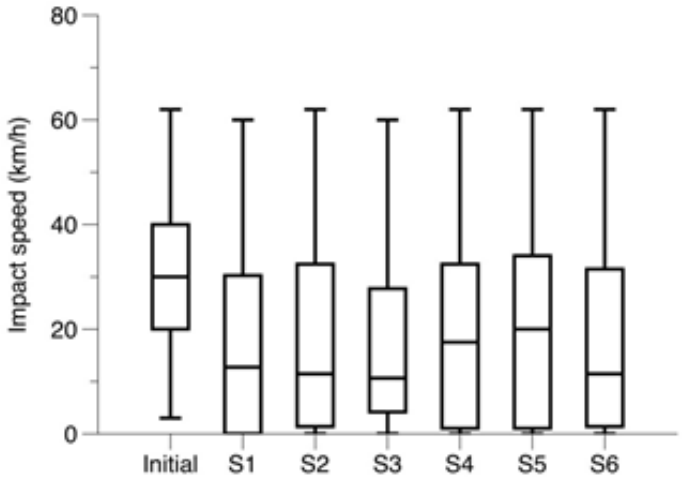

Figure 5.7. Distribution of the impact speed according to the system's reaction

With the deployment of the six pedestrian AEB systems, the average impact speed is reduced from 30 km/h down to 10 km/h. However, there were still cases with no decrease of the maximum speed (60 km/h).

The avoidance rate can also be retrieved in Figure 5.7. It can be noticed that the first quartile (i.e. the quarter of the accidents) has a zero impact speed from the results of the system S1. Excepting the system S3, the remaining systems have results close to the system S1. Hence, the systems appear to have an avoidance rate of about 25%.

Even if the system S3 would have intervened in the accidents less than the other systems, it would have been able to reduce impact speeds to less than 10 km/h in half the cases. The average is below the other systems. This result means that this system was the most effective at mitigating crashes while less effective at avoidance.

The overall impact speed distribution or box plot of the systems S2 and S6 on the one hand and the systems S4 and S5 on the other hand are similar. Looking at the five-number summary (the minimum or smallest observation, the lower quartile or first quartile, the median, the upper quartile or third quartile, the maximum or largest observation), these two pairs of systems have relatively close characteristics. It can be explained by the fact that these systems have approximately the same fields of view for their image sensors.

5.3.Discussion

5.3.1. Implications

The evolution of the detection rate was analysed according to the sample of 100 reconstructed accidents. A comparison is shown between detection at the beginning of the crash simulation (A), 1.0s TTC (B) and overall detection (C) in Figure 5.8. It can be observed that the pedestrians cannot be detected in all the 100 cases. The cases remaining undetectable are in majority cases occurring under poor light conditions and cases where pedestrians were masked by an obstacle.

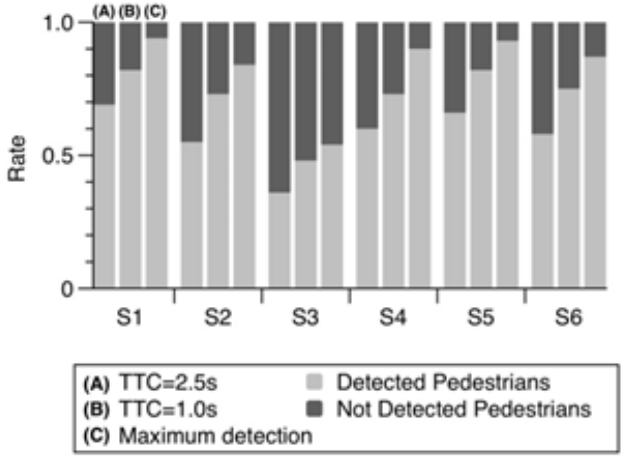

Figure 5.8. Detection rate at different TTC

Moreover, as expected, a sensor with a wide FOV improves the detection rate. For example, the system S1 composed of a radar (60° FOV) and a camera (48° FOV) could detect 94% of cases under study; while the system S6 with radar (60° FOV) and a Near-IR stereo camera (25° FOV) could detect 87% of cases.

According to the sample of reconstructed accidents, most of the systems reached high rates of detection (between 80 and 90%). These rates evolved over the timeline of the simulation. Many of the pedestrians who were, at first, out of range of the sensors entered progressively into the detection coverage area (see Figure 5.2 and Figure 5.3).

At an early stage of the accident simulation (2.5 s TTC), the systems had potentially detected more than 50% of the pedestrians. These earlier detections are important to be noticed regarding complementary systems which aim to warn the driver. Indeed, drivers could potentially trigger an emergency manoeuvre that could prevent or mitigate these accidents. These warning systems were not addressed in this research because it requires implementing in the simulation the driver behaviour (Lubbe and Kullgren, 2015).

The avoidance rate was addressed by studying the trigger of an AEB system at 1s before the impact and with a pedestrian detected in the forward path of the vehicle. About 25%

of the 100 cases could be potentially avoidable and 30 to 40% of cases could be mitigated. The remaining set concerned case where the system didn't respond because:

- The pedestrian was not detected or too late by the sensors giving no opportunity for an AEB system to be deployed (between 12% and 22%)
- The driver has reacted by braking earlier than 1s TTC so before the Ped-CAMS (23%)

It has to be noted that in these last cases, the drivers reacted before the systems would trigger the brakes. These cases represent about a quarter of the database used in this research (see Chapter 4). So if the sensors detected the pedestrian prior to the driver reaction, it could be assumed that the Ped-CAMS could reinforce the braking manoeuvre initiated by the driver. Among the 23 cases where the driver reacted, 15 cases could be covered by the system.

An ideal system would be triggering the emergency braking manoeuvre at LTTB (Last time-to-brake). As shown in Table 5.5, the avoidance rate of the majority of the systems was ranged from 70 to 80% of cases. These rates dropped off significantly to about 20% if the brakes of an active system are assumed to trigger according to two parameters: time-to-collision is 1 second and the detected pedestrian is located in the forward path of the vehicle.

It can be noticed that the time-based parameter has a negligible effect on the performance loss since the average LTTB relative to the accident cases is approximately 0.97s (S.D. 0.42s). Thus, the performance of crash avoidance is sensitive to the second parameter relative to the lateral position of the pedestrians from the vehicle side. In fact, regarding the location of the pedestrians at LTTB (Figure 5.4), there are only 26% of cases that are possibly avoidable. Adding an offset of half a meter from the vehicle path, the rate rises to 39%. So, the avoidance rate could be improved with a better system configuration according to this enhancement. It can be defined a lateral distance relative to the vehicle path from where the pedestrian is considered at risk of a collision. However, it is difficult to assess this parameter. On the task of predicting the pedestrian path (i.e. whether the pedestrian will stop or continue walking), systems are limited and cannot even reach the level of human performance (Keller et al., 2011b).

5.3.2. Limitations of the methodology

In the modelling process, some of the characteristics of a Ped-CAM system may not always be available. Information about processing time for pedestrian detection and decision making are difficult to obtain. These data can be found for some systems in surveys (e.g. Geronimo et al., 2010) or test track results (e.g. Matsui et al., 2011). Having more information about system could provide more realistic simulations.

Since some characteristics of systems are missing, assumptions were made to complete the system modelling. For example, the processing time for a system to detect a pedestrian was assumed to be 10 times the update rate of the camera sensor: that is, time for several repeated detections and also some time to process the image data. If a system

runs at 20 Hz, it was therefore assumed that this process took 0.5s. This assumed processing time appears to accord with published characteristics of systems (Seiniger et al., 2013).

Crash avoidance for systems triggering emergency braking manoeuvre was analysed when the pedestrian was located in the vehicle path. This analysis restrained the study to accident cases with frontal impact. Nevertheless, in the set of reconstructed pedestrian accident, there were 16% of cases with side impacts. As far as for these cases, the distribution of injury severity is comparable to those with frontal impacts (Lenard et al., 2014). So, it could be interesting to deploy systems for pedestrians crossing and reaching a certain critical lateral distance from the vehicle path.

Chapter 6

Challenges in pedestrian active safety

In the previous Chapter, the response of systems with pedestrian detection and autonomous intervention was examined by confronting these systems with real-world accident configurations. For each system under study, numerical simulations associated with a sample of accidents were processed in order to obtain the system's response.

The scope of this chapter is to enhance the previous method. The idea was to run just once the simulations of accidents then, from the results, to estimate the response of each Ped-CAM system. To reach this goal, a generic system was modelled in order to correlate the results of the simulations with the characteristics of a system under study. In other words, the results of the simulations using the generic model enable obtaining the performance metrics of a system with pedestrian detection and autonomous intervention.

Regarding the generic system, it was described by parameters related to detection and autonomous intervention. In this study, it is assumed that the generic system can detect 100% cases (i.e. false negative detections are not taken into account). This means that the generic system is not affected by poor light conditions as described in Chapter 4 and 5. Regarding the intervention of the system, only autonomous braking was considered for the same reason as explained in Chapter 3 (steering manoeuvres are too complicated to be handled). The generic system is then modelling a generic Pedestrian Autonomous Emergency Braking System (Ped-AEBS).

From this new approach, two different methods were successively developed. These two new methods were based on the modelling of a generic system. The generic system model was different from a method to another. Each of the two methods is described in this chapter with its corresponding generic model. They are compared to each other highlighting their strengths and limitations.

6.1.Method 1: Parametric analysis

6.1.1. General approach

A parametric study was conducted based on the functioning of detection sensors and autonomous braking intervention systems. The aim of this parametric study is to establish performance metrics for these systems. These performance metrics presented in graphs are obtained from the results of numerical simulations confronting a generic system with real accident configurations (using the methodology presented in Chapter 3). Hence, this approach enables to run once the simulation of accidents then to assess from the graphs obtained the effectiveness of Ped-AEB systems.

To establish the performance metrics of these Ped-AEB systems, it requires first to define a generic system. Then, the performance metrics is built from the simulation of the effect of this generic model on the 100 reconstructed accidents (the sample of accidents described in Chapter 4). By varying parameters of the generic model, several simulations are computed in order to obtain data clustered into graphs. The variable parameters of the model are related to detection and the activation of the autonomous braking manoeuvre. Hence, the graphs (or performance metrics) are parametric curves expressed in terms of proportion of pedestrians possibly detected and proportion of accidents possibly avoided.

6.1.2. Definition of the generic Ped-AEBS

The generic Ped-AEB system is modelled by two modules: detection and brake modules. For detection, the generic system is composed with solely a camera vision. Even if a system can detect a pedestrian only with merging the data from multiple sensors, images from cameras were systematically included in the detection process (Gandhi and Trivedi, 2007). Besides, the area covered by cameras is overlapped with those of radars or lidars (see Chapter 5). Moreover, for systems using stereo vision, they can be equated with a camera since they detect pedestrians only in the area overlapped by their two lenses (see Figure 6.1). Hence, these multiple sensor based systems can be modelled by a camera placed near the rear-view mirror.

Figure 6.1. Scheme illustrating a stereo vision

Concerning the actuators for triggering the emergency braking manoeuvre, they were modelled with an appropriate level of deceleration. The braking deceleration was estimated for each accident case according to the road surface condition provided by the in-depth database. In order to compare these real conditions with theoretical consideration, two others deceleration were considered:

- a higher deceleration with a value of -8m/s² (Brach and Brach, 2005; Byatt and Watts, 1981; Lechner and Ferrandez, 1990) which can be associated with good road conditions: dry surface, good tires, efficiency brake system …
- a lower deceleration with a value of -5m/s² which can be associated with poor road conditions: wet surface, deflate tires, worn brake system …

The brake force was assumed to have a step response excluding the existing system lag and the transient state. Figure 6.2 displays this brake model and compares it to a conventional one. This system lag and the transient state time interval (noted *L*) can be included in the time reaction of the detection system.

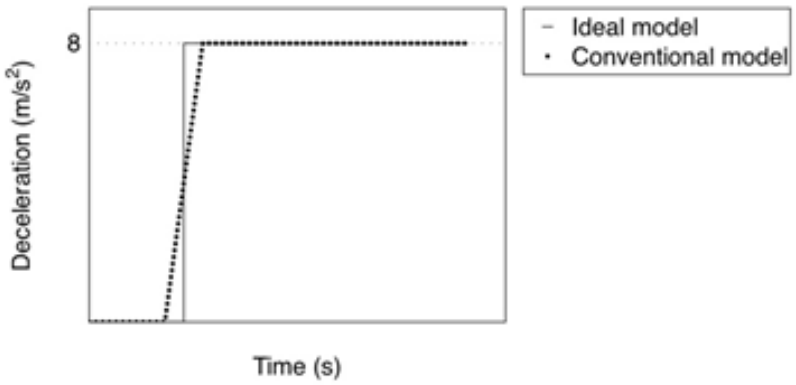

Figure 6.2. Comparison between the current and conventional brake model

6.1.3. Description of the method

Camera sensors have been modelled in this study by their range and Field Of View (FOV). Different FOV's were considered from 20° to 45° in order to evaluate its influence on detection. The range was fixed to 40 m according to the research conducted in the European project SAVE-U (Meinecke et al., 2003). The other characteristics of the camera like image processing or system lag are ignored since it is very difficult to get the required characteristics in the literature and consequently to model it numerically. Figure 6.3 illustrates a configuration of one camera as it has been considered in the accident modelling with a range and a FOV.

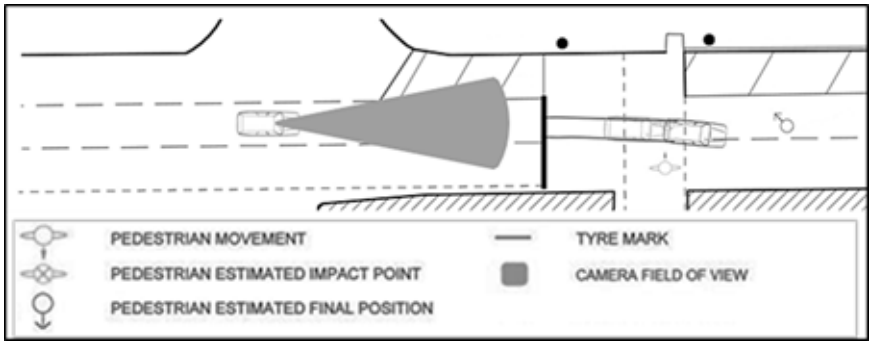

Figure 6.3. Scheme illustrating a crash representation including the active system

From the simulation, a set of data was extracted describing the characteristics of the accident at different pre-defined events. Data included the location of the pedestrian relative to the vehicle (the forward and lateral position), the speed of the vehicle (taking into account when the drivers accelerate or brake) and the Time-To-Collision (TTC). This last value is computed from the remaining travel distance before impact for the vehicle and its speed (Horst and Hogema, 1993).

There is a focus on two specific events occurring in the crash sequence: the first instant when the pedestrian is visible by the sensor (considered as detection) and the last moment when the brakes need to be applied to avoid the crash.

For the detection, it is a question of determining the moment when the pedestrian is entirely inside the camera's Fields Of View and was not masked by any obstacle.

The ability of an AEB system to assist in complete collision avoidance is evaluated with reference to a time in the crash sequence that is the last time-to-brake (LTTB). It corresponds to the time when the vehicle is located at a distance d_{stop} before the impact defined by the following equation:

$$d_{stop} = \frac{v^2}{2 * |a|} + d_{offset} \quad \text{(Equation 6.1)}$$

where V is the vehicle travelling speed (m/s), a is the deceleration that fluctuates depending on the road conditions of the reconstructed accidents (m/s²), d_{offset} is the vehicle longitudinal clearance from pedestrian set at 0.3 m.

At this sequence of the crash, an estimation of the avoidance rate of collisions is established for each camera FOV. It is calculated by verifying if the pedestrian is visible at LTTB even if the pedestrian is not yet on the roadway; i.e. it is possible for a system to avoid the crash (depending on the duration that the pedestrian is visible preceding the LTTB which is not measured here). Otherwise, if the pedestrian is out of the FOV or inside but masked by an obstacle, the case is considered mitigated (according to the moment of visibility before the collision) or unavoidable.

6.1.4. Results of the parametric analysis

Once the structure of the generic pedestrian active safety system has been set up, a batch of simulation are run varying two parameters:
- The sensor's field of view for detection assessment;
- The level of deceleration for avoidance assessment.

In this study, the trigger times (relative to the time of impact) and the distance before impact at which a system is able to trigger an autonomous emergency braking manoeuvre are analyzed.

6.1.4.1. **Graphs for detection assessment**

The detection of the pedestrians in each case is characterized by the Time-To-Collision (TTC) and the pedestrian location relative to the vehicle (the longitudinal and lateral position) at the first instant of detection. These detection parameters were evaluated for different Fields-Of-View (FOV) of the sensor: 20°, 25°, 30°, 35°, 40° and 45°.

Figure 6.4 gives the complementary cumulative frequencies for each of the three kinematics parameters according to the different FOV. From a general point of view, all the curves never reach 100% since there are about 10% of pedestrians that remain undetected till the crash. These undetected pedestrians are mainly due to a pedestrian location outside the sight of view of the sensor. It corresponds mostly with scenarios where vehicles are turning (scenario S2) and obviously cases where pedestrians are masked by obstacles (scenario S1). These scenarios end up with side and front corner impact configurations.

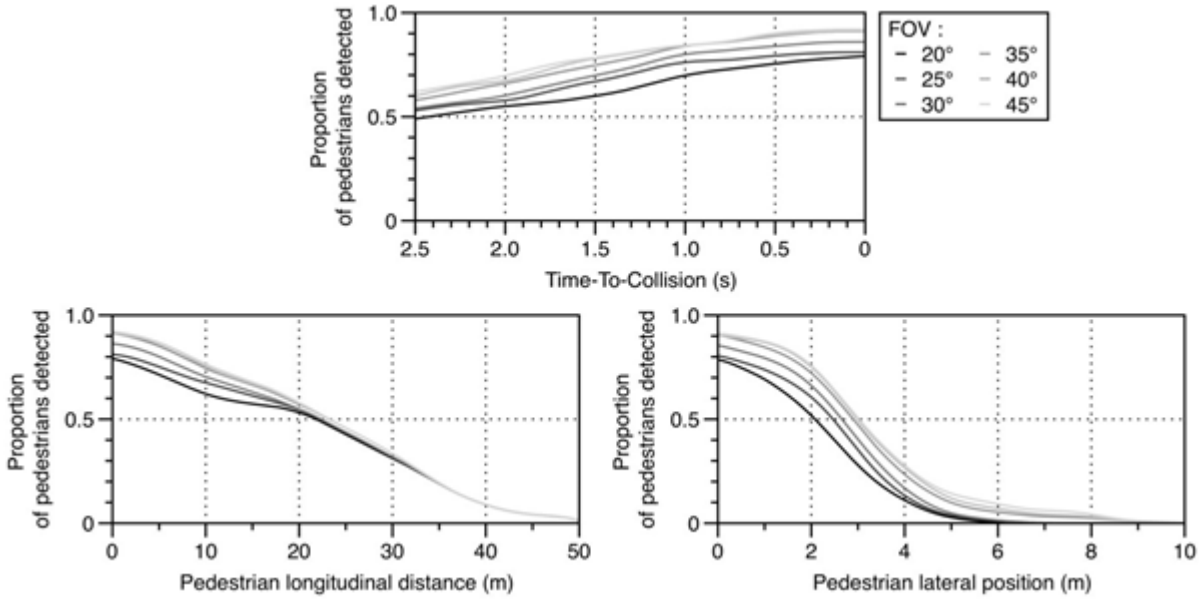

Figure 6.4. Rate of visible pedestrians for each kinematics parameter according to different FOVs

Concerning the time remaining before the impact, about 60% of pedestrians are visible by sensors with a FOV over 35° at 2.5 s before impact (first time of the simulation). Because the number of visible pedestrian remains quite similar with upper FOV, it appears that the optimum FOV for the camera is above 35°. As important as it is, this optimized FOV is expected to detect beyond 80% of hazards 1s before impact.

About the remaining distance before collision, it can be highlight that for all FOV more than half of the pedestrians are visible 20m before the impact and so can be detected. The variation of the FOV has a main role only during the last 20m with a better visibility according to a wider FOV. An angle of 35° seems to be optimal again. It appears also that 10% of the pedestrians are never visible even with a FOV upper than 35°. 40m before the impact, only 10% of pedestrians are visible.

Considering the lateral distance, about 50% of pedestrians are visible with a FOV of 20° from a distance in lateral of 2m. With a FOV upper than 35°, this rate is reached when pedestrians are located above 3m. For a FOV below of 35°, approximately no pedestrians are visible from a lateral distance of 6m. If it is considered a pedestrian situated on the far side of the road (i.e. at about 4.5m in lateral), a FOV lower than 30° allows a visible rate of 10% while for upper FOV, this rate reaches 20%. This rate takes into account all visible pedestrians even if they are not yet on the roadway.

6.1.4.2. **Graphs for braking assessment**

The kinematics parameters (TTC, longitudinal and lateral position of the pedestrian) are analyzed at the LTTB. This defines the requirements of an AEB system that can avoid the collision. The AEB performance refers to the crash avoidance rate obtained from the analysis of the 100 reconstructed crashes.

Figure 6.5 gives the cumulative frequency of the crash avoidance rate as a function of the kinematics parameters according to different sensor's FOV. It appears that 50% of accidents could be avoided if systems are able to be triggered 1s before the impact with a FOV upper than 35°. With a 20° FOV, the avoidance rate decreases to 40%. A threshold is reached at a LTTB equal to about 1.5 s; beyond this LTTB value, there is little improvement in the rate at which crashes can be avoided. Most challenges concerning crash avoidance occur between 0.5 s and 1.5 s (corresponding to the sharp slope of the curve). With a FOV of 35° or more, this threshold reaches an avoidance rate of 80%. Once more, it seems that this FOV is an optimal value as it includes pedestrians not yet on the roadway.

Regarding the longitudinal distance, if the system could be triggered more than 20 m before the impact, about 60% of accidents in this sample would have been avoided with a FOV of 20° (or 75% with a FOV of 35° or more). Beyond 20 m there seems to be no more gain in the rate of avoidance.

For the lateral distance, similar patterns are observed except that the threshold corresponds to a distance of approximately 3 m. The avoidance rate is affected by the FOV only at a distance beyond 2 m. At this lateral distance, about 50% of accidents can be avoided.

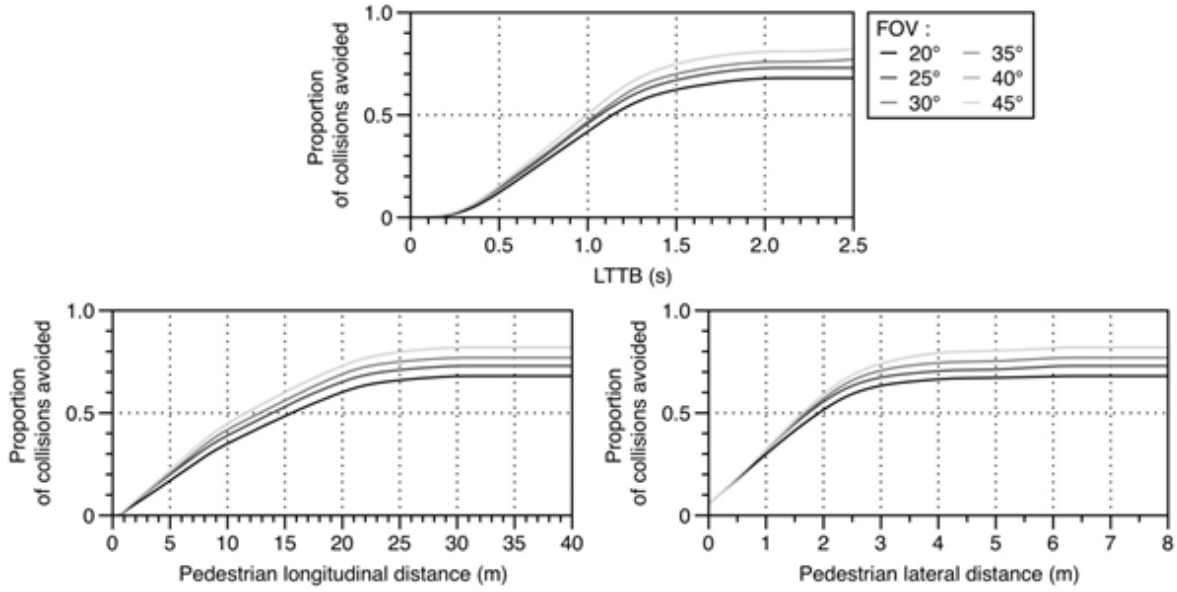

Figure 6.5. Pedestrian avoidance rate in function of kinematic parameters according to the camera FOV and the vehicle braking

A comparison between a "good" condition of deceleration and real condition (i.e. deceleration varying according to the state of the road and so the tyre/road friction coefficient) was conducted. It was observed that there is slightly no difference between the two levels of deceleration. The reason results in the small number of accident cases in our sample where the weather was bad inducing worse road drive conditions (i.e. a low tyre/road friction coefficient).

6.1.4.3. **Graphs for avoidance assessment**

In order to assess the available time for the system to react, the elapsed time between the instant when the pedestrian is visible ($t_{visible}$) and the LTTB was evaluated. Indeed this elapsed time corresponds to the duration available to detect the pedestrian and to trigger an AEB. This duration has been defined by Keller et al. (2011a) as the TTB (Time To Brake). Figure 6.6 shows the evolution of the complementary cumulative frequencies of avoided accidents according to this elapsed time and for the different FOV.

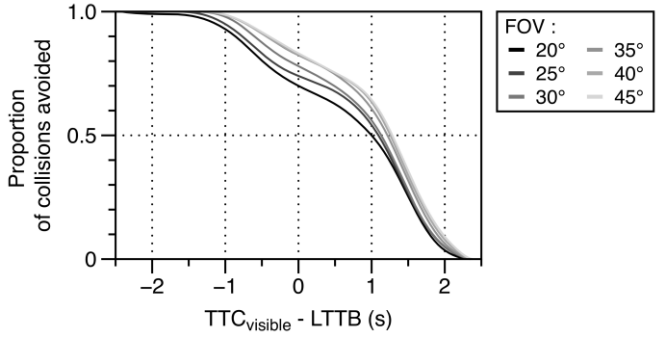

Figure 6.6. Complementary cumulative frequencies of the avoided accidents in function of the elapsed time from the visibility of the pedestrian to the LTTB for different FOV

These curves highlight that if the system is ideal, i.e. needs 0 second to react, the avoidance rate is comprised between 70% with a FOV of 20° and 83% with a FOV of 35°.

The deployment of an AEB system (Autonomous Emergency Braking system) was assessed by computing the LTTB (Last Time To Brake). The system lag and the building rate of a full braking (i.e. the transient phase of an AEB system) were not considered in this research because not enough information was available. However, this delay can be taken into account in the processing time (Figure 6.6). For example, adding the braking system delay of 0.5s (Edwards et al., 2014a) to a processing time of 0.5s leads to increase the elapsed time from the visibility of the pedestrian to the LTTB to 1s. So, according to Figure 6.6, for a FOV of 35°, it would decrease the avoidance rate from 75% to 63%. This rate could drop off considerably if the sum of the processing time and the delay is above 1s. Future systems will have to reduce these aforementioned parameters to improve their effectiveness.

Concerning the reaction time of an active safety system (from detection of the hazard to the decision making and deployment of the emergency manoeuvre), it could be expected to alert the driver by a warning system (visual and/or audible alarm). Since a driver needs in average 1s to react (Lee et al., 2002), only cases with an available time more than 1s can be considered. Such cases represent 50% of our database. So, among this rate, it is possible to avoid some accidents by prompting a response from the driver.

6.2. Method 2: Accident analysis relative to a fixed time

6.2.1. General approach

The second method is to analyse accidents at the time pedestrians walk into the lane of the vehicle; i.e. pedestrians are located at a lateral distance from the vehicles' side of 1 m (which corresponds to 1.8 m distance from the centreline of the vehicle).

This analytical method is conducted first by establishing a diagram presenting the characteristics of the sample of accidents. Given the speed of the vehicle (noted v), the instant when the pedestrian walks into the lane of the vehicle also defines the remaining time before collision (the time-to-collision, noted t) that is available for an AEB system to react. This diagram is then plotted according to the two following parameters:

- The time-to-collision;
- The travel speed of the vehicle.

The response of an AEB system is then examined as follow: the modelling of the effects of an AEB system is overlaid over the diagram which describes the sample of accidents in order to obtain the rate of avoided and mitigated accidents.

6.2.2. Definition of the model

As noticed in Chapter 5, AEB systems have the particularity of triggering an emergency manoeuvre at a determined time-to-collision. This time range or time horizon (noted T_h) corresponds to a longitudinal distance related to a given vehicle speed. This distance then varies according to the vehicle speed. Accordingly, the AEB system reacts only if the pedestrian is located within this distance. Otherwise, beyond that distance, the system ignores the physical presence of the pedestrian on the vehicle's path.

Moreover, the AEB system does not react immediately when the pedestrian is located far from the side of the vehicle although he/she is within the field of view of detection sensors. There is presumably a lateral distance from where the system starts monitoring the forward path.

Before the emergency braking manoeuvre is triggered, the AEB system required a time to react to the hazard (noted T_R). This time includes the processing of data from the detection of the pedestrian to the prediction of the collision. It can include also the lag of different components of a system such as the lag of the detection sensors and the brake lag. The reaction time starts when the pedestrian walks into the coverage area of the system and lasts until the brakes are fully developed (The brake response time can be included in the brake lag as it was assumed in Chapter 5).

From the aforementioned observations, an AEB system can be modelled as illustrated in Figure 6.7 using four parameters:
- the time horizon (noted T_h);
- the lateral distance from the side of the vehicle (noted l);
- the reaction time (noted T_R);
- the average vehicle deceleration (noted a).

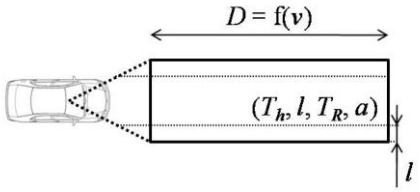

Figure 6.7. Modelling a pedestrian AEB system

In this research, three parameters were varied and analysed. The remaining parameter is the lateral distance of the system's coverage area. This parameter was fixed at 1m which corresponds to 1.8 m distance from the centreline of the vehicle.

To model the effect of a pedestrian AEB system, the reduced impact speed was calculated using the equation of motion assuming a uniform deceleration for the vehicle (Equation 6.2). The term $\min\{t;T_h\}$ was introduced in this equation to define the range of intervention of the system. From this term, the reaction time T_R was subtracted to obtain the effective time before impact when the brakes were fully developed.

$$u = v - |a| \cdot (\min\{t; T_h\} - T_R) \quad \text{(Equation 6.2)}$$

Where *v* is the travelling speed of the vehicle and *u* is its reduced impact speed.

The system may enable the vehicle to stop before collision or reduce the impact speed. Equation 6.2 can be then generalised:

$$u = \max\{0; v - |a| \cdot (\min\{t; T_h\} - T_R)\} \quad \text{(Equation 6.3)}$$

6.2.3. Estimation of AEB response

The objective of modelling the reaction of a Pedestrian AEB system was to examine its effects over various ranges of vehicle speed (*v*) and time-to-Collision (remaining time before the impact occurs, *t*). Equation 5.3 can illustrate the limits of a Ped-AEB system suggesting the three following responses:

- 'Avoidance' for which the AEB system can avoid the accident by stopping the vehicle before impact;
- 'Mitigation' for which the AEB system cannot avoid the accident but reduces the impact speed;
- 'No-effect' for which the challenge is such that the system cannot react quickly enough to respond prior to the collision.

The two first responses are separated by a boundary line where $u = 0$ and according to Equation 6.3: $v = |a| \cdot (t - T_R)$ if $T_R < t < T_h$ and $v = |a| \cdot (T_h - T_R)$ if $t \geq T_h$.

The line between the two last responses is controlled by $u = v$ which, according to Equation 6.3, is: $t = T_R$.

Accordingly, the three responses can be displayed on the diagram including combinations of vehicle speed and time-to-collision of actual accidents (Figure 6.8). Two other lines were added in the diagram to illustrate differences at the level of responses in the mitigated accidents. A first line was plotted for a combination of *v* and *t* where $u = 0.5v$; i.e. the impact speed was reduced to half the travelling speed. Another line was plotted for which $u = \sqrt[3.7]{0.5}v$ identifying the cases where the injury were reduced by half. The expression of the last line was a relationship estimated from the analysis of the risk curve established by Rósen and Sander (2009).

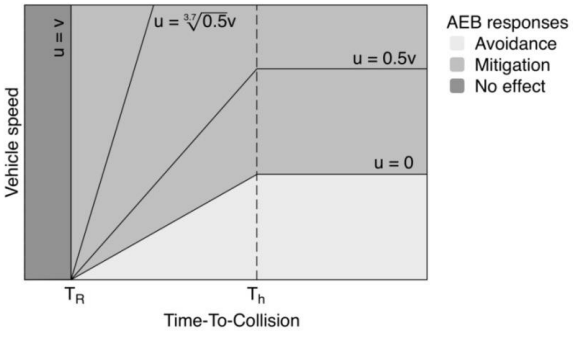

Figure 6.8. Diagram illustrating the different responses of a Ped-AEB system

6.2.4. Results of the analytical method

Figure 6.9 displays combinations of vehicle speed and time-to-collision over the sample of 100 accidents when the pedestrian was located within 1 m from the side of the vehicle. An Example of a Ped-AEB system is presented in this figure too. The system is characterised by a time horizon of 1.5 s, a reaction time of 0.5 s and a braking deceleration of 8 m/s².

According to the sample of crashes used in this research, the system described above can avoid 14% of pedestrians. It can be noticed that this system can avoid accidents for a vehicle approaching speed up to 30 km/h. At this speed, the pedestrians should be located beyond 12 m far from the front of the vehicle.

In the cases of impact speed reduction, the system intervenes in 71% of the cases with: 23% reduced by half and 59% where the injuries are halved.

The system has no effect in 15% of the cases. All the pedestrians in these cases are running. The system is not quickly enough to react to running pedestrians located at 1 m from the side of the vehicle.

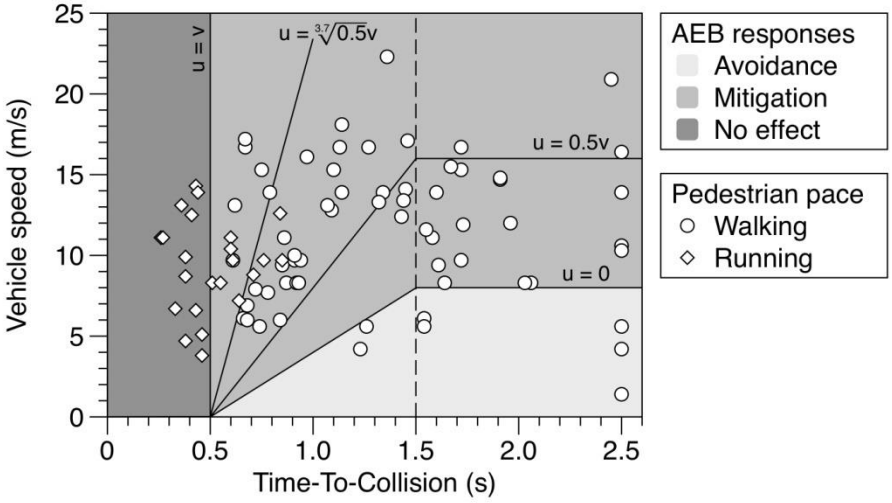

Figure 6.9. Performance of an AEB system with a time horizon of 1.5s, 0.5 s reaction time and a braking deceleration of 8 m/s²

6.3. Discussion

The modelling of the detection function of an active safety system and its implementation in the computational simulation of crash scenarios allows the relevant parameters in detecting pedestrians to be highlighted. It has to be noted that the effect of lighting/weather conditions was not considered in this study. This constraint concerns more specifically the algorithms of detection and the limits of the technology. Additionally, no sensitive analysis was conducted in order to assess the false positive rate. This issue is also considered to be related to the algorithms of detection and probably

differs from one active safety system to another. To include an assessment of the false positives to the simulation process, it suggests that the analysis should be conducted for a determined system.

In the set of 100 real accidents selected for this research, it appears that not all the pedestrians are visible prior to the crash. The remaining set of not visible pedestrians (about 10%) corresponds mostly with scenarios where vehicles are turning (scenario S2) and obviously cases where pedestrians are masked by obstacles (scenario S1). These scenarios end up with side and front corner impact configurations.

Different FOV were evaluated for the sensor model. The evaluation highlighted that the rate of visible pedestrians is increasing with a wider FOV for the camera. This rate is about 79% for a 20° cone angle while it reaches 92% for a 45° cone angle. Additionally, from a 35° FOV, a threshold in the visibility rate is observed. For example, at 1s before impact about 80% of pedestrians could be detected with this FOV. Beyond it, the pattern of the visibility rate is similar for any kinematic parameter: the Time-To-Collision, the longitudinal and lateral pedestrian position relative to the vehicle. These results are complementary and in accordance with those of Rosén et al. (2010) which show a slight reduction of the severely injured (as well as fatality) for camera sensors with a FOV from 40° to 180°. Thus, it can be considered that a FOV of 35° is relevant for pedestrian detection. An expansion of this work could be interesting to study the influence of a 35° FOV on the AEB for vehicle-to-vehicle collisions.

The deployment of an AEB system (Autonomous Emergency Braking system) was assessed by computing the LTTB (Last Time To Brake). The system lag and the building rate of a full braking (i.e. the transient phase of an AEB system) were not considered in this research because not enough information was available. However, this delay can be taken into account in the processing time (Figure 6.6). For example, adding the braking system delay of 0.5s to a processing time of 0.5s leads to increase the elapsed time from the visibility of the pedestrian to the LTTB to 1s. So, according to Figure 6.6, for a FOV of 35°, it would decrease the avoidance rate from 75% to 63%. This rate could drop off considerably if the sum of the processing time and the delay is above 1s. Future systems will have to reduce these aforementioned parameters to improve their effectiveness.

Once the LTTB is calculated, it is possible to determine the effect of the FOV of a camera-based system in terms of avoidance or mitigated cases. As for detection, the avoidance rate increase with the FOV until reaching a threshold at 35°. This FOV can avoid approximately 50% of crashes if the system trigger at 1s before impact. This rate is a little overestimated compared to the literature. Lindman et al. (2010) presented in a Case Study based on accident data from GIDAS the potential effectiveness of an active safety system developed by Volvo Cars (the CWAB-PD). It was estimated that CWAB-PD autonomous braking could avoid about 30% of all pedestrian accidents.

Concerning the reaction time of an active safety system (from detection of the hazard to the decision making and deployment of the emergency maneuver), the elapsed time between the instant when the pedestrian is visible and the LTTB was studied. During this

elapsed time, it could be expected to alert the driver by a warning system (visual and/or audible alarm). Since a driver needs in average 1s to react (Lee et al., 2002), only cases with an available time more than 1s can be considered. Such cases represent 50% of our database. So, among this rate, it is possible to avoid some accidents by prompting a response from the driver.

Finally, the graphs of the parametric study can be used to establish specifications for an active safety system. Indeed, according to the Figure 6.6, it can be observed that the objective of 75% of avoidance rate require 0,5s of reaction time for a 35° FOV.

Chapter 7

Perspectives: Effect of speed reduction

In the previous chapters of this thesis, the scope was to develop a method testing the response of autonomous intervention systems in terms of crash avoidance and speed reduction. This chapter presents an extension of the previous method with a simple example that demonstrates how speed reductions brought about by Ped-CAMS (more specifically Ped-AEB system since only braking is examined) will translate to reduction in biomechanical injury risk.

Several studies have analysed active pedestrian-safety systems and their effects on injury outcomes. There are either physical tests (full body dummy or component tests) or numerical simulation (virtual testing). For example, through numerical simulation of accidents from the GIDAS database, Rosén et al. (2010) evaluated an autonomous braking system that triggered one second prior to collision with a maximum deceleration of 0.6g. With a sensor field of view of 40°, the system was assessed to prevent 40% of fatal injuries and 27% of serious injuries. Moreover, finite element simulations using a pedestrian dummy model (Polar II) were performed by Fredriksson et al. (2011). This study showed that the HIC could drop by 82% for a speed impact reduction of 10 km/h resulting from an autonomous braking.

Pedestrian injury assessment can also be established using risk curves. The effect of speed reduction on changing injury severity was modelled coupling injury risk curve with the new impact speed distribution curve. Knowing this effect of speed reduction, (Anderson et al., 2012) developed a model that can evaluate the reduction in average risk for any given impact test result.

Primary safety systems can reduce the impact speed in case the accident is unavoidable and the pedestrian is detected. But, there is a question on the effect of speed reduction on variations in impact conditions. While the vehicle is braking after system triggering, the

pedestrian may continue walking which would induce a displacement of the pedestrian impact locations on the vehicle. These impacts may move to stiffer or softer areas inducing significant differences in the injury risk assessment.

In this chapter, analysed method is developed to investigate the effect of speed reduction on changing the impact boundary conditions. It is illustrated through the analysis of an accident case. A multibody modelling tool is used to simulate the crash configuration in order to relate the pedestrian injuries to the vehicle damage. A comparison is established between two configurations of the same accident with different impact boundary conditions: a configuration of the real accident and another modelling the mitigation effect of an AEB. The impact boundary conditions reproducing the effect of an AEB model were determined by simulating the functioning of the following attributes: a camera sensor with a 40° FOV, and a deceleration of -8 m/s² for the AEB system. This comparison survey is illustrated through an example of accident provided from in-depth investigation database.

7.1. General approach

The objective is to develop a method to investigate the effect of speed reduction (due to AEB deployment) on biomechanical injury risk. The potential effect of AEB system is estimated by comparing head injury risk between two crash configurations: an "original" accident and one modified by the effect of an AEB.

7.1.1. Methodology description

Figure 7.1 illustrates the method to examine the effects of AEB systems on pedestrian head injury risk. The building blocks of the method are distinguished by separating the effects of active safety from the effects of passive safety. The interaction of these effects is through the modulation of impact speed. Accordingly, the method includes three main parts:

- Initial task: Crash reconstruction;
- Second task: active safety assessment;
- Third task: secondary safety assessment.

The first task of the present method consists in modelling real vehicle/pedestrian accidents provided by in-depth crash investigation databases. As described in Chapter 3, the accidents are reconstructed by modelling the different crash components: the vehicle and pedestrian involved and the road environment (including obstacles that mask the pedestrian). Through a computational simulation, these crash components interact in a virtual environment that represents the real crash scenario.

The second step of the method is to model the AEB with its attributes: these attributes concern the detection system (sensors) and braking (AEB system). In order to test its effect on the reconstructed accidents, the AEB model is then coupled with the pre-crash

trajectory of a vehicle. This step of the assessment provides the potential effectiveness of the selected AEB in terms of crash avoidance and mitigation (speed reduction). But moreover, in the accident mitigation cases, the simulation determines modified pedestrian impact conditions: namely, the new pedestrian impact location and the new vehicle impact speed.

The last step is to estimate the effect of the modified impact conditions on injury risk. The changes in injury risk can then be described between the two crash configurations: the original collision and the mitigated collision.

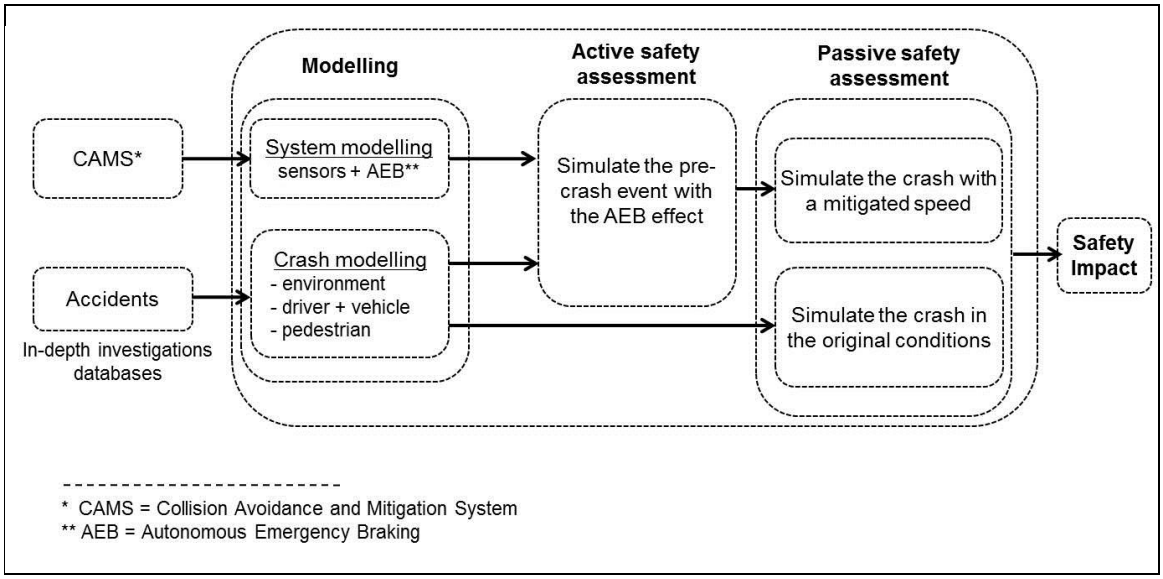

Figure 7.1. Methodology testing the response of AEB systems

7.1.2. Passive safety assessment

Passive safety assessment is obtained through the analysis of injury outcome. Numerical simulation of a pedestrian accident allows an estimation of injury risk and analyses the interfering influences such as the impact speed and the posture of the pedestrian.

For present purposes, the analysis of injury outcome was limited to head injury risks. In Chapter 2 (Section 2.2.4), it was shown that the head and lower extremities were the most frequently injured body region for pedestrians. Among severe injuries (AIS3+), head injuries are the most frequent (Longhitano et al., 2005). Additionally, a study of pedestrian collisions in Germany found that, for all severities, the most frequently injured body region for children is the head regardless of the severity (Yao et al., 2007).

For head injury assessment in pedestrian protection, the most commonly used parameter is the Head Injury Criterion (HIC). This criterion is described in detail in Chapter 2 (Section 2.4.1). To summarize, the HIC measures the head injury severity by expressing the effect of the linear acceleration of the head's centre-of-gravity and the duration of the acceleration. In this study, this duration is fixed to 15 milliseconds.

7.2.Multibody System modelling

Multibody system modelling is based on the theory of solid mechanics (Amirouche, 2006; Blundell and Harty, 2004). This approach allows large deformations to the system (large translations and rotations). Thus, MBS modelling has relatively short computation times compared to the other simulation methods such as the finite element method (since FE models reach high detail level). In this study, the multibody modelling was performed using the MADYMO® software (TNO Automotive, 2001).

MBS studies can also provide details about the transient state of the bodies and joints including accelerations and their contact or boundary conditions as the load-deflections and friction. In the field of accident analysis, multi-body modelling can be used to estimate injury risks. This will be more detailed in a following section describing the pedestrian model used in this study.

Multibody System (MBS) modelling has been used to reconstruct accidents and simulate the impact of pedestrians with vehicles. MBS is suited for parametric-type study; for example, methods have been developed to retrieve the impact configurations that best match the accident data collected such as the impact points on the vehicle, the pedestrian throw distance, the injuries, etc. (Linder et al., 2005; Serre et al., 2004; Untaroiu et al., 2009; Van Rooij et al., 2003).

Additionally, tools that utilise MBS modelling are also designed for injury risk estimation. There are many examples of MBS methods being used to evaluate the effectiveness of vehicle safety systems (Fredriksson et al., 2001; Hamacher et al., 2011; Oh et al., 2008; Sankarasubramanian et al., 2011).

In this study, MBS modelling was used to reconstruct an accident involving a pedestrian struck by a vehicle with or without the effect of an AEB. To set up an accident reconstruction with this approach, it is necessary to start by modelling the pedestrian and the vehicle before modelling the accident configuration. These steps are described in the following sections.

7.2.1. Vehicle model

In pedestrian accidents, the involved vehicles are represented by their front structure for multibody simulations. A vehicle model includes the following structures: the lower bumper, bumper, the bonnet edge, the bonnet, the windscreen and the a-pillar. These structures are modelled by ellipsoids arranged to correspond approximately to the geometry of the genuine vehicle. A number of measures are then performed to sketch the shape of the vehicle model (Serre et al., 2004) (Figure 7.2).

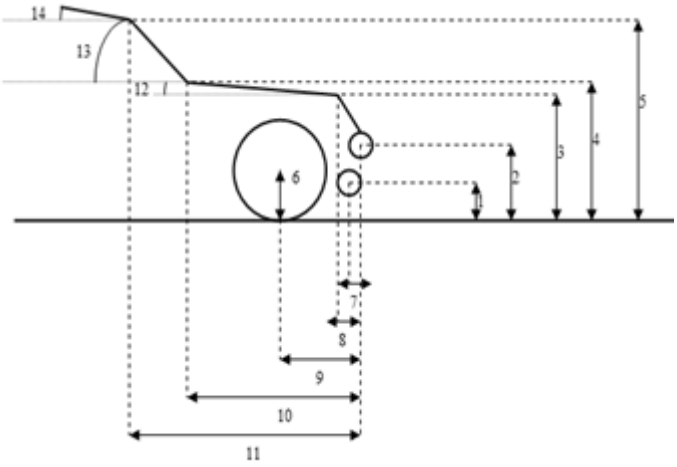

Figure 7.2. Measurement of a front shape vehicle (Serre et al., 2004)

The modelled structures of the vehicle are connected to a reference point in order to emulate the vehicle displacement and the vehicle pitch. Their stiffness characteristics were defined based on the results of experimental tests (Anderson et al., 2009, 2008).

7.2.2. Pedestrian model

The pedestrian model used in this research was developed and validated within a collaboration between the University of Chalmers (Yang et al., 2000), Faurecia (Glasson et al., 2000) and the Laboratory of Biomechanics and Application LBA-IFSTTAR (Cavallero et al., 1983). As described by (Serre et al., 2007), the original model is based on a 50th percentile male (with a height of 1.75 m and a weight of 78 kg) modelled by 35 bodies and joints and 85 ellipsoids. The biomechanical characteristics of the model are provided from the data of previous research (Kajzer et al., 1999; Yamada, 1970).

The selected pedestrian model has the advantage of predicting the risks of injuries sustained by the lower extremities. The leg is modelled by a number of bodies and joints (Figure 6.3) reproducing bone fractures and knee ligament injuries (Coulongeat et al., 2013).

Figure 7.3. Multibody model of a pedestrian (Serre et al., 2004)

7.2.3. Modelling the impact configuration

The objective of the multibody simulation is the validation of the accident reconstruction; i.e. checking if the kinematics of the accident is reproduced through the contact points between the pedestrian and the vehicle and the throw distance.

To reconstruct the real accident configuration, a parametric study is necessary due to a lack of information. Not all the data required for the crash phase reconstruction are available from the data collected and analysed during the in-depth accident investigation. It is not possible to get the posture of the pedestrian prior to impact although the arrangement of dents and marks on the bumper and the injuries related to the lower extremities may reveal some information. Such data required for the simulation are then studied as parameters (or variables) to establish the configuration of the real accident. To validate the configuration, the simulation has to reproduce the kinematics of the accident with the contact points between the pedestrian and the vehicle and the throw distance.

7.3. Case analysis

An accident case is analysed to investigate the effect of speed reduction on changing the impact boundary conditions. The accident case is firstly described by listing the data collected from the in-depth investigation. This accident is then reconstructed using a multibody simulation approach. Accordingly, the vehicle and pedestrian model used for the simulation are presented and the steps for the accident reconstruction are listed. Finally, the accident configuration validated through the simulation is presented.

7.3.1. Description of the accident case

The accident occurred during daytime (mid-morning) in an urban area between a 5-door hatchback and an elderly person crossing a one-way road via a pedestrian crosswalk. The driver did not react before the collision. He stated that he did not see the pedestrian because of sun glare. This information was confirmed by the investigators after filming the crash scene in the direction of the vehicle trajectory prior to impact. The driver started to brake right after the impact with the pedestrian. He assessed that he was driving at about 30 km/h.

The pedestrian was found lying on the ground at about 8 m from the estimated impact location. Using a simple analytical method (Searle and Searle, 1983), investigators estimated the impact speed was 35 km/h.

During the examination of the vehicle involved in the accident, the investigators measured dents and marks observed on the vehicle structures. An impact on the bonnet was located at 0.1 m from the vehicle centre line and for a WAD[1] of 0.87 m. This impact

[1] WAD: Wrap Around Distance measures the distance of the head impact location from the ground up around the front shape of the vehicle.

was assumed to be related to the pedestrian's pelvis. It was thereby inferred that the pedestrian crossed 56% of the vehicle width before the collision. Two impacts on the windscreen were also noted: a first one caused by the pedestrian shoulder (WAD = 1.68 m) and the second by the head (WAD= 2.13 m).

The pedestrian was admitted to hospital and died after 4 days. He sustained several severe injuries (MAIS3+): he suffered from a cerebral contusion and a subarachnoid haemorrhage. For lower extremity injuries, he had fractures of the left tibia and fibula as well as the right tibia and right femoral shaft.

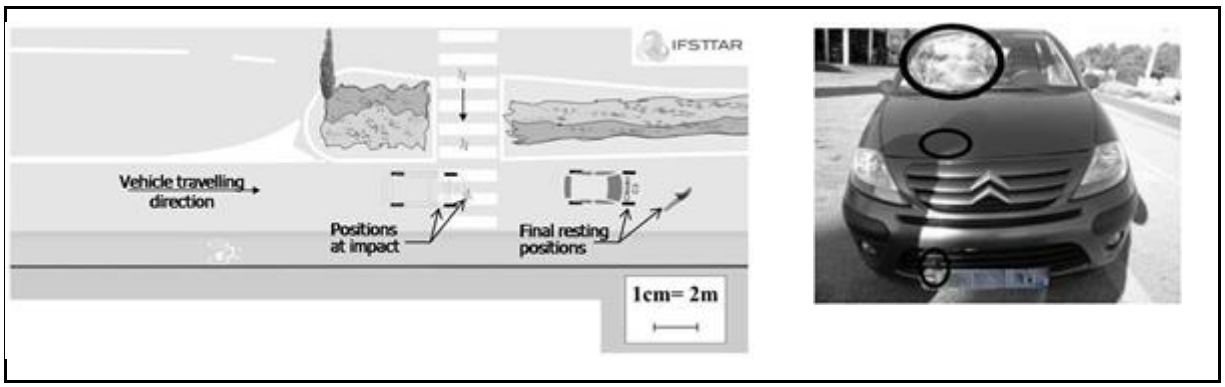

Figure 7.4. An illustration of the site diagram of the accident and a picture of the involved vehicle

7.3.2. Accident case modelling

The vehicle Citroën C3 model was provided from the database of the Laboratory of Biomechanics and Application of IFSTTAR (LBA-IFSTTAR). A Finite Element model of the vehicle front shape was used as a reference to build the geometry of the multibody model out of ellipsoid contact surfaces (Serre et al., 2011) (Figure 7.5).

Figure 7.5. Development of the vehicle multibody system model based on a finite element model

The mechanical properties of the different parts representing the vehicle front shape (bumper, bonnet and windscreen) were defined in a previous project. These properties are presented in Figure 7.6for each component modelling the front shape of the vehicle.

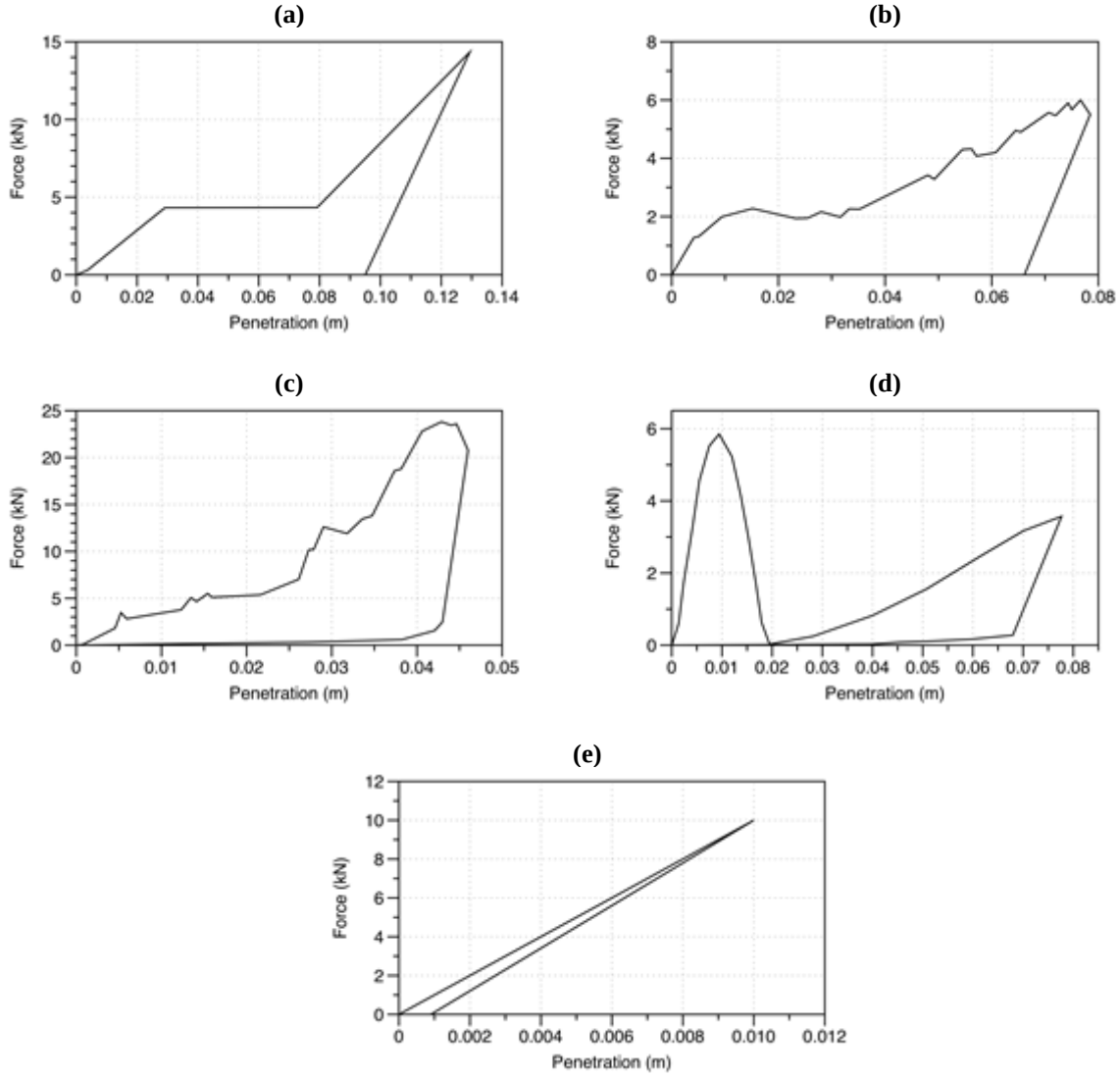

Figure 7.6. Characteristics for a) the bumper-to-leg contact, b) the leg-leading edge and leg/pelvis-lower bonnet contact c) the bonnet, d) windscreen and (e) A-pillar to head contact

The human body model described in Section 7.2.2 is scaled in order to correspond to the anthropometry of the person involved in the selected accident case. A program developed by the LBA-IFSTTAR was used to adapt the pedestrian body model. The program takes into consideration the height and weight of the pedestrian to generate the multibody model. These body dimensions are provided from the datasheet of the accident investigation report. The mechanical properties are not modified.

7.3.3. Reconstruction of the case

A first configuration is performed regarded as the most plausible by the in-depth investigation. The next step is then to realise a parametric study varying the posture of the pedestrian and the impact speed of the vehicle (Figure 7.7). In order to determine the closest configuration, a list of output parameters is correlated with all the data from in-depth investigation: the impact points on the vehicle, the injuries sustained by the

pedestrian and the throw distance. When the results of the simulation are in agreement with in-depth data collection, the correspondent crash configuration is kept as the real configuration.

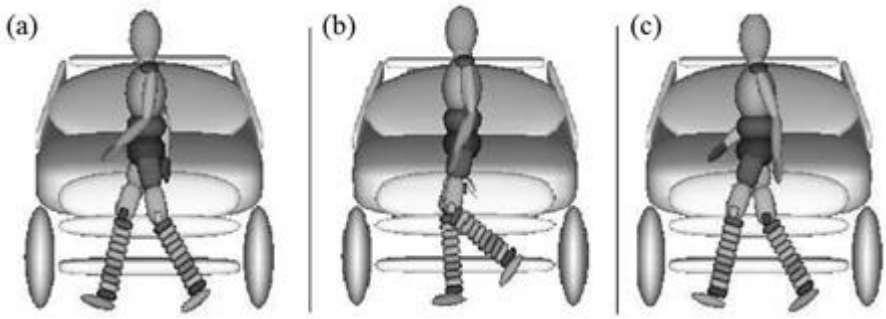

Figure 7.7. Different pedestrian postures

Once the parametric study is completed, the configuration at impact of the real accident is established (Figure 7.8). Describing the figure, the pedestrian model is walking with a constant speed of 3.6 km/h (1 m/s) and oriented perpendicularly to the vehicle trajectory with his right side facing the vehicle. The pedestrian posture corresponds to the switching phase of the weight bearing leg with the right foot positioned forward. The new calculated impact speed is 38 km/h and appears slightly higher than the first estimation provided by the in-depth investigation (35 km/h). Since the driver did not brake before the collision, the travelling speed of the vehicle is equal to the impact speed. The pre-crash phase can be then reconstructed.

Figure 7.8. Configuration of the real accident

The Madymo simulation of the real accident emulated the pedestrian kinematics at impact (Figure 7.9). It can be observed that the pedestrian had a somersault trajectory after hitting the vehicle front structures. The pedestrian body started first wrapping around the front shape of the vehicle. The pedestrian pelvis struck the bonnet (about 70 ms after the first impact), followed by the right shoulder and head hitting the windscreen (about 134 ms after the first impact).

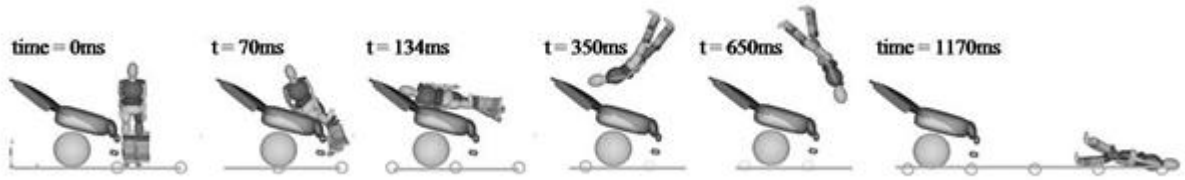

Figure 7.9. Simulation of the pedestrian kinematics at impact for the original accident

7.4. AEB effect on case study

7.4.1. Description of the AEB

In this study, a generic advanced driver assistance system is modelled to analyse its effect on pedestrian secondary safety. The generic system is a pedestrian detection system coupled with an Autonomous Emergency Braking system.

The detection system model is a camera sensor with a 40° field of view and a range of 50 m. It is assumed that the sensor is operating with a detection rate of 100% (no false responses from the system) even under sun glare. The system detects obstacles located within half metre away from the forward path of the vehicle and takes 0.55 seconds to process images from the camera to detect a pedestrian.

The braking manoeuvre is triggered if the pedestrian is detected in the forward path of the vehicle at a time-to-collision under 1 second. The system response is delayed and a building rate of 0.5 seconds is required to reach a full brake at -8 m/s² under good deceleration conditions (which is the case in the selected accident).

7.4.2. Reconstruction of the accident with AEB

The pre-crash scenario of the selected accident was simulated adding the effect of the generic AEB system modelled in this study. Figure 6.10 illustrate the sequence diagram of this pre-crash scenario. The pedestrian was visible to the sensor at 1.43 seconds TTC (i.e. when he was at half metre far from the forward path of the vehicle). The brakes were able to trigger at 0.68 seconds TTC corresponding to a distance of 7.2 m from the pedestrian. Regarding this available distance for braking, the accident was not avoided but the vehicle speed was reduced.

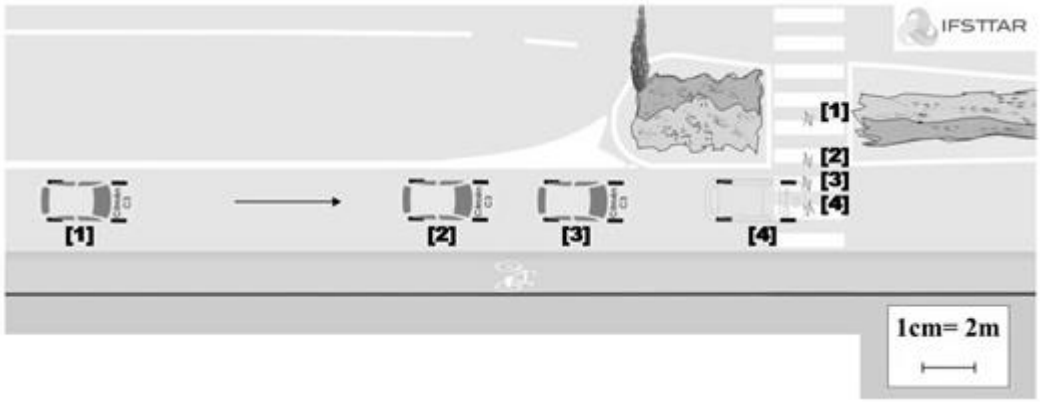

[1] Approaching phase
[2] Detection phase
[3] Brake triggering phase
[4] Impact phase

	[1]	[2]	[3]	[4]
Time-To-Collision (s)	2.5	1.43	0.68	0
Vehicle speed (km/h)	38	38	38	27
Distance to impact for the vehicle (m)	26.5	15.1	7.2	0
Pedestrian speed (m/s)	1	1	1	1
Distance to impact for the pedestrian (m)	2.5	1.43	0.68	0

Figure 7.10. Sequence diagram of the pre-crash scenario of the accident with AEB effect

At impact, the vehicle speed was assessed at 27 km/h. Since the vehicle is braking, a pitch angle was added in modelling the new configuration of the accident. Moreover, the location of the first impact was displaced assuming that the pedestrian was continuing walking. According to his locomotion, the pedestrian posture was also modified moving the weight bearing leg to his right foot (Figure 7.11).

Figure 7.11. Configuration of the accident with AEB effect

The simulation of the accident with AEB effect provided the pedestrian kinematics at impact (Figure 7.12). In this simulation, the pedestrian was projected with a wrap trajectory. The first impact after the contact with the bumper was the pelvis with the bonnet (about 100 ms) and then the head struck the windscreen at a wad of 185 (about 176 ms).

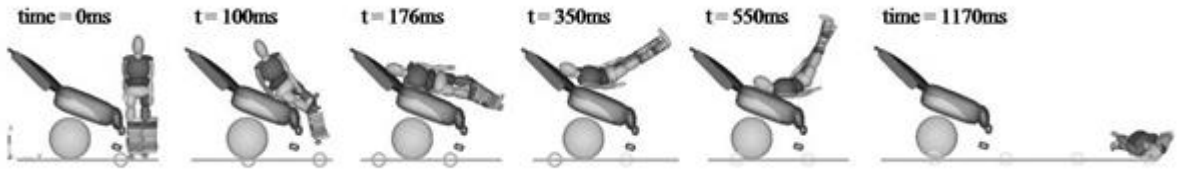

Figure 7.12. Pedestrian kinematics at impact for the accident with AEB effect

7.5. Analysis of changes induced by AEB in an accident scenario

A comparison between outcomes of a pedestrian accident involving a vehicle fitted with and without an AEB is examined starting with the initial impact conditions. The pedestrian kinematics at impact is then analysed describing the successive impacts with the vehicle front structures of the leg, the pelvis and the head of the pedestrian. Finally, injury risk assessments are achieved focusing only on the head injuries.

7.5.1. Impact configurations

The AEB model in our case study reduced the impact speed of the vehicle by 11 km/h (from 38 to 27 km/h). The speed reduction would likely lower the WAD for the head of the pedestrian. Yet, the pitch angle of the vehicle is different in the two accident configurations. In the original accident scenario, the driver did not brake while, in the new accident scenario involving an AEB, full braking is applied inducing a non-neglected pitch angle for the vehicle. This last parameter may affect the WAD as an opposite effect of the speed reduction (Fredriksson and Rosén, 2012). The speed reduction lowers the WAD while the difference in pitch angle elevates it.

Applying a full braking before the collision enabled additional hundredths of a second to the pedestrian crossing (according to our assumption). Consequently, the impact location (first contact with the vehicle structure) has been displaced of about 0.1 m comparing to the original configuration of the accident. The posture of the pedestrian has also evolved from two feet in contact with the ground (switching phase) to a one weight bearing leg corresponding to the right leg. Figure 7.13 illustrates the difference between the pedestrian postures for the two accident configurations. The displacement of impact location and the posture change of the pedestrian would probably induce additional changes in the impact location of the pedestrian head.

Figure 7.13. Configurations of the accidents with and without the AEB effect

7.5.2. Kinematics analysis

Image sequences of the two accidents (with and without the AEB effect) have been recorded in order to compare the pedestrian kinematics at impact (Figure 7.14). In the two cases, the pedestrian wraps around the front shape of the vehicle after the first impact. However, the second impact which corresponds to the head impact with the windscreen occurs differently. For the accident with the AEB effect, the time elapsed from the first impact of lower extremities with the bumper till the impact of the pedestrian head is about 176 ms instead of 134 ms. As expected, the head impact location has moved from the centre ($WAD\_{original}$ = 2,00 m) to the bottom of the windscreen (WAD_{AEB} = 1,85 m).

After the impact with the vehicle, the projection of the pedestrian changed from a configuration to another. It was a somersault trajectory in the original accident case while it was a wrap trajectory in the accident with AEB effect. Since the impact speed is reduced in the second case, the thrown distance of the pedestrian is lower (around 6 m).

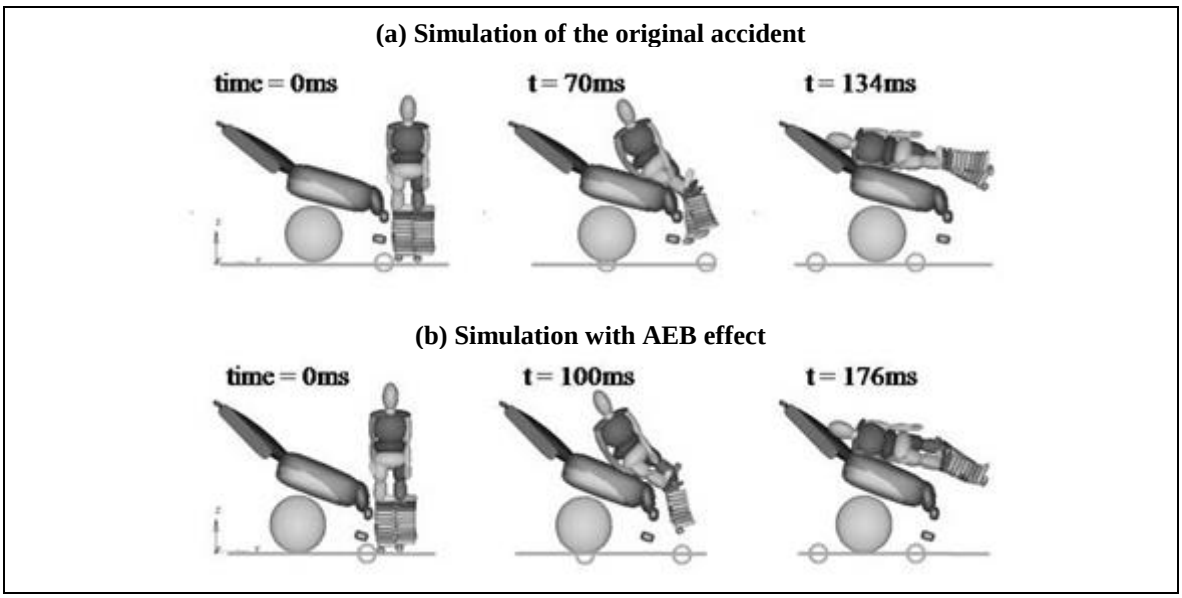

Figure 7.14. Post-impact kinematics of the pedestrian for the accidents with and without AEB effect

7.5.3. Head injury analysis (risk injury assessment)

By reducing the vehicle speed, AEB decreased the head impact velocity by 2.4 m/s (from 6.8 to 4.4 m/s) compared to the outcome of the original accident. Concerning the acceleration of the head, Figure 7.15 superimposes the signals resulting from the simulation of the two accidents (with and without the AEB effect). The two signals shows two distinct peaks of acceleration: one corresponding to the impact of the head with the windscreen and the other with the ground. In the original accident configuration, the acceleration magnitude of the first peak is considerably higher exceeding 80 g for more than 3 ms. For the accident with AEB effect, this magnitude is barely noticeable.

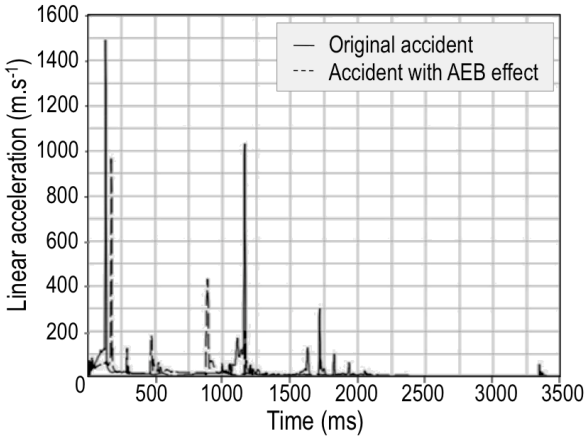

Figure 7.15. Head acceleration signals recorded through the simulation of the accidents with and without AEB effect

The last studied parameter is the head injury criterion assessed from duration of 15 ms (HIC15). In the original accident, the results of the simulation give a HIC of 1306 which corresponds to the head impact with the windscreen. This HIC value exceeds obviously 1000 since the case study concerns a fatal crash. In the case emulating the effect of AEB, the HIC was reduced to 435. Consequently, the risk injury was mitigated.

The HIC values and head impact speeds obtained from the two impact configurations are then verified using the relation established by Searson et al. (2012) expressing the influence of the impact speed on the HIC (Equation 6.1). The results from the simulation comply with this power function.

$$\frac{HIC_1}{HIC_2} = \left(\frac{v_1}{v_2}\right)^{5/2} \qquad \text{(Equation 6.1)}$$

7.6. Discussion

7.6.1. Findings

The consequences of advanced driver assistance systems on impact conditions were addressed in this chapter. This topic has been tackled by several researchers but none have included the impact location as a variable parameter. In this current study, it is

assumed that the pedestrian is likely to continue crossing the vehicle path due to time extension when the vehicle is decelerating. This hypothesis is valid for the case study illustrated in this chapter. The pedestrian involved in this case study stated that he saw the vehicle coming towards him but he continued crossing the road. Besides, Soni et al. (2013) showed that about 50% of pedestrians behaved similarly in the face of this situation. The results of the simulation showed that, for few hundredths of a second (0.1 s), the impact location was moved by 0.1 m. This displacement can be even more significance in the case where the pedestrian is running.

Adding the behaviour of the pedestrian to the emergency situation preceding the collision, the location of the pedestrian at impact is then displaced from the original accident configuration. Fredriksson and Rosén (2012) have explained that the wrap around distance of the pedestrian head changes with the vehicle speed and the pitch of the vehicle (verified according to a minimum height for the pedestrian). The additional displacement of the pedestrian prior to the impact and his/her evolved posture include also changes in impact points on the vehicle front structure. In the case study, the lateral displacements of the impact points (along the width of the vehicle) were minor. I suppose that greater displacements would be remarkable if pedestrians were running.

Head injury assessment was conducted to analyse the outcome of changing the impact conditions induced by an AEB. In our case study, the head acceleration and the head injury criterion were reduced (respectively from 150g to 100g and from 1306 to 435). The HIC and head impact speed reduction could also be verified by the relation established by Searson et al. (2012). This is understandable given that the head impacts of the two configurations remained close to the centre of the windscreen. And, the function of Searson et al. (2012) was set up from data of impact tests (based on component or sub-system tests) conducted on same impact locations but different test speeds.

7.6.2. Limitations

The methodology developed in this chapter is based on multibody modelling. This approach is effective in reproducing a realistic kinematics of the collision of a pedestrian with a vehicle (Anderson et al., 2009; Serre et al., 2005). It enables predicting appropriate head impact locations and head velocities (Anderson et al., 2008; Serre et al., 2007).

The limitation in the multibody modelling approach is the risk injury assessment. In fact, the vehicle is modelled according to its different front structures (lower bumper, bumper, edge and top of the bonnet, windscreen) yet each of these structures have been attributed with homogeneous stiffness properties. The influence of the structure stiffness has been previously studied and it appears that they have slightly effect on the head impact kinematic (Anderson et al., 2008). Actually, the stiffness of the windscreen, for instance, increases from its centre towards the edges. In this current case study, the head impacts of the two simulations (with and without AEB effect) were located not far from the centre of the windscreen. It would have been difficult to assess a HIC if the head would have impacted the bottom of the windscreen. It would have been difficult to estimate injury

risk mitigation. To solve this problem, a possibility is to use hybrid models combining multibody modelling with finite element methods. This last approach was already applied to study head injury mechanisms in several research (Yao et al., 2008).

A generic Ped-CAM system was used in the case study to illustrate the developed method. The system characteristics were representative of a wide range of systems found in the literature review (Edwards et al., 2014b). It was assumed that the performance of the system to detect pedestrians is considered ideal with a detection rate of 100% (i.e. there is no false negatives included in the system responses). This performance can be challenged since, in the case study, the ambient light was inclement caused by the sun glare. Moreover, regarding the characteristics of a system, the system may react and trigger the emergency braking at an earlier or later stage of the pre-crash phase. Hence, in order to analyse the effects of AEB, a sensitivity study could be considered in the simulation of the impact by varying not only the vehicle impact speed but also the impact location (or overlap) and the pedestrian posture.

The scope of this study is to include the displacement of the impact location to the variation of the impact conditions induced by an AEB. It was assumed that the pedestrian was continuing crossing the vehicle path due to time extension when the system was applying the emergency brakes. The evolution of the impact location from an accident configuration to another including the AEB effect depends on the pedestrian velocity. Indeed, if the pedestrian was running, the displacement of the impact location would be greater than if he/she was walking. For example, in an original accident configuration, a pedestrian collides the vehicle after crossing 75% of the vehicle path. For an emergency manoeuvre expanding the time-to-collision of 0.1 s, the pedestrian would cover a distance of 83% of the width of the front of the car if he/she was walking at 5 km/h (1.39 m/s). However, if the pedestrian is running at 10 km/h (2.78 m/s), he/she would cross 92% before impacting the front corner of the vehicle. Even if the increase in time due to the deceleration of the vehicle is short (about 0.1 of a second), the additional distance covered by the pedestrian can be significant depending on his/her speed.

To analyse the effects of a Ped-CAMS on pedestrian protection, effects examined were limited to head injury. It was analysed through the following parameters: the impact velocity of the head, its acceleration and the head injury criterion (HIC15). The last parameter is commonly used in head injury assessment for pedestrian protection. However, this parameter can be disputed since it does not consider the rotations of the head in its formulation.

7.7.Extension

7.7.1. Improve of the assessment methodology

A future step of this research is to improve the methodology to estimate injury mitigation. The real accident cases used for our research involve old model vehicles (from 1969 to 2009). Over the last fifteen years, the design of vehicles has been improved becoming

more pedestrian friendly. Thus, if the estimation of injury mitigation is computed from this sample of crashes, the results would be biased. To solve this issue, a three-step process is designed based on the methodology described in this chapter but with an intermediary stage.

The first step is to reconstruct the real accident in order to obtain the actual risk using the Head Injury Criterion (HIC). Then, the risk needs to be adjusted by reconstructing the same crash again but using a mid-sized sedan class having a 3 stars mark for the pedestrian safety assessment at NCAP (see Chapter 1 about test ranking). This step is important in order to change the implicated vehicle in the reconstruction process to one representing the actual vehicle model tendency. The last step consists of reconstructing the crash by adding the effect of the AEB system so that it will help to find out if the risk is reduced.

7.7.2. Analysis of the ground impact

A further aspect can be studied in the analysis of the effect of an AEB on injury mitigation. It concerns the assessment of the pedestrian impact with the ground. In general, for high impact speeds, the contact of the pedestrian with the vehicle front structures is the most severe impact (as shown through the recorded signals of the pedestrian head acceleration in Figure 7.15). The concern is whether the ground impact remains high when the impact speed is reduced. A comparison study between the impacts with the vehicle and the ground can be considered to complete the injury risk assessment. A first step will be measuring the tangential and normal components of the head acceleration and analysing which of these two parameters are influenced by the impact speed reduction.

7.7.3. Broaden the risk injury assessment

Implication of Ped-CAM systems on secondary pedestrian-safety was addressed in this study through the analysis of injury outcome. This assessment was focused only on head injury. The risk injury assessment could be then extended to lower extremity injury. The pedestrian model used in this study enables realizing an injury assessment on lower extremities. Indeed, this model has been designed to analyse the influence of bumper's geometry on the injuries sustained by the pedestrian lower extremities (Mo et al., 2014). It allows computing the following parameters:

- the elongation or rupture of knee ligaments;
- the shearing displacement and the bending angle of the knee;
- contact forces of the condyloid joints;
- the bending moments and shear forces relative to the leg.

The consequences of changing the impact conditions due to an AEB can be then addressed by analysing lower extremity injuries. The evolution of the pedestrian posture will be of significance regarding injury assessment.

Chapter 8

General discussion

In this chapter, we draw up a review of our research work. Firstly, in Section 8.1, a synthesis of this work is presented. Then, in Section 8.2, a comparison is established between this work and other relevant methods applied in the same research field (pedestrian active safety assessment). Finally, in Section 8.3, a global discussion on the advantages, limitations and some perspectives of this work is proposed.

8.1. Synthesis

The aim of this research was to investigate the response of Pedestrian Collision Avoidance and Mitigation Systems (Ped-CAMS). Indeed, these new technologies are currently integrated in the automotive safety and increasingly implemented in the vehicle market. Most of the studies are focused on developing tests scenarios. Instead of synthesising accidents into reference scenarios, the objective here is to examine the response of Ped-CAMSs to real accident scenarios.

The first objective consisted of gathering a representative sample of 100 real vehicle/pedestrian crashes provided by in-depth crash investigation at both IFSTTAR-LMA and CASR. These crashes have been recorded in sufficient details to reconstruct the trajectories of the vehicle and the pedestrian prior to the collision. This dataset of accidents was then represented in a parametric form as input to a computational simulation.

Accordingly, an assessment tool was developed to firstly reconstruct numerically various accidents and then to highlight the functional requirements for Ped-CAMS. Each crash was modelled by representing the vehicle, the pedestrian involved and the road environment. Every Ped-CAMS of interest was represented by the sensor and actuator parameters provided by literature review. Assumptions have been adopted due to lack of

data in the bibliography. The program was developed in order to insure modularity. Every processed accident can be saved and reused for complementary analysis like the investigation of a new system. His structure allows easily changes to be applied and updates according to different Ped-CAMS characteristics.

The main interest of the program is to compute the instant when the pedestrian was detected by the sensor. It determined in particular the eventual blind spot due to obstacles located on the sensor's field of view which mask the pedestrian.

According to the 100 reconstructed accidents, the relevant factors affecting the pedestrian detection concerned the travel speed of the vehicle, the pedestrian trajectory and his walking speed, the scene configuration with obstacles and the weather conditions. In particular, the results highlighted that one second before the impact, only 30% of pedestrian are located in front of the car and 90% of them are less than 20 m from the front of car.

The next step consisted in running a simulation batch confronting several existing pedestrian CAM systems to the set of 100 crash scenarios. Two groups from the outcomes were generated. One is representing the set of avoidable crashes relative to the active system. In this set, relevant outputs were processed to describe the ability of these systems to avoid the impact with the pedestrian. From the detection instant to the last moment for applying the appropriate countermeasure, several time-related measures were recorded determining the functional steps of the Active System. On the other hand, there was a set of non-avoidable crashes. This dataset informed on an estimated impact speed accordingly to the deployment of an Automatic Emergency Brake (AEB).

The safety potential of six Pedestrian CAM systems has been estimated. This analysis showed the functional requirements for these systems concerning the crash avoidance issues: weather condition, road curvature, obstacles, vehicle speed, pedestrian velocity, etc. It has been shown that about 40% of pedestrian accident could be avoided with most of the systems considered at 1s before the impact. It highlights the great interest to implement Ped-CAMS in vehicles for safety issue.

A generic AEB system based on a camera sensor for pedestrian detection was also modelled in order to identify the functionality of its different attributes in the timeline of each crash scenario: the detection, reaction and triggering of the brakes. These attributes were assessed to determine their relevance on pedestrian safety. The influence of the detection and the activation of the AEB system were explored by varying the Field Of View (FOV) of the sensor and the level of deceleration. According to these attribute, a system based on a camera with a FOV of 35° appeared relevant in terms of efficiency. It could allow high rates in detection (~90%) and if the system triggers at the Last Time To Brake, approximately 75% of accidents could be avoided. For the reaction of a system (from hazard detection to triggering the brakes), between 0,5 and 1s appears necessary. The results obtained in this work allowed evaluating the efficiency of active safety systems but can be used also to define their specifications.

The last step of the study is presented as a perspective describing a method to investigate the influence of the AEB on pedestrian injury risk. Previous studies have established a relationship between impact severity and speed impact variations. This project introduced a method to analyse the effect of speed reduction specifically on head impact conditions. These impact conditions were calculated through the use of multi-body system software. The first step was to reconstruct the real accident in order to obtain the actual risk using the Head Injury Criterion (HIC). Finally, a simulation was run with new impact conditions (impact location, vehicle speed…) induced by the deployment of an Automatic Emergency Brake (AEB).

8.2. Comparison to other methods

A comparison of different studies related to pedestrian active safety systems is first summarised in Table 8.1. A comparative analysis is then expanded according to the following features: method, data selection, accident modelling, system modelling and outcomes.

Table 8.1. Key features of comparable studies related to pedestrian active safety systems

	ASPECSS project	Helmer method	Seiniger et al. method	Rosén et al. method	Lindman et al. method	Hamdane
Objectives	Evaluation of speed reduction	Evaluation of the injury severity	Evaluation of speed reduction	Evaluation of fatalities and severely injured pedestrians	Evaluation of the injury risk for the Volvo system	Investigation of speed reduction
Approach	Experimental	Numerical simulation	Numerical simulation	Numerical simulation	Numerical simulation	Numerical simulation
Method	Test tracks	Stochastic method	Scenario tests	Accident reconstruction	Accident reconstruction	Accident reconstruction
Input data	Accident scenarios (60 config.) Frontal config.	Virtual scenarios (accident and non-accident scenarios) (18 million situations) Frontal config.	Accident scenarios (90 config.) Frontal config.	Real scenarios (243 cases) Frontal config.	Real scenarios Frontal config.	Real scenarios (100 cases) Frontal + side config.
Source	German national road traffic statistics GIDAS STATS19 SETRA	GIDAS PCDS (US)	GIDAS	GIDAS	GIDAS	IFSTTAR CASR

Table 8.1. (continued)

	ASPECSS project	Helmer method	Seiniger et al. method	Rosén et al. method	Lindman et al. method	Thesis
Vehicle modelling	Tested speeds: 10-60km/h	Speed: probability distribution < 80km/h	Tested speeds: 10-60km/h	Speeds from database	Speeds from database	Speeds from database
Pedestrian modelling	Slow walking: 3km/h Walking: 5km/h Running: 8km/h	Speed: probability distribution	Walking adults: 5km/h Running children: 8km/h	Speed estimation from Eberhardt and Himbert (1977)	Speed estimation from Eberhardt and Himbert (1977)	Speed estimation from Huang et al. (2008)
Detection modelling	-	No influence of light and weather conditions	Delay: 0.1, 0.2, 0.5s No influence of light and weather conditions	in FoV No influence of light and weather conditions	in FoV for 10 consecutive frames Influence of light conditions	in FoV for 10 consecutive frames Influence of light and weather conditions
AEB modelling	-	Actuation: 0.4s< TTC< 1.2s Deceleration: 4m/s² < Decel< 11 m/s² No influence of road conditions	Actuation: ped in veh path + predicted impact Deceleration max: 10m/s² No influence of road conditions	Actuation: 1s TTC Deceleration: max: 6m/s² No influence of road conditions	Deceleration: 3m/s² < Decel< 9 m/s² Influence of road conditions	Actuation: ped in veh path + 1s TTC Deceleration: 5m/s² < Decel< 8 m/s² Influence of road conditions
AES modelling	-	-	Lateral acceleration: 0m/s², 6m/s², 10m/s²	-	-	Maximum lateral acceleration: 6m/s²
End users	Consumer and regulatory tests car manufacturers	Automotive industry	Automotive industry	Automotive industry	Automotive industry	Automotive industry
References	Wisch et al. (2013b) Seiniger et al. (2014)	Helmer (2014)	Seiniger et al. (2013)	Rosén et al. (2010)	Lindman et al. (2010)	Hamdane et al. (2016) Hamdane et al. (2015)

8.2.2. Method

The simulation approach proposed in this research can be seen as an exploratory work for designing purposes. It is an investigation of the challenges in pedestrian active safety. It is an upstream work prior to develop on-board safety systems.

Experimental tests (track testing) based on accident scenarios are conducted to validate system design. As shown in Chapter 1 (Section 2.3.2.2), these track testing were developed from the analysis of accident data in terms of fatally and severely injured pedestrians in order to obtain weighting test scenarios. They are then limited in the number of test scenarios (see Table 2.2) unlike the numerical approach. Moreover, it is difficult to increase test scenarios since it is already time consuming to run the existing ones.

Concerning the outcomes of assessment methods found in the literature, two approaches were employed to measure the effectiveness of active safety systems in terms of pedestrian protection. The first approach is based on risk reduction at a level of injury severity (Lindman et al., 2010; Rosén et al., 2010). The second approach is estimating the gain in terms of speed reduction. This last approach was used in this current research even if the objective is not to evaluate but investigate the relevance of these safety systems.

8.2.3. Data selection

For simulation approaches, one of the main difficulties is to have enough accurate elements on the accidents to be able to describe them reliably in respect of factors important to autonomous detection. Detailed information are required like the impact location, the trajectories and velocities of the parts involved in the collision, the vehicle features and the location of eventual obstacles that masks the visibility of the pedestrian. In many cases, historical crash data provided from national databases (those maintained by the police, hospitals or insurance agencies) may not have been collected with such needs in mind. However, databases maintained by organizations conducting in-depth accident investigations (such as GIDAS, CASR, IFSTTAR…) include high level of details allowing robust accident reconstructions. Indeed, the validity of the present results depends on the quality of the numerical reconstructions of the accident. Accordingly, the accident data used in this research were provided from in-depth investigations. In return, these last databases are limited in the number of accident comparing to national accident data.

Through the analysis of in-depth investigation, accident cases have to be selected. As most of the studies (experimental and numerical approaches), accident cases occurred when vehicles were attempting reversing manoeuvres were excluded. Indeed, the assessment methods were not evaluating reverse camera systems. Contrary to most of the assessment methods, the sample of accidents used in the current research was not only covering frontal impact configuration but also including side impacts along the fender of

the vehicle. As a matter of fact, the distribution of injury severity for these cases is comparable to those with frontal impacts (Lenard et al., 2014). So, it was interesting to include these cases in the set of test scenarios in the current research.

Concerning cases where the braking was difficult to estimate, they were excluded contrary to what is considered in other methods. It concerns mainly cases where the driver reacted prior to impact with a partial braking. Indeed, these cases were considered problematic to reconstruct since it was difficult to nominate the timing or the strength of the reported braking and consequently the speed of the car. So, only cases with physical evidence of braking (skid marks) observed on the accident scene were reconstructed assuming that the driver reacted by a full braking. In these cases, it was easier to reconstruct the accident by assuming a constant braking deceleration according to the road surface condition (i.e. the deceleration is assumed to be -8m/s² for dry conditions and -6m/s² for wet conditions).

8.2.4. Accident modelling

All evaluation or investigation methods on active safety systems are based on accident data. Nevertheless, the use of accident data varies regarding the methods. Track tests and stochastic methods need specific analysis of accident data: from this analysis, accident features such as the vehicle and pedestrian speeds are gathered into test scenarios. These features are fixed in experimental tests, while, in the stochastic method (Helmer, 2015), they are presented in probabilistic distributions. Unlike the two aforementioned methods, the data required for accident reconstruction is directly provided from databases for the case-by-case simulation methods.

Vehicle speeds are generally provided in accident databases. These speeds are estimated from various techniques using information such as the length of the tire marks (found on the accident scene) and the pedestrian throw distance. The methods of Lindman et al. (2010) and Rosén et al. (2010) were both using vehicle travelling and impact speeds provided from GIDAS data. In this current research, although vehicle travelling speeds were also available in the databases, only impact speeds were used. Indeed, vehicle travelling speeds were recalculated in order to consider additional factors affecting the deceleration capacity such as the initiation of the brakes. For cases where drivers were assumed to apply a full braking, a mean deceleration is estimated for wet and dry road conditions corresponding with friction coefficient values found in the accident databases.

Although the accident data are massive and detailed (since it is provided from in-depth investigations), there is definitely a lack of specific information. The pedestrian walking speed is generally missing since it is very difficult to find relevant clues at scene. Therefore, in accident reconstruction as well as in track tests, pedestrian speed is provided from various other sources in the literature. These observational and/or experimental studies usually present pedestrian speed according to the pace, age and gender. Within the ASPECSS project, pedestrian speed values proposed in test scenarios were not differentiated according to the age and gender but varied according to the pace: walking

(5km/h) and running (8km/h) (Wisch et al., 2013b). Seiniger et al. (2013) used the same pedestrian speeds as in ASPECSS project focusing on running children (8km/h) and walking adults (5km/h). In this current research, the pedestrian speed data was provided from the work of Eubanks et al. (2004) quoted by Huang et al. (2008) and was estimated for 50% percentile speed according to the age and pace of the pedestrian: walking and running. The studies of Lindman et al. (2010) and Rosén et al. (2010) were also using estimated speeds, but from another source (Eberhardt and Himbert, 1977) and for different categories of pedestrian pace: walking, walking slowly, walking briskly and running.

During simulations, the visibility of the pedestrian from the sight of detection sensors is assessed. Obstacles that may obstruct this visibility have to be included in the accident modelling since they may reduce the time for an active safety system to trigger before impact. In one of their pedestrian test scenarios, Seiniger et al. (2013) have modelled an obstacle around 1 m away from the side of the vehicle in accordance with the findings in the ASPECSS project (Wisch et al., 2013b). Lindman et al. (2010) assumed that the pedestrian was not ASPECSS masked when he/she was located at 1.6 m or less from the vehicle front centre. Contrary to the other methods, Rosén et al. (2010) as well as the current method were modelling obstacles for each case according to information in the accident databases. In this study, it was then possible to test the relevance of systems for scenarios where pedestrians came out from obstacles located at less than 1m from the vehicle side.

8.2.5. System modelling

System modelling is required for the numerical simulation of the pedestrian active safety systems. Ped-CAMSs are typically modelled according to their functions: detection including the processing time and the actuation of the emergency manoeuvre.

Detection modelling was addressed by Rosén et al. (2010) as the pedestrian enters in the field of view of one sensor positioned next to the rear view mirror. Lindman et al. (2010) assessed the Volvo system (CWAB-PD: Collision Warning with Full Auto Brake and Pedestrian Detection) and considered the pedestrian detected if he is located entirely in the field of view of the camera for five consecutive frames. Similarly, the current method assumed detection for pedestrians inside the coverage area of the system (demarcated by the overlap of the sight of different sensors integrated in the system) for 10 consecutive frames. The last assumption was somehow in accordance with the model described by Seiniger et al. (2013): i.e. if a system, for instance, works at 20 Hz, it would require 0.5s to detect a pedestrian. The sensitivity of this last parameter was nevertheless investigated in Chapter 6 through the analysis of the elapsed time between the instant when the pedestrian was visible ($t_{visible}$) and the last time the brakes needed to be applied to avoid the accident.

Another important feature in the detection modelling is the effect of light conditions. Most of the numerical approaches (case-by-case studies as well as the stochastic method) considered the system operating independently from light and weather conditions. Only

Lindman et al. (2010) have introduced briefly the influence of light conditions without distinguishing day and night time crashes but through estimating the relevance of light condition. In this current research, light and weather conditions (darkness, sun glare, heavy rain) were taken into account in the analysis of test results of the system response. The test results were presented according to two approaches: an optimistic view excluding the effect of these conditions (under-estimating boundary) and a pessimistic view considering systems not functioning under these conditions (over-estimating boundary).

For the emergency braking manoeuvre, it was modelled according to its actuation and level of deceleration. Rosén et al. (2010) used a time based measure (1s TTC), while Helmer (2014) varied this time characteristic from 0.4 to 1.2s TTC. Seiniger et al. (2013) have not defined a time but conditions were tested to consider the system triggering: pedestrian almost in the vehicle path and predicted collision if braking was not applied. In this current research, it was assumed that the autonomous intervention would be deployed under two conditions: 1) the pedestrian (previously detected) is located in the forward path of the vehicle, 2) at 1s before impact. The sensitivity of these two last conditions were assessed in Chapter 6 by analysing the response of a system at the last time the brakes needed to be applied to avoid the accident.

Most of the numerical methods were not considering the influence of road-tire friction in the deceleration applied by the system. While Seiniger et al. (2013) and Rosén et al. (2010) have fixed a maximum deceleration of 10m/s², Helmer (2014) presented a study varying the level of deceleration from 4 to 11 m/s². Contrary to these methods, Lindman et al. (2010) included in their model the influence of road conditions on deceleration capacity and differentiated the level of deceleration for dry, moist or wet roads, and those covered with ice or snow. In line with the last method, the deceleration was related to road conditions in this current research in order to reproduce a level of deceleration in accordance with the original accident.

Concerning the emergency steering manoeuvre, it was only investigated by Seiniger et al. (2013). In this current research, it was, however, modelled in the simulation tool (see Chapter 3 Section 3.5.3.2) but not tested on the accident sample. The steering manoeuvre was excluded because it is restricted by factors not available for the simulation such as the traffic situation (missing in the accident databases).

8.2.6. Outcomes

Six pedestrian collision avoidance and mitigation systems were selected to apply the method developed in this research. Among these systems, one was slightly similar to the system evaluated in the study of Lindman et al. (2010). For this system (CWAB-PD), it was estimated here that 24% of the considered cases were completely avoided, while Lindman et al. (2010) have shown that this number represented 30% of their cases. This difference can be explained by the choices in the system modelling: the current method assumed detection for pedestrians inside the coverage area of the system for 5 more

consecutive frames than the other method. This means that the system had a longer time delay to detect a pedestrian which led to later braking actuation and so less cases to be avoided.

The method developed in this thesis has shown the rate of visible pedestrians increased with a wider sensor coverage area. For a camera field of view of 35°, a threshold in the visibility rate was observed. At 1 s before impact about 80% of pedestrians could be detected with this FOV. Beyond it, the pattern of the visibility rate was similar for any kinematic parameter: the time-to-collision, the longitudinal and lateral pedestrian position relative to the vehicle. These results were complementary and in accordance with those of Rosén et al. (2010) which showed a slight reduction of the severely injured (as well as fatality) for camera sensors with a FOV from 40° to 180°. Thus, it can be considered that a FOV of 35° is relevant for pedestrian detection.

8.3.Limits and perspective

The first limitation which could be considered concerns the size of the sample (100 accident cases). The present study could be obviously extended to a larger panel of accidents in order to ensure a better representativeness of the sample and to cover a broad range of configurations. However, a previous study showed that a sample of one hundred crashes can reduce the probability of not considering an accident scenario less than 5% (Brenac and Megherbi, 1996). This result tends to show that the possible statistical bias due to the sample size is limited. The representativeness issue could be also resolved by using cluster analyses of vehicle/pedestrian crash data. Weighting factors could be added to crash scenarios reflecting real accident frequencies and, thus, leading to estimate the benefits of each technology.

Modelling the crash scenario depends of the availability and the quality of crash data required for the reconstruction. There is inevitably some fuzzy and even missing data to complete the reconstruction of a crash. This matter led to establish assumptions and define a procedure for modelling the different components of an accident in order to realize reliable computational simulations of the crash scenarios. For example, the pedestrian speed is only estimated in in-depth investigations from a qualitative approach (statements). It was so assumed that for each age group this speed was constant before the impact and corresponded to the 50th percentile velocity. These hypotheses raise an important issue concerning the accuracy of the accident reconstruction. To remove any doubt, a detailed sensitivity study has to be developed in order to evaluate the influence of specific factors (e.g. pedestrian speed, vehicle speed) on the pedestrian CAM systems benefits.

Otherwise, false activation calls were not considered in this study. Indeed, this issue concerns more specifically the algorithms of detection and the limits of the used technology. Then, the false positive rate varies from one specific active safety system to another. To include an assessment of the false positives to this study, the analysis should integrate this characteristic for each system.

In terms of perspective concerning global pedestrian safety, it should be also interesting to evaluate the benefits of integrated safety systems which coupled active and passive safety features. Future works can be addressed in three steps by analysing the injury risk for the main injured body segments (head, lower leg, thorax, and pelvis):

- The original accident configuration is firstly simulated to calculate the actual risk.
- The second step consists of reconstructing the crash by adding the effect of the AEB system so that it will help to find out if the risk is reduced.
- The last step is to adjust the risk by reconstructing the same crash again but using a mid-sized sedan class having a good rate for the pedestrian safety assessment at NCAP.

This current research was focused on the two first points. But since the accident database is represented by cases over a wide period of time (1995-2011), it is important to change the implicated vehicle in the reconstruction process to one representing the actual vehicle model tendency. This assessment methodology could be even validated by performing full-scale crash tests and sub-system tests.

Finally, the methodology developed in this research has been applied on analysing the impact of CAM systems for only pedestrian. But this methodology can be used for other road users. For example, it would be interesting to study the influence of the system's attributes for others vulnerable users (cyclists, powered two wheelers) and vehicle-to-vehicle collisions. An expansion of this work could be considered in future work.

Appendices

Appendix A

Listing data of the selected accident cases

The 100 accident cases selected for this research are described below. The first 40 cases are from the database of IFSTTAR-LMA and the remaining from CASR. They are described according to the different components of a crash: the road environment, driver, vehicle and the pedestrian. The description includes:

- the time when the crash occurred (D:daytime; N:nighttime; N+L: nighttime with street lights);
- the light condition (BC: bad condition as heavy rain or sun glare);
- the road condition (Wet: wet road);
- the road curvature (LT: left turn or RT: right turn);
- the obstacles that mask the pedestrian from sight view of the detection systems;
- the travel speed of the vehicle;
- the impact speed;
- the age of the pedestrian;
- the pace of the pedestrian according to the statements declared by the involved parts or witnesses (S: static; walking; W f.: walking fast; R: running);
- the pedestrian velocity corresponding to his age and pace;
- the impact location on the front–end of the vehicle (LS: left side of the driver; FC: front centre; RS: right side);
- The trajectory of the pedestrian according to the driver (L: from the left towards the vehicle; R: from the right).

Table A.1. Listing data of the accident cases from the database of IFSTTAR (1/2)

Case	Environment					Vehicle		Pedestrian				
	Day/Night	Light Cond.	Road Cond.	Road curve	Obstacles masking	Travel Speed (km/h)	Impact Speed (km/h)	Age	Pace	Speed (m/s)	Impact Locat.	Traject.
1	D					45.5	32	52	R	2.83	FC	L
2	N+L		Wet			50	50	40	W	1.62	RS	L
3	D					42.4	10	12	R	1.68	RS	R
4	D					117.6	86	66	R	2.47	RS	L
5	N+L					75.2	45	79	W	1.07	RS	L
6	D			LT		0	22	17	W	1.65	LS	R
7	N					130	130	33	W	1.62	LS	R
8	D			LT		11.1	20	79	W	1.07	LS	R
9	D					53	53	74	W	1.28	RS	L
10	D					55	55	86	W	1.07	FC	R
11	D					50	50	79	W	1.28	RS	R
12	D				Vehicle	35	35	62	W	1.46	FC	R
13	D					30	30	65	W	1.28	RS	R
14	D			LT		2.1	15	76	W	1.28	LS	R
15	D	BC			Tree	44.7	40	85	W	1.28	FC	L
16	D				Vehicle	39.9	5	27	W	1.62	LS	L
17	N+L					33.9	27	69	W	1.28	FC	R
18	N+L					40	40	40	W	1.62	RS	L
19	D	BC	Wet	LT		22	8	51	W	1.52	FC	L
20	D			LT		20	20	64	W	1.46	LS	R

Table A.1. Listing data of the accident cases from the database of IFSTTAR (2/2)

Case	Environment					Vehicle		Pedestrian				
	Day/Night	Light Cond.	Road Cond.	Road curve	Obstacles masking	Travel Speed (km/h)	Impact Speed (km/h)	Age	Pace	Speed (m/s)	Impact Locat.	Traject.
21	D+L*				Vehicle	43.3	10	21	W	1.62	RS	R
22	D				Vehicle	40	10	15	R	4.2	LS	L
23	D+L	BC	Wet			35	35	17	W	1.65	FC	L
24	D	BC				50	50	69	W	1.28	FC	L
25	D					30	30	77	W	1.28	LS	L
26	D			LT		35	35	60	W	1.46	FC	R
27	N+L					38.3	3	82	W	0.5	RS	L
28	D					30	30	70	W	1.28	LS	L
29	D					30	30	73	W	1.28	FC	R
30	D				Vehicle	20	20	60	S	0	RS	-
31	D				Bus	39.7	17	6	R	3.94	FC	L
32	D			RT		20	20	14	W	1.68	FC	R
33	D				Vehicle	34.7	5	5	R	3.94	FC	R
34	N+L					55	15	11	R	4.2	FC	L
35	D					36.3	11	37	W	1.34	RS	R
36	D					22	22	19	W	1.65	RS	R
37	D	BC				36	36	68	W	1.28	RS	R
38	D					5	5	24	W f.	2.8	RS	R
39	D	BC	Wet	RT	Billboard	30	30	10	R	4.2	FC	L
40	D	BC				30	30	82	W	1.07	FC	L

* Dawn

Table A.2. Listing data of the accident cases from the database of CASR (1/3)

Case	Environment					Vehicle		Pedestrian				
	Day/Night	Light Cond.	Road Cond.	Road curve	Obstacles masking	Travel Speed (km/h)	Impact Speed (km/h)	Age	Pace	Speed (m/s)	Impact Locat.	Traject.
41	D					35	35	21	W	1,62	RS	R
42	D				Vehicle	45	45	13	R	4,2	FC	R
43	D					55	55	75	W	1,46	LS	L
44	D					40	40	29	R	4,2	FC	L
45	D	BC		RT		20	20	75	W	1,28	FC	L
46	D					53,4	30	75	W	1,28	RS	L
47	D		Wet			56,4	44	47	R	2,9	LS	L
48	D				Bus	40	40	13	R	4,2	LS	L
49	N+L					60	60	24	W	1,4	LS	L
50	D		Wet		Vehicle	20	20	18	W	1,65	LS	R
51	D					50	50	47	R	2,9	FC	L
52	D				Bin	35	35	3	R	2,41	FC	L
53	D					55,7	30	50	W	1,52	LS	R
54	D		-		Vehicle	35	35	14	R	4,2	LS	R
55	D				Vehicle	65,5	40	38	W	1,62	FC	L
56	D					47	47	16	W	1,65	LS	L
57	D					58,9	14	57	S	0	LS	-
58	D			RT		0	43,1	71	W	1,28	FC	L
59	D					42,7	29	45	W	1,52	RS	L
60	N+L					60	60	17	W	1,65	FC	R

Table A.2. Listing data of the accident cases from the database of CASR (2/3)

Case	Environment					Vehicle		Pedestrian				
	Day/Night	Light Cond.	Road Cond.	Road curve	Obstacles masking	Travel Speed (km/h)	Impact Speed (km/h)	Age	Pace	Speed (m/s)	Impact Locat.	Traject.
61	D				Bus	43,1	36	14	W	1,68	RS	L
62	D				Vehicle	25	25	19	W	1,65	LS	L
63	D					60	60	16	W	1,65	LS	L
64	D					56,1	22	6	R	3,94	FC	R
65	D				Vehicle	17	17	11	R	4,2	FC	R
66	D					58	58	89	W	1,28	LS	L
67	D					30	30	67	W	1,28	RS	L
68	N+L					43	30	35	R	3,35	LS	L
69	N+L					37	37	35	S	0	FC	-
70	N+L					47	47	28	R	3,54	FC	R
71	D					46,2	36	65	W	1,28	FC	L
72	N+L		-			50	50	67	W	1,28	RS	R
73	D					50,9	31	18	W	1,46	FC	L
74	D			RT		15	15	65	W	1,28	RS	-
75	N+L		-	RT		15	15	24	W	1,62	FC	L
76	N+L				Pole	62	62	44	W	1,62	LS	L
77	D					48,2	21	76	W	1,28	FC	R
78	D					62,6	27	80	W	1,28	FC	L
79	D					60	50	30	W	1,62	FC	R
80	D					35	35	67	R	2,71	LS	L

Table A.2. Listing data of the accident cases from the database of CASR (3/3)

Case	Environment					Vehicle		Pedestrian				
	Day/Night	Light Cond.	Road Cond.	Road curve	Obstacles masking	Travel Speed (km/h)	Impact Speed (km/h)	Age	Pace	Speed (m/s)	Impact Locat.	Traject.
81	D		-			49,5	5	7	R	3,94	FC	R
82	D	-	-			41,8	41,8	82	W	1,28	FC	R
83	D					55	55	13	W	1,68	FC	R
84	N+L			RT		20	20	53	W	1,52	LS	L
85	D				Vehicle	14,4	25	19	R	4,2	FC	R
86	D	-		RT		30	30	78	W	1,28	LS	L
87	D				Vehicle	27,3	12	20	R	3,54	FC	L
88	D					40	40	23	W	1,62	LS	L
89	D		-			49,1	30	48	R	2,9	LS	L
90	D			LT		15	15	50	W	1,52	LS	L
91	D	-		LT		15	15	33	W	1,62	FC	R
92	N+L					50	50	39	W	1,62	RS	R
93	D		-			29,6	20	19	W	1,65	LS	L
94	D					30	20	17	W	1,65	FC	R
95	D				Vehicle	55,1	20	58	W	1,46	RS	R
96	D					35,1	10	30	W	1,62	LS	L
97	D		-	RT		20	20	41	W	1,62	RS	L
98	D					94,3	49	84	W	1,28	FC	L
99	D					47,7	30	73	W	1,28	FC	L
100	D			LT		7,9	15	9	R	3,94	LS	L

Appendix B

Assessing the pedestrian detection

The benefits of the Pedestrian-AEB systems were presented according to two different views: 'optimistic' view which includes the assumption of detecting under poor light conditions and 'pessimistic' view without taking into account the aforementioned assumption. The results were presented separately expressing these two views.

Some systems may detect easily the pedestrian under poor light conditions with combining multiple sensors. Cameras using visible light (excluding near or infrared radiation –IR–) were assumed not able to detect pedestrians under poor light condition. In these last cases, the pedestrian could be located in the coverage area of the camera but still considered "not detected". Nevertheless, cameras coupled with other kind of sensors (radar, scanner, IR…) were assumed to overcome the limited performance of each sensor (see Chapter 2, Section 2.3.1). It is then possible for a multiple sensor system to detect pedestrians under poor light condition.

Algorithms for assessing pedestrian detection were classified according to the type of sensors and the width of the field of view (FOV) of radars and lidars compared to visible light cameras:

- Only stereo camera: which corresponds to system S3

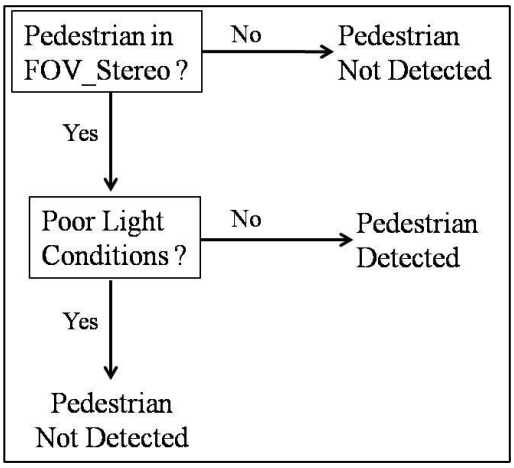

- FOV_camera (or stereo) is smaller than FOV_radar (or lidar): which corresponds to the systems S1, S2, S5 and S6

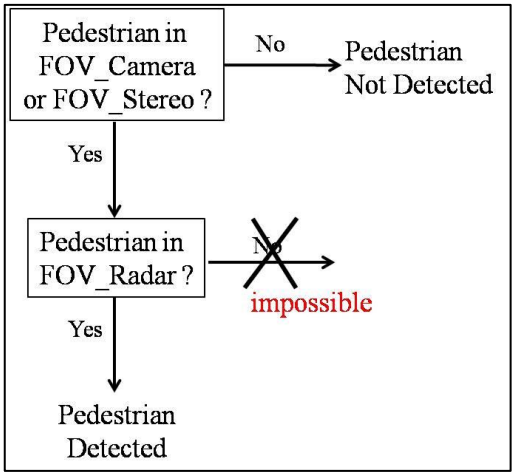

- FOV_camera (or stereo) is wider than FOV_radar (or lidar): which corresponds to system S4

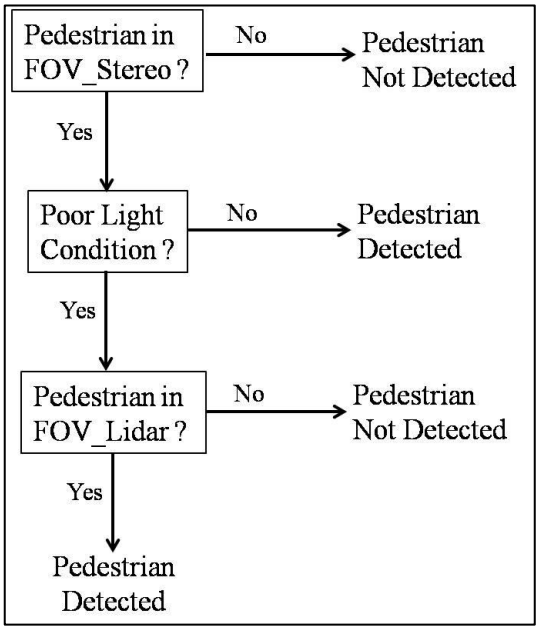

Bibliography

AAAM, 2008. The Abbreviated Injury Scale: 2005 (No. Update 2008). Association for the Advancement of Automotive Medicine, Des Plaines, Illinois, USA.

Amirouche, F., 2006. Fundamentals of multibody dynamics: theory and applications. Birkhäuser Engineering.

Anderson, R., Streeter, L., Ponte, G., Van de Griend, M., McLean, J., 2003. Vehicle design and operation for pedestrian protection: accident simulations and reconstructions (No. Vehicle Safety Standards Report (VSSR 1)). Commonwealth Department of Transport and Regional Services, Australia.

Anderson, R.W., Long, A.D., Serre, T., 2009. Phenomenological continuous contact–impact modelling for multibody simulations of pedestrian–vehicle contact interactions based on experimental data. Nonlinear Dyn. 58, 199–208.

Anderson, R.W., Searson, D.J., Hutchinson, T.P., 2012. Integrating the assessment of pedestrian safety in vehicles with collision detection and mitigation systems. Presented at the 2012 IRCOBI Conference, International Research Council on Biomechanics of Injury, Dublin Ireland, pp. 751–760.

Anderson, R.W.G., Long, A.D., Serre, T., Masson, C., 2008. Determination of boundary conditions for pedestrian collision reconstructions. Presented at the 2008 ICrash Conference, Kyoto, Japan.

Arnoux, P.-J., Cesari, D., Behr, M., Thollon, L., Brunet, C., 2005. Pedestrian lower limb injury criteria evaluation: A finite element approach. Traffic Inj. Prev. 6, 288–297.

Bertozzi, M., Broggi, A., Felisa, M., Vezzoni, G., Del Rose, M., 2006. Low-level Pedestrian Detection by means of Visible and Far Infra-red Tetra-vision. Presented at the 2006 IEEE Conference on Intelligent Vehicles Symposium, Tokyo, Japan, pp. 231–236.

Blundell, M., Harty, D., 2004. The multibody systems approach to vehicle dynamics. Elsevier.

Brach, R.M., Brach, R.M., 2005. Vehicle accident analysis and reconstruction methods. SAE International.

Brannstrom, M., Coelingh, E., Sjoberg, J., 2010. Model-Based Threat Assessment for Avoiding Arbitrary Vehicle Collisions. IEEE Trans. Intell. Transp. Syst. 11, 658–669. doi:10.1109/TITS.2010.2048314

Brenac, T., Megherbi, B., 1996. Diagnostic de sécurité routière sur une ville : intérêt de l'analyse fine de procédures d'accidents tirées aléatoirement. Rech.-Transp.-Sécurité RTS 59–71.

Brenac, T., Nachtergaële, C., Reigner, H., 2004. Scenarions types d'accidents impliquant des piétons et éléments pour leur prévention (No. 256), Rapport INRETS. INRETS.

Broggi, A., Cerri, P., Ghidoni, S., Grisleri, P., Ho Gi Jung, 2009. A New Approach to Urban Pedestrian Detection for Automatic Braking. IEEE Trans. Intell. Transp. Syst. 10, 594–605.

Burgett, A., Srinivasan, G., Ranganathan, R., 2008. A methodology for estimating potential safety benefits for pre-production driver assistance systems (Final report No. DOT HS 810 945).

Byatt, R., Watts, R., 1981. Manual of road accident investigation. Pitman.

Carhs, 2012. SafetyWissen afetyWissen : Pedestrian Saf. Companion 65–68.

Cavallero, C., Cesari, D., Ramet, M., Billault, P., Farisse, J., Seriat-Gautier, B., Bonnoit, J., 1983. Improvement of pedestrian safety: influence of shape of passenger car-front structures upon pedestrian kinematics and injuries: evaluation based on 50 cadaver tests (No. SAE Technical Paper 830624). Society of Automotive Engineers.

Cesari, D., Arnoux, P.-J., Borde, P., Cassan, F., Chalandon, S., Martin, J., Masson, C., Minne, F., Hermitte, T., Perrin, C., Serre, T., Sjoonekindt, S., Vallee, H., 2007. Amélioration de la protection des piétons en cas d'accident (No. Rapport final no. 3 DSCR 403).

Coelingh, E., Eidehall, A., Bengtsson, M., 2010. Collision Warning with Full Auto Brake and Pedestrian Detection - a practical example of Automatic Emergency Braking. Presented at the 13th International IEEE Conference on Intelligent Transportation Systems (ITSC), Funchal, Madeira Island, Portugal, pp. 155–160. doi:10.1109/ITSC.2010.5625077

Coulongeat, F., Anderson, R., Llari, M., Serre, T., 2013. Relations de dépendance entre la configuration d'un accident VL-piéton et le déroulement du choc. Presented at the 4ème colloque francophone international du GERI COPIE, Salon-de-Provence, France, p. 12p.

Crandall, J.R., Bhalla, K.S., Madeley, N.J., 2002. Designing road vehicles for pedestrian protection. Br. Med. J. 324, 1145.

DaCoTA, 2013. DaCoTA EU Road Safety Project [WWW Document]. URL http://www.dacota-project.eu/ (accessed 2.15.16).
Daniel, S., 1982. The role of the vehicle front end in pedestrian impact protection. SAE Technical paper.
Demetriades, D., Murray, J., Martin, M., Velmahos, G., Salim, A., Alo, K., Rhee, P., 2004. Pedestrians injured by automobiles: Relationship of age to injury type and severity. J. Am. Coll. Surg. 199, 382–387. doi:10.1016/j.jamcollsurg.2004.03.027
Depriester, J.-P., Perrin, C., Serre, T., Chalandon, S., 2005. Comparison of several methods for real pedestrian accident reconstruction. Presented at the 19th International Technical Conference on the Enhanced Safety of Vehicles (ESV), Washington D.C., USA.
Eberhardt, W., Himbert, G., 1977. Bewegungs-Geschwindigkeiten. Ing. -Büro Simon-Himbert-Eberhardt, Grossherzog-Friedrich-Str 86, 6600 Saarbrüken, Germany.
Ebner, A., Helmer, T., Samaha, R.R., Scullion, P., 2011. Identifying and Analyzing Reference Scenarios for the Development and Evaluation of Active Safety: Application to Preventive Pedestrian Safety. Int. J. Intell. Transp. Syst. Res. 9, 128–138. doi:10.1007/s13177-011-0035-z
Eckert, A., Hohm, A., Lueke, S., 2013. An integrated ADAS solution for pedestrian collision avoidance. Presented at the 23rd International Technical Conference on the Enhanced Safety of Vehicles (ESV), Seoul, Republic of Korea, pp. 13–0298.
Edwards, M., Nathanson, A., Carroll, J., Wisch, M., Zander, O., Lubbe, N., 2015. Assessment of integrated pedestrian protection systems with autonomous emergency braking (AEB) and passive safety components. Traffic Inj. Prev. 16, S2–S11.
Edwards, M., Nathanson, A., Wisch, M., 2014a. Estimate of Potential Benefit for Europe of Fitting Autonomous Emergency Braking (AEB) Systems for Pedestrian Protection to Passenger Cars. Traffic Inj. Prev. 15, S173–S182. doi:10.1080/15389588.2014.931579
Edwards, M., Nathanson, A., Wisch, M., 2014b. Benefit estimate and assessment methodologies for pre-crash braking part of forward-looking integrated pedestrian safety systems (No. ASPECSS D1.3).
EEVC, 1998. Improved Test Methods to Evaluate Pedestrian Protection Afforded by Passenger Cars (No. EEVC Working Group 17 report). European Enhanced Vehicle-safety Committee, Brussels, Belgium.
Eubanks, J., Haight, W., 1992. Pedestrian involved traffic collision reconstruction methodology. SAE Technical Paper 921591. doi:10.4271/921591
Eubanks, J., Hill, F.P., Casteel, A.D., 2004. Pedestrian Accident Reconstruction and Litigation, second. ed. Lawyers & Judges Publishing Company, Tuscon, Arizona, USA.
Euro NCAP, 2015. Assessment protocol – Pedestrian protection (No. Version 8.1).
Euro NCAP, 2009. Pedestrian testing protocol - Testing Protocol Version 5.0. European New Car Assessment Programme.
Evrard, B., 2011. Innovative Bonnet Active Actuator (B2A) For Pedestrian Protection. Presented at the 22nd International Technical Conference on the Enhanced Safety of Vehicles (ESV), Washington D.C., USA.
Fang, Y., Yamada, K., Ninomiya, Y., Horn, B., Masaki, I., 2003. Comparison between infrared-image-based and visible-image-based approaches for pedestrian detection. Presented at the 2003 IEEE Conference on Intelligent Vehicles Symposium, Columbus, Ohio, USA, pp. 505–510.
Ference, J.J., Szabo, S., Najm, W., 2006. Performance evaluation of integrated vehicle-based safety systems. Presented at the Performance Metrics for Intelligent Systems Worshop (PerMIS), Gaitherburg, Maryland, USA.
Ferguson, D., Darms, M., Urmson, C., Kolski, S., 2008. Detection, prediction, and avoidance of dynamic obstacles in urban environments. Presented at the 2008 IEEE Conference on Intelligent Vehicles Symposium, Eindhoven, Netherlands, pp. 1149–1154. doi:10.1109/IVS.2008.4621214
Ferrandez, F., Brenac, T., Girard, Y., Lechner, D., Jourdan, J.-L., Michel, J.-E., Nachtergaële, C., 1995. L'étude détaillée d'accidents orientée vers la sécurité primaire, méthodologie de recueil et de pré-analyse : Méthodologie de recueil et de pré-analyse. Presses de l'Ecole Nationale des Ponts et Chaussées, Paris.
Fleury, D., Brenac, T., 2001. Accident prototypical scenarios, a tool for road safety research and diagnostic studies. Accid. Anal. Prev. 33, 267–276.
FOT-Net, 2014. FESTA Handbook, Version 5.
Fredriksson, R., 2011. Priorities and Potential of Pedestrian Protection Accident Data: Accident data, Experimental tests and Numerical Simulations of Car-to- Pedestrian Impacts. Karolinska Institutet, Stockholm, sweden.
Fredriksson, R., Håland, Y., Yang, J., 2001. Evaluation of a new pedestrian head injury protection system with a sensor in the bumper and lifting of the bonnet's rear part (No. SAE2001-06-0089). Society of Automotive Engineers, Warrendale Pa, USA.

Fredriksson, R., Rosén, E., 2014. Head Injury Reduction Potential of Integrated Pedestrian Protection Systems Based on Accident and Experimental Data–Benefit of Combining Passive and Active Systems. Presented at the 2014 IRCOBI Conference, Berlin, Germany.
Fredriksson, R., Rosén, E., 2012. Integrated pedestrian countermeasures – Potential of head injury reduction combining passive and active countermeasures. Saf. Sci. 50, 400–407. doi:10.1016/j.ssci.2011.09.019
Fredriksson, R., Rosén, E., Kullgren, A., 2010. Priorities of pedestrian protection—A real-life study of severe injuries and car sources. Accid. Anal. Prev. 42, 1672–1681. doi:10.1016/j.aap.2010.04.006
Fredriksson, R., Shin, J., Untaroiu, C.D., 2011. Potential of Pedestrian Protection Systems—A Parameter Study Using Finite Element Models of Pedestrian Dummy and Generic Passenger Vehicles. Traffic Inj. Prev. 12, 398–411. doi:10.1080/15389588.2011.566655
Gandhi, T., Trivedi, M.M., 2007. Pedestrian Protection Systems: Issues, Survey, and Challenges. IEEE Trans. Intell. Transp. Syst. 8, 413–430. doi:10.1109/TITS.2007.903444
Gavrila, D.M., Giebel, J., Munder, S., 2004. Vision-based pedestrian detection: the PROTECTOR system. Presented at the 2004 IEEE Conference on Intelligent Vehicles Symposium, Parma, Italy, pp. 13–18.
Geronimo, D., Lopez, A.M., Sappa, A.D., Graf, T., 2010. Survey of pedestrian detection for advanced driver assistance systems. IEEE Trans. Pattern Anal. Mach. Intell. 32, 1239–1258. doi:10.1109/TPAMI.2009.122
Glasson, E., Bonnoit, J., Cavallero, C., Basile, F., 2000. A numerical analysis of the car front end module regarding pedestrian lower limb safety. Presented at the International Conference on Vehicle Safety, London, UK.
Hamacher, M., Eckstein, L., Kühn, M., Hummel, T., 2013. Integrated pedestrian safety assessment procedure. Presented at the 23rd International Technical Conference on the Enhanced Safety of Vehicles (ESV), Seoul, Republic of Korea, pp. 13–0268.
Hamacher, M., Eckstein, L., Kühn, M., Hummel, T., 2011. Assessment of active and passive technical measures for pedestrian protection at the vehicle front. Presented at the 22nd International Technical Conference on the Enhanced Safety of Vehicles (ESV), Washington D.C., USA.
Hamdane, H., Serre, T., Masson, C., Anderson, R., 2016. Relevant factors for active pedestrian safety based on 100 real accident reconstructions. Int. J. Crashworthiness 21, 51–62.
Hamdane, H., Serre, T., Masson, C., Anderson, R., 2015. Issues and challenges for pedestrian active safety systems based on real world accidents. Accid. Anal. Prev. 82, 53–60. doi:10.1016/j.aap.2015.05.014
Han, I., Brach, R.M., 2002. Impact throw model for vehicle-pedestrian collision reconstruction. Proc. Inst. Mech. Eng. Part J. Automob. Eng. 216, 443–453.
Hayashi, H., Inomata, R., Fujishiro, R., Ouchi, Y., Suzuki, K., Nanami, T., 2013. Development of pre-crash safety system with pedestrian collision avoidance assist. Presented at the 23rd International Conference on the Enhanced Safety of Vehicles (ESV), Seoul, Republic of Korea, pp. 13–0271.
Hayashi, R., Isogai, J., Raksincharoensak, P., Nagai, M., 2012. Autonomous collision avoidance system by combined control of steering and braking using geometrically optimised vehicular trajectory. Veh. Syst. Dyn. 50, 151–168. doi:10.1080/00423114.2012.672748
Hayward, J.C., 1972. Near miss determination through use of a scale of danger (No. Report no. TTSC 7115). The Pennsylvania State University, Pennsylvania, USA.
Hayward, J.C., 1972. Near-miss determination through use of a scale of danger (No. Report no. TTSC 7115). The Peennsylvania State University, Pennsylvania.
Helmer, T., 2015. Development of a methodology for the evaluation of active safety using the example of preventive pedestrian protection. Springer.
Helmer, T., Ebner, A., Samaha, R.R., Scullion, P., Kates, R., 2010. Injury risk to specific body regions of pedestrians in frontal vehicle crashes modeled by empirical, in-depth accident data. Stapp Car Crash J. 54, 93.
Hillman, M., Adams, J., Whitelegg, J., 1990. One false move. A study of children's independent mobility. Policy Stud. Inst.
Horst, A.R.A.V. der, Hogema, J.H., 1993. Time-to-collision and collision avoidance systems. Presented at the 6th ICTCT Congress, Salzburg, Austria.
Hu, J., Klinich, K.D., 2014. Toward designing pedestrian–friendly vehicles. Int. J. Veh. Saf. 8, 22–54.
Hu, J., Klinich, K.D., 2012. Toward designing pedestrian-friendly vehicles (No. Report no. UMTRI-2012-19). The University of Michigan Transportation Research Institute, Ann Arbor, Michigan, USA.
Huang, S., Yang, J., Eklund, F., 2008. Evaluation of remote pedestrian sensor system based on the analysis of car-pedestrian accident scenarios. Saf. Sci. 46, 1345–1355. doi:10.1016/j.ssci.2007.08.004

Huber, P., Kirschbichler, S., Prüggler, A., Steidl, T., 2014. Three-Dimensional Occupant Kinematics During Frontal, Lateral and Combined Emergency Maneuvers. Presented at the 2014 IRCOBI Conference, Berlin, Germany.
IGLAD, 2015. Initiative for the global harmonisation of accident data [WWW Document]. URL http://www.iglad.net/ (accessed 2.15.16).
Isermann, R., Schorn, M., Stählin, U., 2008. Anticollision system PRORETA with automatic braking and steering. Veh. Syst. Dyn. 46, 683–694. doi:10.1080/00423110802036968
Kaempchen, N., Schiele, B., Dietmayer, K., 2009. Situation assessment of an autonomous emergency brake for arbitrary vehicle-to-vehicle collision scenarios. IEEE Trans. Intell. Transp. Syst. 10, 678–687. doi:10.1109/TITS.2009.2026452
Kajzer, J., Matsui, Y., Ishikawa, H., Schroeder, G., Bosch, U., 1999. Shearing and bending effects at the knee joint at low speed lateral loading. Presented at the 1999 SAE International Congress and Exposition, Society of Automotive Engineers (SAE), Detroit,Michigan, USA, p. 14. doi:10.4271/1999-01-0712
Keller, C.G., Dang, T., Fritz, H., Joos, A., Rabe, C., Gavrila, D.M., 2011a. Active Pedestrian Safety by Automatic Braking and Evasive Steering. IEEE Trans. Intell. Transp. Syst. 12, 1292–1304.
Keller, C.G., Hermes, C., Gavrila, D.M., 2011b. Will the pedestrian cross? Probabilistic path prediction based on learned motion features, in: Pattern Recognition. Springer, pp. 386–395.
Kent, R., Trowbridge, M., Lopez-Valdes, F.J., Ordoyo, R.H., Segui-Gomez, M., 2009. How Many People Are Injured and Killed as a Result of Aging? Frailty, Fragility, and the Elderly Risk-Exposure Tradeoff Assessed via a Risk Saturation Model. Presented at the 53rd Annual Conference on Association for the Advancement of Automotive Medicine (AAAM), Baltimore, Maryland, USA, pp. 41–50.
Kirschbichler, S., Huber, P., Prüggler, A., Steidl, T., Sinz, W., Mayer, C., DAddetta, G.A., 2014. Factors Influencing Occupant Kinematics during Braking and Lane Change Maneuvers in a Passenger Vehicle. Presented at the 2014 IRCOBI Conference, Berlin, Germany.
Kompass, K., 2012. Accident research 2.0: New methods for representative evaluation of integral safety in traffic. Presented at the 5th International Conference on ESAR "Expert Symposium on Accident Research," Hannover, Germany.
Kuehn, M., Froeming, R., Schindler, V., 2005. Assessment of vehicle related pedestrian safety. Presented at the 19th International Technical Conference on the Enhanced Safety of Vehicles (ESV), Washington D.C., USA, pp. 05–0044.
Lechner, D., Ferrandez, F., 1990. Analysis and reconstruction of accident sequences. Presented at the XXIII FISITA Congress, ATA, Torino, Italy, pp. 931–939.
Lee, J.D., McGehee, D.V., Brown, T.L., Reyes, M.L., 2002. Collision warning timing, driver distraction, and driver response to imminent rear-end collisions in a high-fidelity driving simulator. Hum. Factors 44, 314–334.
Lenard, J., Badea-Romero, A., Danton, R., 2014. Typical pedestrian accident scenarios for the development of autonomous emergency braking test protocols. Accid. Anal. Prev. 73, 73–80. doi:10.1016/j.aap.2014.08.012
Lenard, J., Danton, R., Avery, M., Weekes, A., Zuby, D., Kühn, M., 2011. Typical pedestrian accident scenarios for the testing of autonomous emergency braking systems. Presented at the 22nd International Technical Conference on the Enhanced Safety of Vehicles (ESV), Washington DC, USA, pp. 11–0196.
Linder, A., Douglas, C., Clark, A., Fildes, B., Yang, J., Otte, D., 2005. Mathematical simulations of real-world pedestrian-vehicle collisions. Presented at the 19th International Technical Conference on the Enhanced Safety of Vehicles (ESV), Washington D.C., USA, pp. 05–285.
Lindman, M., Oedblom, A., Bergvall, E., Eidehall, A., Svanberg, B., Lukaszewicz, T., 2010. Benefit estimation model for pedestrian auto brake functionality. Presented at the 4th International Conference on ESAR "Expert Symposium on Accident Research," Hanover, Germany, pp. 05–285.
Liu, X.J., Yang, J.K., Lövsund, P., 2002. A Study of Influences of Vehicle Speed and Front Structure on Pedestrian Impact Responses Using Mathematical Models. Traffic Inj. Prev. 3, 31–42. doi:10.1080/15389580210517
Longhitano, D., Henary, B., Bhalla, K., Ivarsson, J., Crandall, J., 2005. Influence of vehicle body type on pedestrian injury distribution. SAE Trans. 114, 2283–2288.
Lubbe, N., Kullgren, A., 2015. Assessment of Integrated Pedestrian Protection Systems with Forward Collision Warning and Automated Emergency Braking. Presented at the 2015 IRCOBI Conference, Lyon, France, pp. 385–397.

Luo, Y., Remillard, J., Hoetzer, D., 2010. Pedestrian detection in near-infrared night vision system. Presented at the 2010 IEEE Conference on Intelligent Vehicles Symposium, San Diego, California, USA, pp. 51–58. doi:10.1109/IVS.2010.5548089
Machida, T., Naito, T., 2011. GPU & CPU cooperative accelerated pedestrian and vehicle detection. Presented at the 2011 IEEE International Conference on Computer Vision Workshops (ICCV Workshops), Barcelona, Spain, pp. 506–513. doi:10.1109/ICCVW.2011.6130285
Martin, J.-L., Lardy, A., Laumon, B., 2011. Pedestrian injury patterns according to car and casualty characteristics in France. Presented at the 55th Annual Conference on Annals of Advances in Automotive Medicine (AAAM), Paris, France.
Masson, C., Arnoux, P.-J., Brunet, C., Cesari, D., 2005. Pedestrian injury mechanisms & criteria: a coupled experimental and finite element approach. Presented at the 19th International Technical Conference on the Enhanced Safety of Vehicles (ESV), Washington DC, USA.
Masson, C., Brunet, C., 2006. The influence of the impact point on pedestrian lower limb injury and criteria. J. Biomech. 39, 535.
Masson, C., Serre, T., Cesari, D., 2007. Pedestrian-vehicle accident: Analysis of 4 full scale tests with PMHS. Presented at the 20th International Conference on the Enhanced Safety of Vehicles (ESV), Lyon, France.
Matlab, 2008. . The MathWorks Inc.
Matsui, Y., Han, Y., Mizuno, K., 2011. Performance of collision damage mitigation braking systems and their effects on human injury in the event of car-to-pedestrian accidents. Stapp Car Crash J. 55, 461–478.
Matsui, Y., Hitosugi, M., Takahashi, K., Doi, T., 2013. Situations of Car-to-Pedestrian Contact. Traffic Inj. Prev. 14, 73–77. doi:10.1080/15389588.2012.678511
McLean, A.J., Kloeden, C.N., Anderson, R.W., Baird, R.P., Farmer, M.J.B., 1996. Data collection and analysis of vehicle factors in relation to pedestrian brain injury. Presented at the 15th International Technical Conference on the Enhanced Safety of Vehicles (ESV), National Highway Traffic Safety Administration, Melbourne, Australia, pp. 1408–1411.
McLean, J., Anderson, R.W.G., Farmer, M.J.B., Lee, B.H., Brooks, C.G., 1994. Vehicle travel speeds and the incidence of fatal pedestrian collisions. Federal Office of Road Safety, Transport and Communiations.
Meinecke, M.-M., Obojski, M.A., Gavrila, D., Marc, E., Morris, R., Töns, M., Letellier, L., 2003. Deliverable D6: Strategies in Terms of Vulnerable Road User Protection (EU-Project SAVE-U No. Deliverable D6).
Meinecke, M.M., Obojski, M.A., Töns, M., Dehesa, M., 2005. SAVE-U: First Experiences with a Pre-Crash System for Enhancing Pedestrian Safety. Presented at the 5th European Congress and Exhibition on Intelligent Transportation Systems and Services (ITS), ERTICO, Hanover, Germany.
Michalke, T.P., Jebens, A., Schafers, L., 2011. A dynamic approach for ensuring the functional reliability of next-generation driver assistance systems. Presented at the 2011 IEEE Conference on Intelligent Transportation Systems, IEEE, Washington D.C., USA, pp. 408–415. doi:10.1109/ITSC.2011.6082881
Mizuno, K., Kajzer, J., 2000. Head injuries in vehicle-pedestrian impact (No. SAE paper n° 2000-01-0157). SAE Technical paper.
Mizuno, Y., 2005. Summary of IHRA pedestrian safety WG activities (2005) -izuno, Y. test methods to evaluate pedestrian protection aforded by passenger cars. Presented at the 19th International Technical Conference on the Enhanced Safety of Vehicles (ESV), Washington D.C., USA, p. 15.
Mizuno, Y., 1998. International harmonized research activities (IHRA) status report of the Pedestrian Safety Working Group. Presented at the 16th International Technical Conference on the Enhanced Safety of Vehicles (ESV), National Highway Traffic Safety Administration, Windsor, Ontario, Canada, pp. 2120–2121.
Mo, F., Arnoux, P.J., Cesari, D., Masson, C., 2014. Investigation of the injury threshold of knee ligaments by the parametric study of car–pedestrian impact conditions. Saf. Sci. 62, 58–67.
Montufar, J., Arango, J., Porter, M., Nakagawa, S., 2007. Pedestrians' Normal Walking Speed and Speed When Crossing a Street. Transp. Res. Rec. J. Transp. Res. Board 90–97.
NHTSA, 2016. Special Crash Investigations (SCI) | National Highway Traffic Safety Administration (NHTSA) [WWW Document]. URL http://www.nhtsa.gov/SCI (accessed 2.12.15).
Niewöhner, W., Roth, F., Gwehenberger, J., Gruber, C., Kuehn, M., Sferco, R., Pastor, C.-H., Nagel, U., Stanzel, M., 2011. Proposal for a test procedure of assistance systems regarding preventive pedestrian protection. Presented at the 22nd International Technical Conference on the Enhanced Safety of Vehicles (ESV), Washington D.C., USA.

Oh, C., Kang, Y., Kim, W., 2008. Assessing the safety benefits of an advanced vehicular technology for protecting pedestrians. Accid. Anal. Prev. 40, 935–942. doi:10.1016/j.aap.2007.10.010
Okamoto, Y., Sugimoto, T., Enomoto, K., Kikuchi, J., 2003. Pedestrian head impact conditions depending on the vehicle front shape and its construction--full model simulation. Traffic Inj. Prev. 4, 74–82.
ONISR, 2013. La sécurité routière en France : Bilan de l'accidentalité de l'année 2013 (Pre-edition). Observatoire National Interministériel de la Sécurité Routière.
Otte, D., Jänsch, M., Haasper, C., 2012. Injury protection and accident causation parameters for vulnerable road users based on German In-Depth Accident Study GIDAS. Accid. Anal. Prev., Safety and Mobility of Vulnerable Road Usears: Pedestrians, Bicyclists, and Motorcyclists 44, 149–153. doi:10.1016/j.aap.2010.12.006
Peng, R.Y., Bongard, F.S., 1999. Pedestrian versus motor vehicle accidents: an analysis of 5,000 patients. J. Am. Coll. Surg. 189, 343–348. doi:10.1016/S1072-7515(99)00166-0
Reed, W.S., Keskin, A.T., 1989. Vehicular Deceleration and Its Relationship to Friction (SAE Technical Paper No. 890736). SAE International, Warrendale, PA.
Rodarius, C., Seiniger, P., Baurès, S., Waagmeester, K., Aparicio, A., Vissers, J.P.M., Ranovona, M., McCarthy, M., Lloyd, L., Muirhead, M., 2012. Pre-crash evaluation: final status (No. ASSESS D4.3b).
Rosén, E., Källhammer, J.-E., Eriksson, D., Nentwich, M., Fredriksson, R., Smith, K., 2010. Pedestrian injury mitigation by autonomous braking. Accid. Anal. Prev. 42, 1949–1957.
Roudsari, B.S., Mock, C.N., Kaufman, R., 2005. An evaluation of the association between vehicle type and the source and severity of pedestrian injuries. Traffic Inj. Prev. 6, 185–192.
Sankarasubramanian, H., Mukherjee, S., Chawla, A., 2011. Optimization of vehicle front for safety of pedestrians. Presented at the 22nd International Technical Conference on the Enhanced Safety of Vehicles (ESV), Washington D.C., USA.
Schaller, T., Aparicio, A., Gruber, C., Pla, M., 2012. Report describing the comparative survey of existing test protocols and test facilities (No. ASPECSS D2.2).
Scheunert, U., Cramer, H., Fardi, B., Wanielik, G., 2004. Multi sensor based tracking of pedestrians: a survey of suitable movement models. Presented at the 2004 IEEE Conference on Intelligent Vehicles Symposium, Parma, Italy, pp. 774–778.
Schoenmarkers, F., 2011. MADYMO human models for Euro NCAP pedestrian safety assessment.
Schofer, J.L., Christoffel, K.K., Donovan, M., Lavigne, J.V., Tanz, R.R., Wills, K.E., 1995. Child pedestrian injury taxonomy based on visibility and action. Accid. Anal. Prev. 27, 317–333.
Schram, R., Williams, A., van Ratingen, M., 2013. Implementation of autonomous emergency braking (AEB), the next step in Euro NCAP's safety assessment. Presented at the 23rd International Technical Conference on the Enhanced Safety of Vehicles (ESV), Seoul, Republic of Korea.
Searle, J.A., Searle, A., 1983. The trajectories of pedestrians, motorcycles, motorcyclists etc following a road accident. Presented at the 1983 IRCOBI Conference, International Research Council on Biomechanics of Injury, San Diego, California, USA, pp. 277–286.
Searson, D.J., Anderson, R.W., Hutchinson, T.P., 2012. The effect of impact speed on the HIC obtained in pedestrian headform tests. Int. J. Crashworthiness 17, 562–570.
Seiniger, P., Bartels, O., Kunert, M., Schaller, T., 2014. Test procedure including test target and misuse tests, based on test results (No. ASPECSS D2.5).
Seiniger, P., Bartels, O., Pastor, C., Wisch, M., 2013. An open simulation approach to identify chances and limitations for vulnerable road user (VRU) active safety. Traffic Inj. Prev. 14, S2–S12. doi:10.1080/15389588.2013.797574
Serre, T., Bohn, M., Llari, M., Cavallero, C., Perrin, F.C., 2004. Detailed investigation and reconstructions of real accidents involving vulnerable road users. Presented at the 1st International Conference on ESAR "Expert Symposium on Accident Research," Hannover, Germany.
Serre, T., Llari, M., Cassagne, J., 2011. Analyse du choc piéton par une approche numérique multicorps ulticorps : différences entre le choc véhicule et la chute au sol, in: 3ème Colloque Francophone International Du GERI COPIE. Salon de ProvenceSerre, T., Masson, C., Perrin, C., Chalandon, S., Llari, M., Py, M., Cavallero, C., Cesari, D., 2007. Real accidents involving vulnerable road users: in-depth investigation, numerical simulation and experimental reconstitution with PMHS. Int. J. Crashworthiness 12, 227–234. doi:10.1080/13588260701441050
Simms, C.K., Wood, D.P., Walsh, D.G., 2004. Confidence limits for impact speed estimation from pedestrian projection distance. Int. J. Crashworthiness 9, 219–228.
Soni, A., Robert, T., Rongiéras, F., Beillas, P., 2013. Observations on pedestrian pre-crash reactions during simulated accidents. Stapp Car Crash J. 57, 157.
Suard, F., 2006. Kernel Machines for Pedestrian Detection. Institut National des Sciences Appliquées de Rouen, Rouen, France.

Subaru Australia, 2014. EyeSight™ Principle Of Operation [WWW Document]. URL http://www.subaru.com.au/about/eyesight/eyesight-principle-of-operation (accessed 5.28.14).
Szarvas, M., Sakai, U., Ogata, J., 2006. Real-time Pedestrian Detection Using LIDAR and Convolutional Neural Networks. Presented at the 2006 IEEE Conference on Intelligent Vehicles Symposium, Tokyo, Japan, pp. 213–218.
Tamke, A., Thao Dang, Breuel, G., 2011. A flexible method for criticality assessment in driver assistance systems. Presented at the 2011 IEEE Conference on Intelligent Vehicles Symposium, Baden-Baden, Germany, pp. 697–702. doi:10.1109/IVS.2011.5940482
Tanno, K., Kohno, M., Ohashi, N., Ono, K., Aita, K., Oikawa, H., Honda, K., Misawa, S., 2000. Patterns and mechanisms of pedestrian injuries induced by vehicles with flat-front shape. Leg. Med. 2, 68–74.
TNO Automotive, 2001. Theory manual – Madymo V6.0.
Tons, M., Doerfler, R., Meinecke, M.-M., Obojski, M.A., 2004. Radar sensors and sensor platform used for pedestrian protection in the EC-funded project SAVE-U. Presented at the 2004 IEEE Conference on Intelligent Vehicles Symposium, Parma, Italy, pp. 813–818.
Toyota-global, 2016. Rescue | TOYOTA GLOBAL SITE [WWW Document]. URL http://www.toyota-global.com/innovation/safety_technology/safety_technology/rescue/ (accessed 2.16.16).
TRL, 2016. Our History - TRL [WWW Document]. URL http://www.trl.co.uk/about-us/our-history/ (accessed 2.12.15).
Untaroiu, C.D., Meissner, M.U., Crandall, J.R., Takahashi, Y., Okamoto, M., Ito, O., 2009. Crash reconstruction of pedestrian accidents using optimization techniques. Int. J. Impact Eng. 36, 210–219. doi:10.1016/j.ijimpeng.2008.01.012
Van Rooij, L., Bhalla, K., Meissner, M., Ivarsson, J., Crandall, J., Longhitano, D., Takahashi, Y., Dokko, Y., Kikuchi, Y., 2003. Pedestrian crash reconstruction using multi-body modeling with geometrically detailed, validated vehicle models and advanced pedestrian injury criteria. Presented at the 18th International Technical Conference on the Enhanced Safety of Vehicles (ESV), Nagoya, Japan.
Volvocars, 2012. Volvo Car Corporation's pedestrian airbag: here's how it works - Volvo Car Group Global Media Newsroom [WWW Document]. URL https://www.media.volvocars.com/global/en-gb/media/pressreleases/43844 (accessed 2.16.16).
WHO, 2013. Global status report on road safety 2013: supporting a decade of action. World Health Organization, Geneva, Switzerland.
WHO, 2009. Global status report on road safety: time for action. World Health Organization, Geneva, Switzerland.
Wisch, M., Seiniger, P., Edwards, M., Schaller, T., Pla, M., Aparicio, A., Geronimi, S., Lubbe, N., 2013a. European project ASPECSS - interim result: Development of test scenarios based on identified accident scenarios. Presented at the 23rd International Technical Conference on the Enhanced Safety of Vehicles (ESV), Seoul, Republic of Korea, pp. 13–0405.
Wisch, M., Seiniger, P., Pastor, C., Edwards, M., Visvikis, C., Reeves, C., 2013b. Assessment methodologies for forward looking integrated pedestrian and further extension to cyclists safety (No. ASPECSS D1.1).
Wood, D.P., 1988. Impact and movement of pedestrians in frontal collisions with vehicles. Proc. Inst. Mech. Eng. Part J. Automob. Eng. 202, 101–110.
Yamada, H., 1970. Strength of biological materials. The Williams and Wilkins, Baltimore MD, USA.
Yang, J., 2003. Pedestrian head protection from car impacts. Int. J. Veh. Des. 32, 16–27.
Yang, J.K., Lövsund, P., Cavallero, C., Bonnoit, J., 2000. A human-body 3D mathematical model for simulation of car-pedestrian impacts. Traffic Inj. Prev. 2, 131–149.
Yao, J., Yang, J., Otte, D., 2008. Investigation of head injuries by reconstructions of real-world vehicle-versus-adult-pedestrian accidents. Saf. Sci. 46, 1103–1114. doi:10.1016/j.ssci.2007.06.021
Yao, J., Yang, J., Otte, D., 2007. Head Injuries in Child Pedestrian Accidents—In-Depth Case Analysis and Reconstructions. Traffic Inj. Prev. 8, 94–100. doi:10.1080/15389580600944243
Yuasa, H., Nakanishi, M., Mochida, T., Yamada, N., Nakai, M., 2013. Research into evaluation method for pedestrian pre-collision system. Presented at the 23rd International Technical Conference on the Enhanced Safety of Vehicles (ESV), Seoul, Republic of Korea, pp. 13–0110.
Zębala, J., Ciępka, P., RezA, A., 2012. Pedestrian acceleration and speeds. Probl. Forensic Sci. 91, 227–234.
Zhang, X., Chen, P., Nakamura, H., Asano, M., 2013. Modeling pedestrian walking speed at signalized crosswalks considering crosswalk length and signal timing. Presented at the 10th International Conference on Eastern Asia Society for Transportation Studies, Taipei, Taiwan.